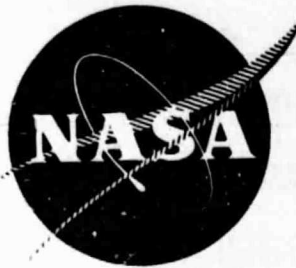# N O T I C E

THIS DOCUMENT HAS BEEN REPRODUCED FROM
MICROFICHE. ALTHOUGH IT IS RECOGNIZED THAT
CERTAIN PORTIONS ARE ILLEGIBLE, IT IS BEING RELEASED
IN THE INTEREST OF MAKING AVAILABLE AS MUCH
INFORMATION AS POSSIBLE

# NASA

# QUIET CLEAN SHORT-HAUL EXPERIMENTAL ENGINE (QCSEE)
# OVER-THE-WING (OTW)
# PROPULSION SYSTEMS TEST REPORT

## VOLUME IV
## ACOUSTIC PERFORMANCE

by

D. L. Stimpert

GENERAL ELECTRIC COMPANY

Prepared for

## National Aeronautics and Space Administration

NA

# FOREWORD

Technical contributors to this report are listed below:

### Advanced Systems Acoustics

| Manager | H.D. Sowers |
| Engineer | D.L. Stimpert |

### Acoustic Evaluation Engineering

| Engineer | W.R. Minzner |

### Acoustic Treatment Development

| Manager | R.E. Kraft |

### Advanced Measurements and Analysis

Senior Engineer  M.T. Moore

iii

# TABLE OF CONTENTS

# TABLE OF CONTENTS  (Concluded)

# LIST OF FIGURES

## LIST OF FIGURES (Continued)

## LIST OF FIGURES (Continued)

## LIST OF FIGURES (Concluded)

## LIST OF TABLES

# 1.0 SUMMARY

As part of the Quiet Clean Short-haul Experimental Engine (QCSEE) Program sponsored by NASA Lewis Research Center, a series of acoustic tests were conducted on the Over-the-Wing (OTW) engine. These tests evaluated the fully suppressed noise levels in forward and reverse thrust operation and provided insight into the component noise sources of the engine plus the suppression achieved by various components.

System noise levels using the contract specified calculation procedure indicate that the in-flight noise level on a 152m (500 foot) sideline at takeoff and approach are 97.2 and 94.6 EPNdB, respectively, compared to a goal of 95.0 EPNdB. In reverse thrust, the system noise level was 106.1 PNdB compared to a goal of 100 PNdB.

Baseline source noise levels agreed very well with pretest predictions. Inlet-radiated noise suppression of 14 PNdB was demonstrated with the high throat Mach number inlet at 0.79 throat Mach number.

# 2.0 INTRODUCTION

The General Electric Company is currently engaged in the Quiet Clean Short-haul Experimental Engine Program (QCSEE) under Contract NAS3-18021 to the NASA Lewis Research Center. The Over-the-Wing (OTW) experimental engine was designed and built under the program to develop and demonstrate technology applicable to engines for future commercial short-haul turbofan aircraft. The initial buildup of the OTW engine and boilerplate nacelle was tested at General Electric's Peebles, Ohio, Outdoor Test Site 4D during the period from March 31, 1977 through June 9, 1977.

Initial testing included a mechanical and systems checkout with hard wall acoustic panels and a bellmouth inlet. Performance data were taken over a range of fan speeds and at three exhaust nozzle areas (side door angles). This phase of testing provided data in the range of takeoff and approach operating conditions to explore "uninstalled" performance with maximum inlet total pressure recovery. Fan performance characteristics were mapped over a range of fan speeds and operating lines. An acoustic baseline was also run in the unsuppressed forward thrust configuration.

The inlet was then changed to the boilerplate high throat Mach number design to investigate installed performance with real inlet total pressure recovery. Points were repeated at takeoff and approach operating conditions. Reverse thrust testing included 105° and 115° blocker angles with a 0.6 lip length ratio. A reingestion shield, 3.66m (12 ft) in diameter and 9.14m (30 ft) long, was used to reduce reingestion of hot exhaust gases during reverse thrust testing, and the effect of this shield on thrust measurements was calibrated in the forward thrust mode.

Following reverse thrust performance testing, all hard wall panels were replaced with acoustically treated panels and an acoustic splitter was added in the fan duct. Fully suppressed acoustic data were taken in the reverse and forward thrust modes. Additional acoustic tests in forward thrust were then conducted to evaluate the contribution of inlet treatment and the combined effect of the splitter and core exhaust nozzle treatment.

Following the completion of acoustic testing, additional tests were conducted to evaluate control characteristics and engine throttle response in the forward thrust mode.

The engine was inspected, refurbished, and delivered to NASA Lewis Research Laboratory on June 30, 1977 for further planned testing adjacent to a wing section.

This volume of the propulsion system test report includes results of the analysis of internal and far field acoustic measurements and the adjustment of this data to reflect the specified four engine, 66700 kg (147000 lb) OTW aircraft for comparison with sideline noise goals. These adjustments include the addition of jet/flap interaction noise levels to the engine alone noise levels measured during the test program. Detailed acoustic data used in this analysis may be found in a separate volume, Appendix B.

2

# 3.0 TEST CONFIGURATIONS

The QCSEE OTW engine was tested on pad IV-D at the General Electric Company Peebles Test Operation near Peebles, Ohio. Acoustic testing occurred between April 29 and June 9, 1977. This section documents the configurations tested and the data acquisition and reduction processes.

The engine incorporated many low noise design features as indicated in Figure 1 and in Table I. Included are wide rotor-stator spacing, frame treatment and treated vanes, stacked treatment in the core to attenuate both high frequency turbine noise and low frequency core noise, removable treated fan exhaust wall panels and splitter, and a hybrid inlet which combined high throat Mach number acceleration suppression with inlet wall treatment.

Details of the OTW acoustic design are available in References 1, 2, 3 and 4.

Five configurations were tested as part of the acoustic investigation on this engine. An overview of the five configurations is given in Table II and indicates the general set-up of each. Tables III through VII present the specific data points acquired for each test and the corresponding engine operating parameters.

## 3.1 FORWARD THRUST

Of the five configurations tested, four were in the forward thrust mode, Figure 2 is a photograph of the fully suppressed configuration. The inlet is the hybrid inlet or high-throat Mach number inlet with treatment. Note in Figure 3 that this OTW engine has a "D" shaped nozzle with variable side doors for varying discharge nozzle area. The engine was mounted inverted from what it would be when installed over a wing on an aircraft.

A schematic of the baseline engine is shown in Figure 4. It was tested with a hard wall bellmouth, no fan exhaust duct treatment, and no core treatment. The fan frame treatment and the treatment on the pressure side of the vanes was not removable and was therefore included in the baseline engine test configuration.

The fully suppressed engine schematic is presented in Figure 5. This configuration is the one used to determine the system noise levels. Its suppression features include high throat Mach number treated inlet, fan aft duct and core wall suppression, and an acoustic splitter. These are in addition to the fan frame treatment mentioned above.

Inlet acoustic performance with a high-throat Mach number inlet without treatment was given by the configuration in Figure 6. The treatment panels in the inlet were replaced with hardwall panels to allow separate determination

3
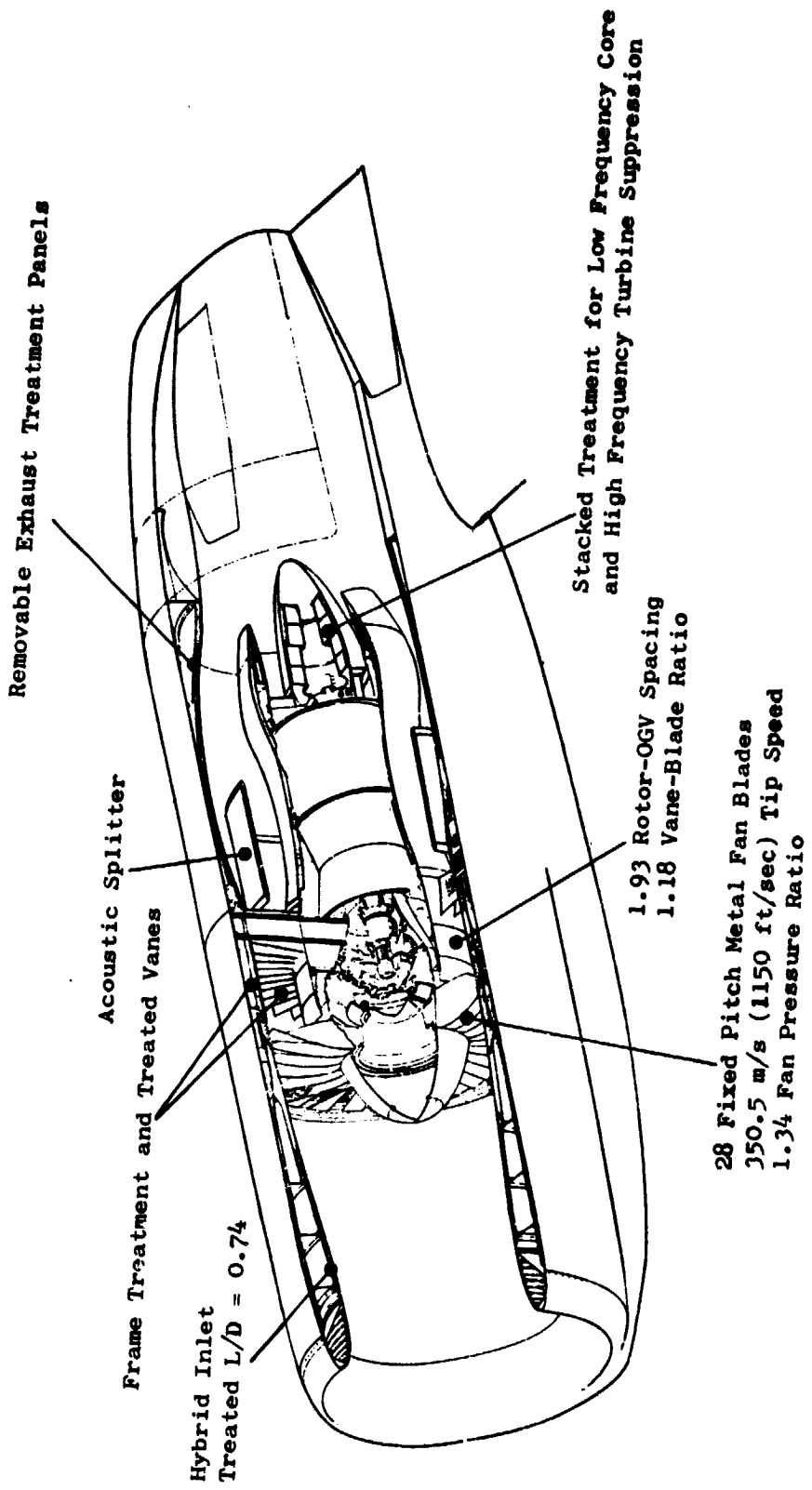
Figure 1. Acoustic Design Features.

Removable Exhaust Treatment Panels

Stacked Treatment for Low Frequency Core
and High Frequency Turbine Suppression

Acoustic Splitter

1.93 Rotor-OGV Spacing
1.18 Vane-Blade Ratio

Frame Treatment and Treated Vanes

28 Fixed Pitch Metal Fan Blades
350.5 m/s (1150 ft/sec) Tip Speed
1.34 Fan Pressure Ratio

Hybrid Inlet
Treated L/D = 0.74

4

Table 1. Acoustic Design Parameters.

- 41 m/sec (80 knots) Aircraft Speed
- 61 m (200 ft) Altitude

| | |
|---|---|
| Number of Fan Blades | 28 |
| Fan Diameter | 180.4 cm (71 in.) |
| Fan Pressure Ratio | 1.34 |
| Fan rpm (takeoff) | 3778 rpm |
| Fan rpm (design, 100 percent) | 3793 rpm |
| Fan Tip Speed | 350.5 m/sec (1150 ft/sec) |
| Number of OGV's | 33 |
| Fan Weight Flow (Corrected) | 405.5 kg/sec (894 lb/sec) |
| Inlet Mach Number (throat) | 0.79 |
| Rotor/OGV Spacing | 1.93 |
| Treated Inlet Length to Fan Diameter Ratio | 0.74 |
| Exhaust Area ("D" nozzle) | 1.747 $m^2$ (2708 in.$^2$) |
| Gross Thrust (Uninstalled) | 93.4 kN (21,000 lb) |
| Blade Passing Frequency (Fan) | 1760 Hz |
| Vane/Blade Ratio | 1.18 |

Table II. QCSEE OTW Acoustic Test Configurations.

| Configuration | Test Number | Inlet Type | Fan Wall Treatment | Acoustic Splitter | Core Treatment | Thrust |
|---|---|---|---|---|---|---|
| Baseline | 6 | Bellmouth | No | No | No | Forward |
| Fully Suppressed* | 11 | Hybrid | Yes | Yes | Yes | Reverse |
| Fully Suppressed | 12 | Hybrid | Yes | Yes | Yes | Forward |
| Accelerating Inlet | 13 | Hard Wall Accelerating | Yes | Yes | Yes | Forward |
| Partial Exhaust Suppression | 14 | Hybrid | Yes | No | No | Forward |

*With reingestion shield
105° blocker door angle
0.6 lip length
0° side doors

All configurations have frame treatment with treated vanes and compressor inlet wall treatment.

Table III. Test 6 - Baseline Data Points.

| Acoustic Reading | % $N/\sqrt{\theta}$ | Physical $N_F$ | Physical $N_C$ | Side Door Angle (Degrees) | $A_{18}$ in.² | $A_{18}$ m² | Type Data Taken[1] | Comments |
|---|---|---|---|---|---|---|---|---|
| 1 | 0 | 0 | 0 | 11.5 | 2666 | 1.72 | M, A, K | Background noise facility off |
| 2 | 0 | 0 | 0 | 11.5 | 2666 | 1.72 | M, A, K | Slave lube pump |
| 3 | 0 | 0 | 0 | 11.5 | 2666 | 1.72 | M, A, K | Digital control cooling air |
| 4 | 0 | 0 | 0 | 11.5 | 2666 | 1.72 | M, A, K | Undercowl cooling (500 counts) |
| 5 | 0 | 0 | 0 | 11.5 | 2666 | 1.72 | M, A, K | Undercowl cooling (1000 counts) |
| 6 | 0 | 0 | 0 | 11.5 | 2666 | 1.72 | M, A, K | Vortex destroyer fans |
| 7 | 0 | 0 | 0 | 11.5 | 2666 | 1.72 | M, A, K | All facility items |
| 8 | 44.5 | 1696 | 10880 | 11.5 | 2666 | 1.72 | M, A, K | |
| 9 | 75.6 | 2879 | 12360 | 11.5 | 2666 | 1.72 | M, A, K | |
| 10 | 81.4 | 3100 | 12677 | 11.5 | 2666 | 1.72 | M, A, K | Vortex destroyer fans on |
| 11 | 81.4 | 3099 | 12650 | 11.5 | 2666 | 1.72 | M, A, K | |
| 12 | 85.4 | 3252 | 12860 | 11.5 | 2666 | 1.72 | M, A, K | Vortex destroyer fans on |
| 13 | 85.4 | 3252 | 12860 | 11.5 | 2666 | 1.72 | M, A, K | |
| 14 | 93.4 | 3556 | 13259 | 11.5 | 2666 | 1.72 | M, A, K | Vortex destroyer fans on |
| 15 | 93.3 | 3551 | 13258 | 11.5 | 2666 | 1.72 | M, A, K | |
| 16 | 95.2 | 3622 | 13640 | 11.5 | 2666 | 1.72 | M, A, K | Vortex destroyer fans on |
| 17 | ---- | ---- | ----- | 11.5 | 2666 | 1.72 | M, A, K | No signal on tape |
| 18 | 45.0 | 1713 | 10929 | 25 | 2947 | 1.90 | M, A, K | |
| 19 | 75.4 | 2867 | 12580 | 25 | 2947 | 1.90 | M, A, K | |
| 20 | 81.4 | 3090 | 12580 | 25 | 2947 | 1.90 | M, A, K | |
| 21 | 93.3 | 3540 | 13130 | 25 | 2947 | 1.90 | M, A, K | |
| 22 | 95.3 | 3596 | 13279 | 25 | 2947 | 1.90 | M, A, K | |
| 23 | 98.5 | 3712 | 13460 | 25 | 2947 | 1.90 | M, A, K | |
| 24 | 81.5 | 3078 | 12595 | 25 | 2947 | 1.90 | M, A, K | |
| 25 | 95.4 | 3597 | 13425 | 0 | 2444 | 1.58 | M, A, K | |
| 26 | 97.1 | 3652 | 13313 | 11.5 | 2666 | 1.72 | DA | 120° from inlet |
| 27 | 97.1 | 3652 | 13313 | 11.5 | 2666 | 1.72 | DA | 110° from inlet |
| 28 | 97.1 | 3652 | 13313 | 11.5 | 2666 | 1.72 | DA | 100° from inlet |
| 29 | 97.1 | 3652 | 13313 | 11.5 | 2666 | 1.72 | DA | 80° from inlet |
| 30 | 97.1 | 3652 | 13313 | 11.5 | 2666 | 1.72 | DA | 60° from inlet |
| 31 | 80.7 | 3032 | 12470 | 25 | 2947 | 1.90 | DA | 60° from inlet |
| 32 | 80.7 | 3032 | 12470 | 25 | 2947 | 1.90 | DA | 80° from inlet |
| 33 | 80.7 | 3052 | 12470 | 25 | 2947 | 1.90 | DA | 100° from inlet |
| 34 | 80.7 | 3052 | 12470 | 25 | 2947 | 1.90 | DA | 110° from inlet |
| 35 | 80.7 | 3052 | 12470 | 25 | 2947 | 1.90 | DA | 120° from inlet |
| 63[2] | 81.4 | 3110 | 12750 | 25 | 2947 | 1.90 | P-FF, P-N | 3 immersions at position 1 for P-N and 6 immersions for P-T |
| 64 | 81.7 | 3126 | 12770 | 25 | 2947 | 1.90 | P-O | 15 immersions |
| 67 | 95.4 | 3646 | 13600 | 11.5 | 2666 | 1.72 | P-FF, P-N | 6 immersions for P-T, 3 immersions at Position 1 for P-N |
| 68 | 95.5 | 3656 | 13520 | 11.5 | 2666 | 1.72 | P-O | 15 immersions |
| 69 | 95.3 | 3656 | 13490 | 11.5 | 2666 | 1.72 | P-N | 3 immersions at Position 2 |
| 70 | 81.5 | 3131 | 12780 | 25 | 2947 | 1.90 | P-N | 3 immersions at Position 2 |
| 70 | 98.0 | ---- | ----- | 11.5 | 2666 | 1.72 | M, A, | 30 second of data |
| 71 | 81.0 | 3109 | 12700 | 2.5 | 2947 | 1.90 | P-N | 3 immersions at Position 3 |
| 72 | 94.4 | 3622 | 13580 | 11.5 | 2666 | 1.72 | P-N | 3 immersions at Position 3 |
| 73 | 94.4 | 3622 | 13580 | 11.5 | 2666 | 1.72 | P-N | 1 immersion at Position 4 |

[1] M    Far field microphones, near field microphones and ground plane microphones
A    Asymmetry microphones
K    Wall Kulites
DA    Directional array
P-T    Throat probe
P-FF    Fan Face probe
P-O    OGV probe
P-N    Core probe
    (See Figure 12 for Kulite and probe locations)

[2] Number sequence changed to agree with engine log system.

Table IV.  Test 11 – Fully Suppressed Reverse Thrust Data Points.

| Acoustic Reading(1) | % $N/\sqrt{\theta}$ | Physical | | $\dfrac{\% \, PNR_{Reverse}}{PNR_{FWD} \, T/O}$ | Type Data Taken(2) | Comments |
|---|---|---|---|---|---|---|
| | | $N_F$ | $N_C$ | | | |
| 117A | 0 | 0 | 0 | --- | M, K | Background noise – no facility on |
| 117B | 0 | 0 | 0 | --- | M, K | Undercowl cooling at 500 counts |
| 117C | 0 | 0 | 0 | --- | M, K | Undercowl cooling at 1000 counts |
| 118 | 40.7 | 1570 | 10991 | --- | M, K | High winds – data not reduced |
| 120 | 62.1 | 2394 | 12254 | --- | P-FF | 6 immersions |
| 121 | 62.1 | 2394 | 12254 | --- | P-OGV | 6 immersions |
| 124 | 78.5 | 3025 | 13117 | 33 | M, K | |
| 125 | 83.7 | 3226 | 13399 | 37 | M, K | |
| 126 | 78.5 | 3026 | 13119 | 33 | M, K | |
| 127 | 78.0 | 3005 | 13063 | 37 | DA | |
| 128 | 78.0 | 3005 | 13020 | --- | DA | High winds data not reduced |
| 129 | 78.0 | 3005 | 13044 | --- | DA | High winds data not reduced |
| 130 | 78.0 | 3005 | 13026 | --- | M, K | |
| 131 | 83.1 | 3200 | 13250 | 37 | M, K | 100° from inlet |
| 132 | 69.7 | 2682 | 12615 | 27 | M, K | 80° from inlet |
| 133 | 59.4 | 2286 | 12126 | 19 | M, K | 60° from inlet |
| 134 | 41.2 | 1590 | 10980 | 5 | M, K | |

(1) Engine log numbering system

(2) M   Microphones at engine centerline height plus ground plane microphones
    A   Asymmetry microphones
    K   Wall Kulites
    DA  Directional array
    P-T   Throat probe
    P-FF  Fan Face probe
    P-O   OGV probe
    P-N   Core probe
    (See Figure 12 for Kulite and probe locations)

# Table V. Test 12 - Fully Suppressed Forward Thrust Data Points.

| Acoustic Reading | % N/√θ | Physical | | XN11 | Side Door Angle (Degrees) | $A_{18}$ | | Type Data Taken[1] | Comments |
|---|---|---|---|---|---|---|---|---|---|
| | | $N_F$ | $N_C$ | | | in.² | m² | | |
| 1 | 0 | 0 | 0 | 0 | 11.5 | 2666 | 1.72 | N, A, K | Background noise facility off |
| 2 | 0 | 0 | 0 | 0 | 11.5 | 2666 | 1.72 | N, A, K | All facility on |
| 3 | 0 | 0 | 0 | 0 | 11.5 | 2666 | 1.72 | N, A, K | All facility on except undercowl cooling |
| 4 | 0 | 0 | 0 | 0 | 11.5 | 2666 | 1.72 | N, A, K | All facility on |
| 5 | 42.9 | 1656 | 10881 | 0.260 | 11.5 | 2666 | 1.72 | N, A, K | |
| 6 | 75.1 | 2872 | 12513 | --- | 11.5 | 2666 | 1.72 | N, A, K | |
| 7 | 80.0 | 3058 | 12729 | 0.536 | 11.5 | 2666 | 1.72 | N, A, K | |
| 8 | 85.8 | 3287 | 13070 | 0.599 | 11.5 | 2666 | 1.72 | N, A, K | |
| 9 | 94.9 | 3637 | 13495 | 0.720 | 11.5 | 2666 | 1.72 | N, A, K | |
| 10 | 96.3 | 3691 | 13614 | 0.759 | 11.5 | 2666 | 1.72 | N, A, K | |
| 11 | 96.3 | 3691 | 13603 | 0.760 | 11.5 | 2666 | 1.72 | N, A, K | |
| 12 | 42.1 | 1608 | 10878 | --- | 25 | 2947 | 1.90 | N, A, K | |
| 13 | 75.6 | 2896 | 12468 | 0.500 | 25 | 2947 | 1.90 | N, A, K | |
| 14 | 80.5 | 3118 | 12715 | 0.561 | 25 | 2947 | 1.90 | N, A, K | |
| 15 | 80.3 | 3108 | 12967 | 0.561 | 25 | 2947 | 1.90 | N, A, K | Core stators closed 5° from nominal |
| 16 | 80.2 | 3107 | 13400 | 0.561 | 25 | 2947 | 1.90 | N, A, K | Core stators closed 10° from nominal |
| 17 | 84.5 | 3270 | 12909 | 0.613 | 25 | 2947 | 1.90 | N, A, K | |
| 18 | 95.3 | 3689 | 13485 | 0.789 | 25 | 2947 | 1.90 | N, A, K | |
| 19 | 80.1 | 3100 | 12685 | 0.557 | 25 | 2947 | 1.90 | N, A, K | |
| 20 | 41.9 | 1603 | 10880 | --- | 0 | 2444 | 1.58 | N, A, K | |
| 21 | 75.1 | 2910 | 12583 | 0.455 | 0 | 2444 | 1.58 | N, A, K | |
| 22 | 78.2 | 3028 | 12783 | 0.482 | 0 | 2444 | 1.58 | N, A, K | |
| 23 | 84.9 | 3287 | 13146 | 0.552 | 0 | 2444 | 1.58 | N, A, K | |
| 24 | 79.3 | 3030 | 12765 | --- | 0 | 2444 | 1.58 | N, A, K | |
| 25 | 94.3 | 3651 | 13411 | 0.791 | 25 | 2947 | 1.90 | N, A, K | |
| 26 | 94.8 | 3672 | 13463 | 0.778 | 25 | 2947 | 1.90 | N, A, K | |
| 27 | 80.8 | 3084 | 12651 | --- | 25 | 2947 | 1.90 | P-T | 6 immersions |
| 28 | 82.2 | 3142 | 12746 | --- | 25 | 2947 | 1.90 | P-FF | 6 immersions |
| 29 | 82.2 | 3143 | 12736 | --- | 25 | 2947 | 1.90 | P-O | 15 immersions |
| 30 | 82.2 | 3144 | 12748 | --- | 25 | 2947 | 1.90 | P-N | 3 immersions at Position 1 |
| 31 | 41.7 | 1594 | 10863 | --- | 25 | 2947 | 1.90 | P-O | 6 immersions |
| 32 | 41.9 | 1603 | 10872 | --- | 25 | 2947 | 1.90 | P-N | 3 immersions at Position 1 |
| 33 | 94.7 | 3667 | 13582 | --- | 11.5 | 2666 | 1.72 | DA | 60° from inlet |
| 34 | 94.7 | 3667 | 13582 | --- | 11.5 | 2666 | 1.72 | DA | 80° from inlet |
| 35 | 94.7 | 3667 | 13582 | --- | 11.5 | 2666 | 1.72 | DA | 100° from inlet |
| 36 | 94.7 | 3667 | 13582 | --- | 11.5 | 2666 | 1.72 | DA | 110° from inlet |
| 37 | 94.7 | 3667 | 13582 | --- | 11.5 | 2666 | 1.72 | DA | 120° from inlet |
| 38 | 80.6 | 3122 | 12756 | --- | 25 | 2947 | 1.90 | DA | 120° from inlet |
| 39 | 80.6 | 3122 | 12756 | --- | 25 | 2947 | 1.90 | DA | 110° from inlet |
| 40 | 80.6 | 3122 | 12756 | --- | 25 | 2947 | 1.90 | DA | 120°, Repeat aiming points 1,2,3 |
| 41 | 80.6 | 3122 | 12756 | --- | 25 | 2947 | 1.90 | DA | 100° from inlet |
| 42 | 80.6 | 3122 | 12756 | --- | 25 | 2947 | 1.90 | DA | 80° from inlet |
| 43 | 80.6 | 3122 | 12756 | --- | 25 | 2947 | 1.90 | DA | 60° from inlet |
| 44 | 93.6 | 3633 | 13640 | --- | 11.5 | 2666 | 1.72 | P-T | 6 immersions |
| 45 | 93.6 | 3633 | 13640 | --- | 11.5 | 2666 | 1.72 | P-FF | 6 immersions |
| 46 | 93.7 | 3637 | 13620 | --- | 11.5 | 2666 | 1.72 | P-O | 15 immersions |

[1] N    Far field microphones, near field microphones and ground plane microphones
    A    Asymmetry microphones
    K    Wall Kulites
    DA    Directional array
    P-T    Throat probe
    P-FF    Fan Face probe
    P-O    OGV probe
    P-N    Core probe (see Figure 12)

9

Table VI. Test 13 - Hard Wall Accelerating Inlet Data Points.

| Acoustic Reading | % $N/\sqrt{\theta}$ | Physical $N_F$ | $N_C$ | XM11 | Side Door Angle (Degrees) | $A_{18}$ in.² | $A_{18}$ m² | Type Data Taken[1] | Comments |
|---|---|---|---|---|---|---|---|---|---|
| 1 | 0 | 0 | 0 | 0 | 11.5 | 2666 | 1.72 | M, A, K | Background noise - all facility off |
| 2 | 0 | 0 | 0 | 0 | 11.5 | 2666 | 1.72 | M, A, K | Full undercowl cooling air |
| 3 | 41.8 | 1625 | 10889 | 0.252 | 11.5 | 2666 | 1.72 | M, A, K | Reading no good |
| 4 | 41.8 | 1625 | 10889 | 0.252 | 11.5 | 2666 | 1.72 | M, A, K | |
| 5 | 75.3 | 2908 | 12513 | 0.487 | 11.5 | 2666 | 1.72 | M, A, K | |
| 6 | 80.3 | 3115 | 12785 | 0.540 | 11.5 | 2666 | 1.72 | M, A, K | |
| 7 | 85.3 | 3289 | 13005 | --- | 11.5 | 2666 | 1.72 | M, A, K | |
| 8 | 94.3 | 3640 | 13475 | 0.715 | 11.5 | 2666 | 1.72 | M, A, K | |
| 9 | 95.8 | 3696 | 13590 | 0.741 | 11.5 | 2666 | 1.72 | M, A, K | |
| 10 | 95.6 | 3689 | 13592 | 0.741 | 11.5 | 2666 | 1.72 | M, A, K | |
| 11 | 75.5 | 2911 | 12527 | 0.499 | 25 | 2947 | 1.90 | M, A, K | |
| 12 | 81.0 | 3145 | 12802 | --- | 25 | 2947 | 1.90 | M, A, K | |
| 13 | 85.5 | 3290 | 12990 | 0.611 | 25 | 2947 | 1.90 | M, A, K | |
| 14 | ---- | ---- | --- | --- | 25 | 2947 | 1.90 | M, A, K | No good |
| 15 | 96.3 | 3704 | 13533 | 0.779 | 25 | 2947 | 1.90 | M, A, K | |
| 16 | 81.6 | 3140 | 12750 | 0.563 | 25 | 2947 | 1.90 | M, A, K | |
| 17 | 42.1 | 1619 | 10876 | 0.253 | 25 | 2947 | 1.90 | M, A.,K | |
| 18 | 80.8 | 3100 | 12755 | --- | 25 | 2947 | 1.90 | DA | 60° from inlet |
| 19 | 80.8 | 3100 | 12755 | --- | 25 | 2947 | 1.90 | DA | 80° from inlet |
| 20 | 80.8 | 3100 | 12755 | --- | 25 | 2947 | 1.90 | DA | 100° from inlet |
| 21 | 95.6 | 3665 | 13533 | --- | 11.5 | 2666 | 1.72 | DA | 100° from inlet |
| 22 | 95.6 | 3665 | 13533 | --- | 11.5 | 2666 | 1.72 | DA | 80° from inlet |
| 23 | 95.6 | 3665 | 13533 | --- | 11.5 | 2666 | 1.72 | DA | 60° from inlet |
| 24 | 95.6 | 3662 | 13513 | --- | 11.5 | 2666 | 1.72 | P-T | 6 immersions |
| 25 | 95.6 | 3662 | 13513 | --- | 11.5 | 2666 | 1.72 | P-FF | 6 immersions |
| 26 | 95.6 | 3662 | 13513 | --- | 11.5 | 2666 | 1.72 | P-N | 3 immersions at Position 4 |
| 27 | 90.6 | 3471 | 13183 | 0.663 | 11.5 | 2666 | 1.72 | M, A, K | |
| 28 | 80.9 | 3100 | 12728 | --- | 25 | 2946 | 1.90 | P-T | 6 immersions |
| 29 | 80.9 | 3100 | 12728 | --- | 25 | 2946 | 1.90 | P-FF | 6 immersions |
| 30 | 80.9 | 3100 | 12728 | --- | 25 | 2946 | 1.90 | P-N | 3 immersions at Position 4 |
| 31 | 40.9 | 1568 | 10875 | --- | 25 | 2946 | 1.90 | P-N | 3 immersions at Position 4 |
| 32 | 46.3 | 1775 | 11220 | --- | 25 | 2946 | 1.90 | P-N | 3 immersions at Position 3 |
| 33 | 80.0 | 3064 | 12800 | --- | 25 | 29446 | 1.90 | P-N | 3 immersions at Position 3 |
| 34 | 95.1 | 3638 | 13506 | --- | 11.5 | 2667 | 1.72 | P-N | 3 immersions at Position 3 |
| 35 | 94.6 | 3619 | 13368 | --- | 11.5 | 2667 | 1.72 | P-N | 3 immersions at Position 1 |
| 36 | 41.0 | 1570 | 10870 | --- | 25 | 2946 | 1.90 | P-N | 3 immersions at Position 1 |
| 37 | 80.0 | 3076 | 12682 | --- | 25 | 2946 | 1.90 | P-N | 3 immersions at Position 1 |
| 38 | 41.9 | 1602 | 10880 | --- | 25 | 2946 | 1.90 | P-N | 3 immersions at Position 2 |
| 39 | 80.6 | 3082 | 12694 | --- | 25 | 2946 | 1.90 | P-N | 3 immersions at Position 2 |
| 40 | 95.1 | 3637 | 13453 | --- | 11.5 | ---- | ---- | P-N | 3 immersions at Position 2 |

[1]
| | |
|---|---|
| M | Far field microphones, near field microphones and ground plane microphones |
| A | Asymmetry microphones |
| K | Wall Kulites |
| DA | Directional array |
| P-T | Throat probe |
| P-FF | Fan Face probe |
| P-0 | OGV probe |
| P-N | Core probe |
| | (See Figure 12 for Kulite and probe locations) |

10

Table VII.   Test 14 - Partial Exhaust Suppression Data Points.

| Acoustic Reading | $\frac{X}{N\sqrt{\theta}}$ | Physical $N_F$ | $N_C$ | XM11 | Side Door Angle (Degrees) | $A_{18}$ in.$^2$ | m$^2$ | Type Data Taken[1] | Comments |
|---|---|---|---|---|---|---|---|---|---|
| 1 | 0 | 0 | 0 | 0 | 11.5 | 2666 | 1.72 | M, A, K | Background noise - slave lube pump on |
| 2 | 0 | 0 | 0 | 0 | 11.5 | 2666 | 1.72 | M, A, K | Undercowl cooling full on |
| 3 | 42.1 | 1620 | 10880 | 0.249 | 11.5 | 2666 | 1.72 | M, A, K | |
| 4 | 85.8 | 3297 | 13064 | 0.611 | 11.5 | 2666 | 1.72 | M, A, K | |
| 5 | 93.9 | 3611 | 13527 | 0.729 | 11.5 | 2666 | 1.72 | M, A, K | |
| 6 | 94.5 | 3631 | 13490 | 0.738 | 11.5 | 2666 | 1.72 | M, A, K | |
| 7 | 90.7 | 3485 | 13328 | 0.678 | 11.5 | 2666 | 1.72 | M, A, K | |
| 8 | 94.6 | 3636 | 13515 | 0.734 | 11.5 | 2666 | 1.72 | M, A, K | |
| 9 | 92.9 | 3567 | 13509 | 0.710 | 11.5 | 2666 | 1.72 | P-O | 6 immersions |
| 10 | 93.3 | 3582 | 13509 | --- | 11.5 | 2666 | 1.72 | P-N | 3 immersions at Position 2 |
| 12 | 41.3 | 1584 | 10883 | --- | 25 | 2947 | 1.90 | P-N | 3 immersions at Position 2 |
| 13 | 41.3 | 1584 | 10883 | --- | 25 | 2947 | 1.90 | M, A, K | |
| 14 | 75.8 | 2905 | 12407 | 0.501 | 25 | 2947 | 1.90 | M, A, K | |
| 15 | 81.9 | 3138 | 12726 | 0 564 | 25 | 2947 | 1.90 | M, A, K | |
| 16 | 84.9 | ---- | --- | --- | 25 | 2947 | 1.90 | M, A, K | |
| 17 | 82.1 | 3148 | 12758 | 0.567 | 25 | 2947 | 1.90 | M, A, K | |
| 18 | 81.6 | ---- | --- | --- | 25 | 2947 | 1.90 | P-N | 3 immersions at Position 2 |
| 19 | 81.5 | ---- | --- | --- | 25 | 2947 | 1.90 | P-O | 6 immersions |
| 20 | 41.5 | ---- | --- | --- | 25 | 2947 | 1.90 | P-O | 6 immersions |
| 21 | 80.9 | ---- | --- | --- | 25 | 2947 | 1.90 | DA | 100° from inlet |
| 22 | 80.9 | ---- | --- | --- | 25 | 2947 | 1.90 | DA | 110° from inlet |
| 23 | 80.9 | ---- | --- | --- | 25 | 2947 | 1.90 | DA | 120° from inlet |
| 24 | 80.9 | ---- | --- | --- | 25 | 2947 | 1.90 | P-N | 3 immersions at Position 1 |
| 25 | 42.0 | ---- | --- | --- | 25 | 2947 | 1.90 | P-N | 3 immersions at Position 1 |
| 26 | 94.0 | ---- | --- | --- | 11.5 | 2666 | 1.72 | DA | 120° from inlet |
| 27 | 94.0 | ---- | --- | --- | 11.5 | 2666 | 1.72 | DA | 110° from inlet |
| 28 | 94.0 | ---- | --- | --- | 11.5 | 2666 | 1.72 | DA | 100° from inlet |
| 29 | 92.3 | ---- | --- | --- | 11.5 | 2666 | 1.72 | P-N | |
| 199[2] | 95.7 | ---- | --- | --- | 25 | 2947 | 1.90 | P-FF | 6 immersions |
| 200 | 95.7 | ---- | --- | --- | 25 | 2947 | 1.90 | P-T | 6 immersions |

[1] M Far field microphones, near field microphones and ground microphones
A Asymmetry microphones
K Wall Kulites
DA Directional array
P-T Throat probe
P-FF Fan Face probe
P-O OGV probe
P-N Core probe
 (See Figure 12 for Kulite and probe locations)

[2] Number sequence changed to agree with engine log system

Aero Acoustic Lip

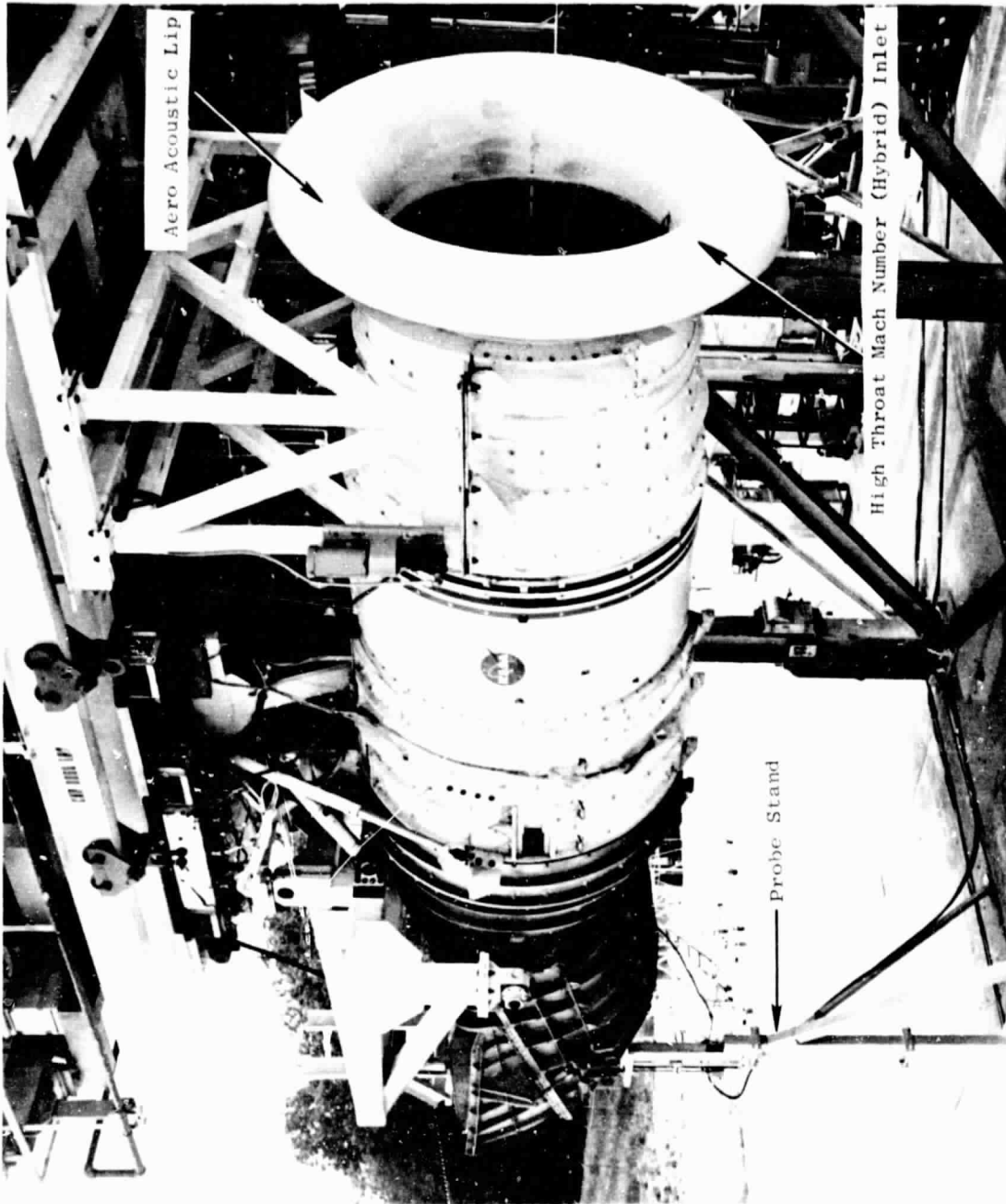High Throat Mach Number (Hybrid) Inlet

Probe Stand

Figure 2.  Fully Suppressed Engine.

12
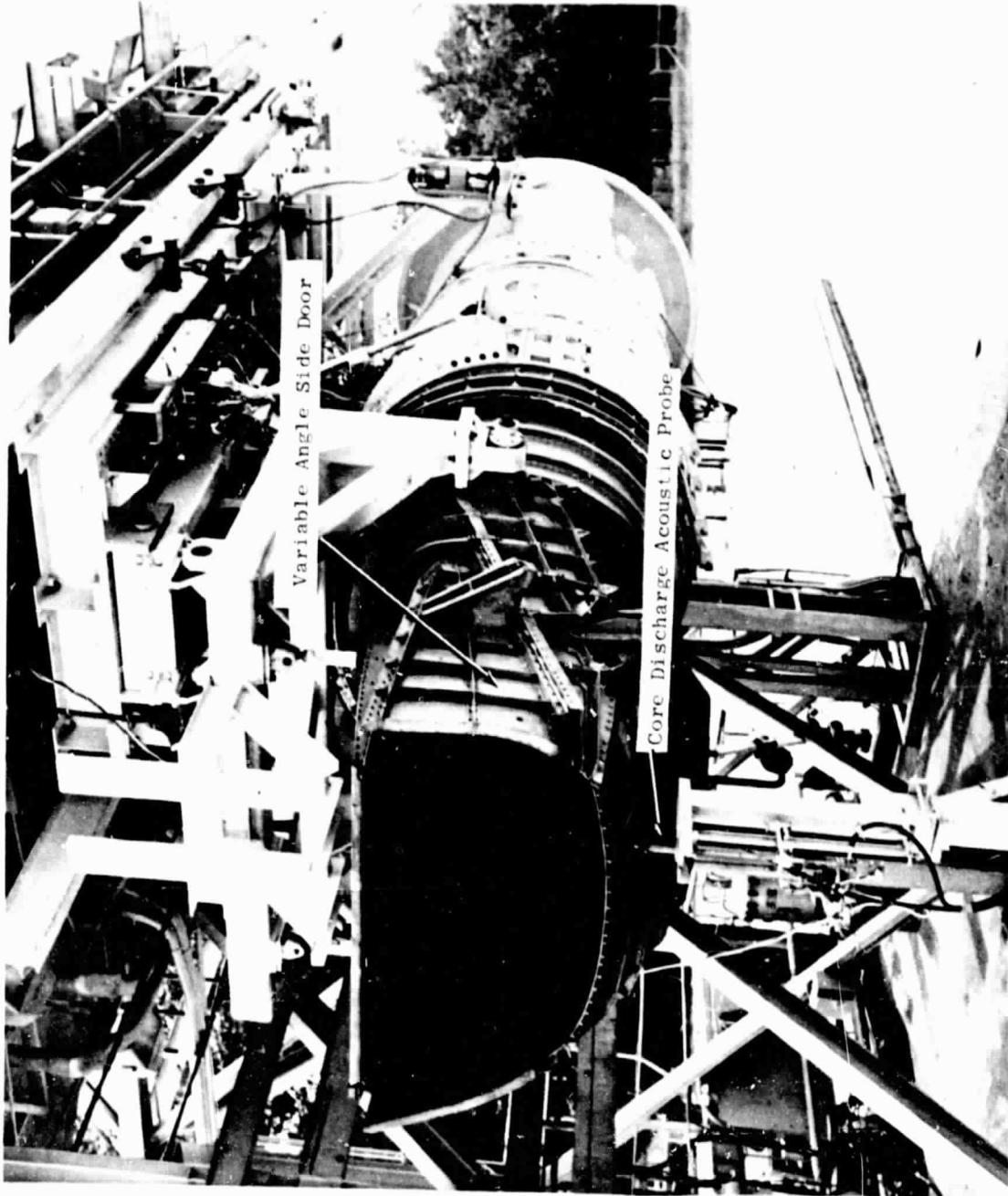
Figure 3. Exhaust "D" Nozzle.

Variable Angle Side Door

Core Discharge Acoustic Probe

13

- Test 6
- Baseline Bellmouth (Hard Wall)
- Frame and Vane Treatment
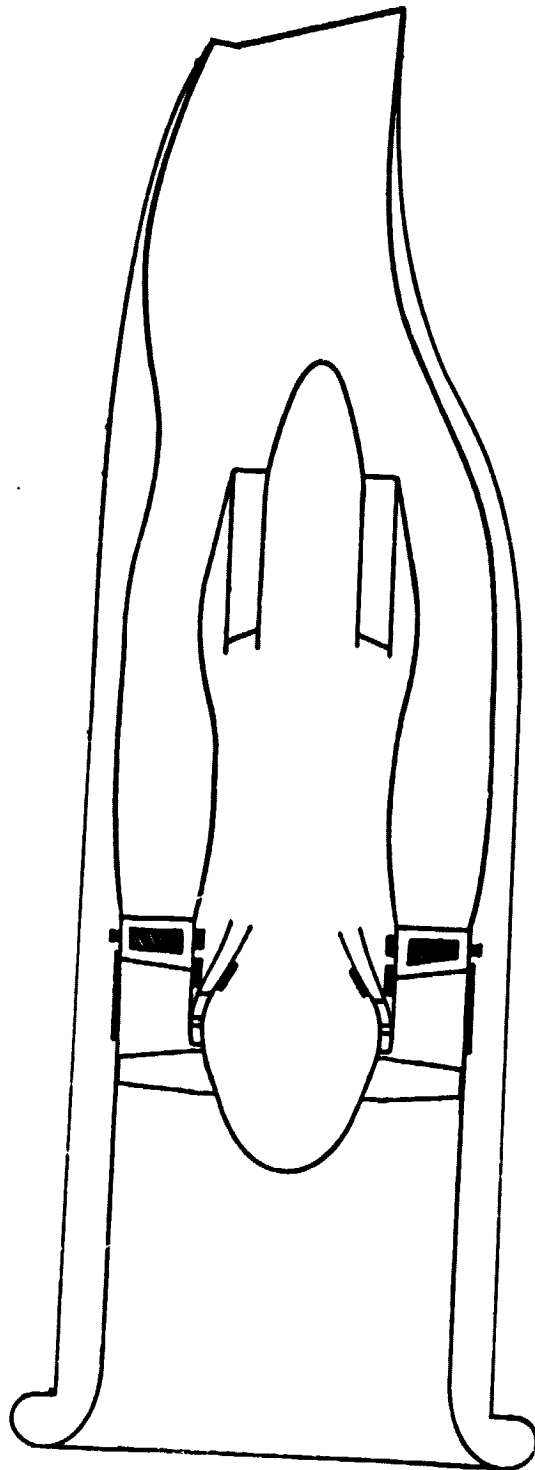- Hard Wall Fan Exhaust
- Hard Wall Core

Figure 4.  Baseline Engine Schematic.

14

- Test 12
- Hybrid Inlet
- Frame and Vane Treatment
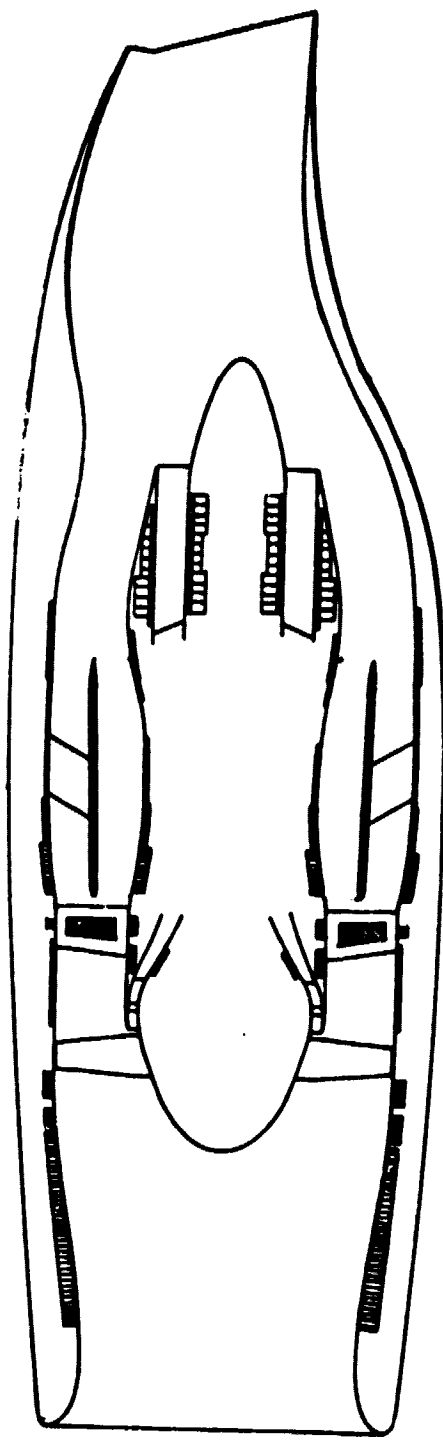- Fan Exhaust Treatment with Splitter
- Core Treatment

Figure 5. Fully Suppressed Engine Schematic.

- Test 13
- Hard Wall Accelerating Inlet
- Frame and Vane Treatment
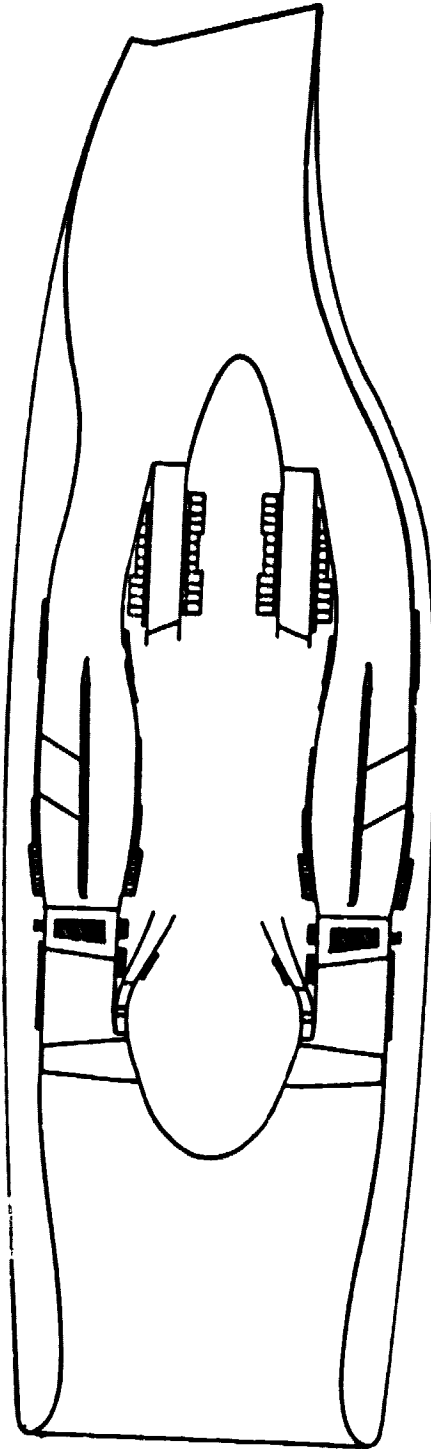- Fan Exhaust Treatment with Splitter
- Core Treatment

Figure 6.   Hard Wall Accelerating Inlet Schematic.

16

of the acceleration effect and treatment on inlet radiated noise. Exhaust radiated noise remain fully treated.

The final forward thrust configuration was designed to determine effect of reduced exhaust suppression on system noise. For example, an aircraft which was powered by OTW engines and which was designed to operate out of longer runways than the QCSEE design criteria would require less suppression to meet the noise goals (see Reference 1). Reduced suppression was achieved by removing the splitter and the stacked core treatment as shown schematically in Figure 7.

## 3.2 REVERSE THRUST

For reverse thrust operation of this engine, the roof of the "D" nozzle was positioned to form a target thrust reverser. The exhaust nozzle was run in the inverted position so that the exhaust gases would be directed downward rather than into the test facility and instrumentation lines. To prevent hot gas reingestion, a reingestion shield 3.66m (12 ft) in diameter and 9.14m (30 ft) long was mounted ahead of the inlet as shown in Figure 8. The engine was fully suppressed for this test and had the blocker door positioned at 105° with a 0.6 lip length. The variable-position side doors were at 0 degrees or closed during reverse thrust operation.

- Test 14
- Hybrid Inlet
- Frame and Vane Treatment
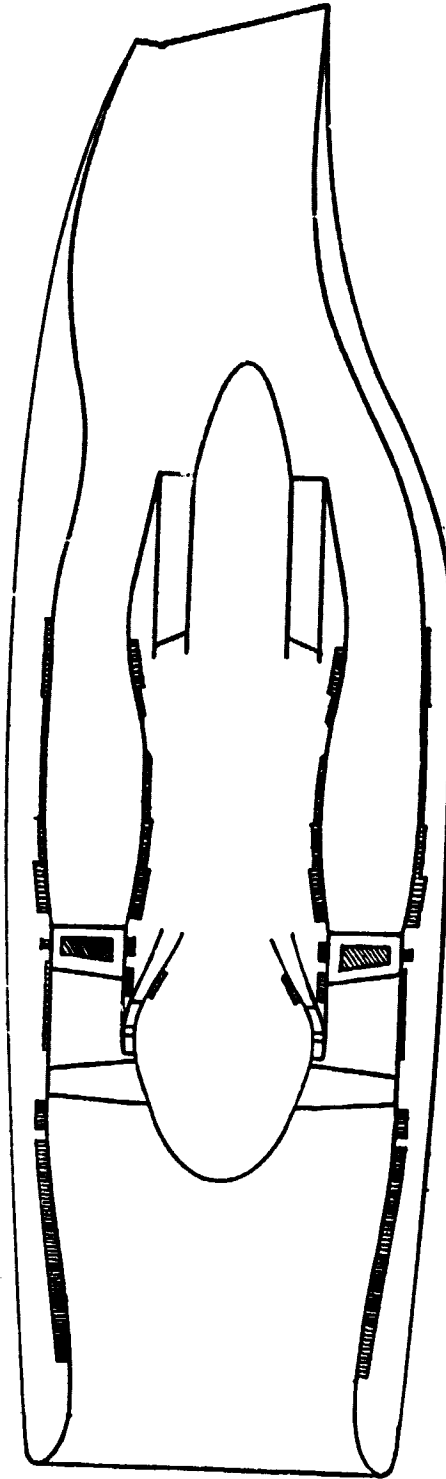- Fan Exhaust Wall Treatment without Splitter
- Hard Wall Core

Figure 7. Partially Suppressed (Hard Core/No Splitter) Schematic.
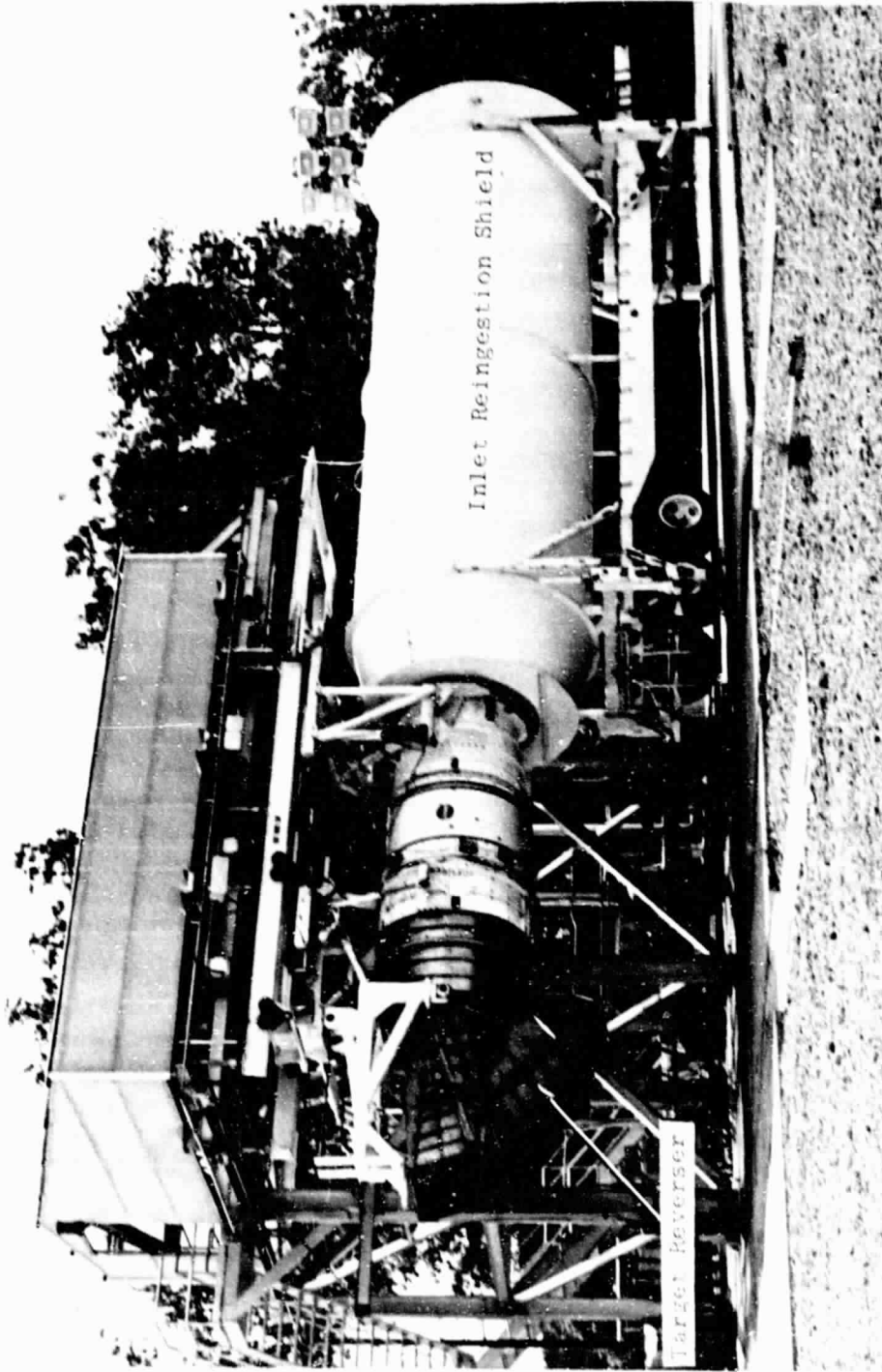
18

Figure 8. Fully Suppressed Reverse Thrust Configuration.

19

# 4.0 ACOUSTIC INSTRUMENTATION

## 4.1 DATA ACQUISITION

Acoustic data were acquired on this engine using a variety of instrumentation including the usual far field microphones, near field microphones, ground plane microphones, a directional acoustic array, in-duct wall kulites, and in-duct sound separation probes.

### 4.1.1 Sound Field Microphones

The test arena, shown on Figure 9, consists of a leveled semicircle of approximately 76 meters (250 ft) radius with a crushed rock surface composed of rock sizes of approximately 2.5 - 7.5 cm (1 in. - 3 in.) diameter. The standard far field microphones setup for forward thrust tests consisted of microphones located at acoustic angles of 10° through 160° at 10° increments, on permanently fixed towers located on a 45.7 meter (150 ft) arc centered near the fan rotor plane. Standard microphone height was 12.2 meters (40 ft) above ground level, or 8.2 meters (27 ft) above engine centerline height of 4.0 meters (13.0 ft), with a distance from the arc center to microphone location of 46.5 meters (152.4 ft). The 12.2 meter (40 ft) microphone height was chosen in the early 1970's to simulate the ground reflection effects experienced during flyover testing with a 1.22 meter (4 ft) microphone height. For reverse thrust testing the microphones were mounted on the towers at engine centerline height of 4.0 m (13.0 ft) at angles of 30° through 150°.

Ground plane microphones were located at acoustic angles of 60°, 90°, and 120° for all tests to allow determination of ground reflection corrections at these selected angles.

Additional far field microphones were utilized during forward thrust testing to monitor "D" nozzle asymmetry effects. Three microphones were located on the 90°, 120°, and 150° poles at engine centerline height. A fourth was located on the 150° pole at a height of 7.8 m (25.6 ft). Figure 10 shows the location of these microphones.

Five near field microphones were located on a 3 m (10 ft) sideline. These microphones are shown schematically in Figures 9 and 10 and were used to aid in evaluation of engine source noise characteristics by correlation with the far field microphones.

A directional acoustic broadside array (Reference 5) was used in the sound field to separate sources of noise at select angles. The array was positioned on a 30 m (100 ft) arc at 60°, 80°, 100°, and 120° acoustic angles and aimed at seven points on the engine. Postrun analysis then was performed to determine the relative contribution from each aiming point on the engine at each acoustic angle.
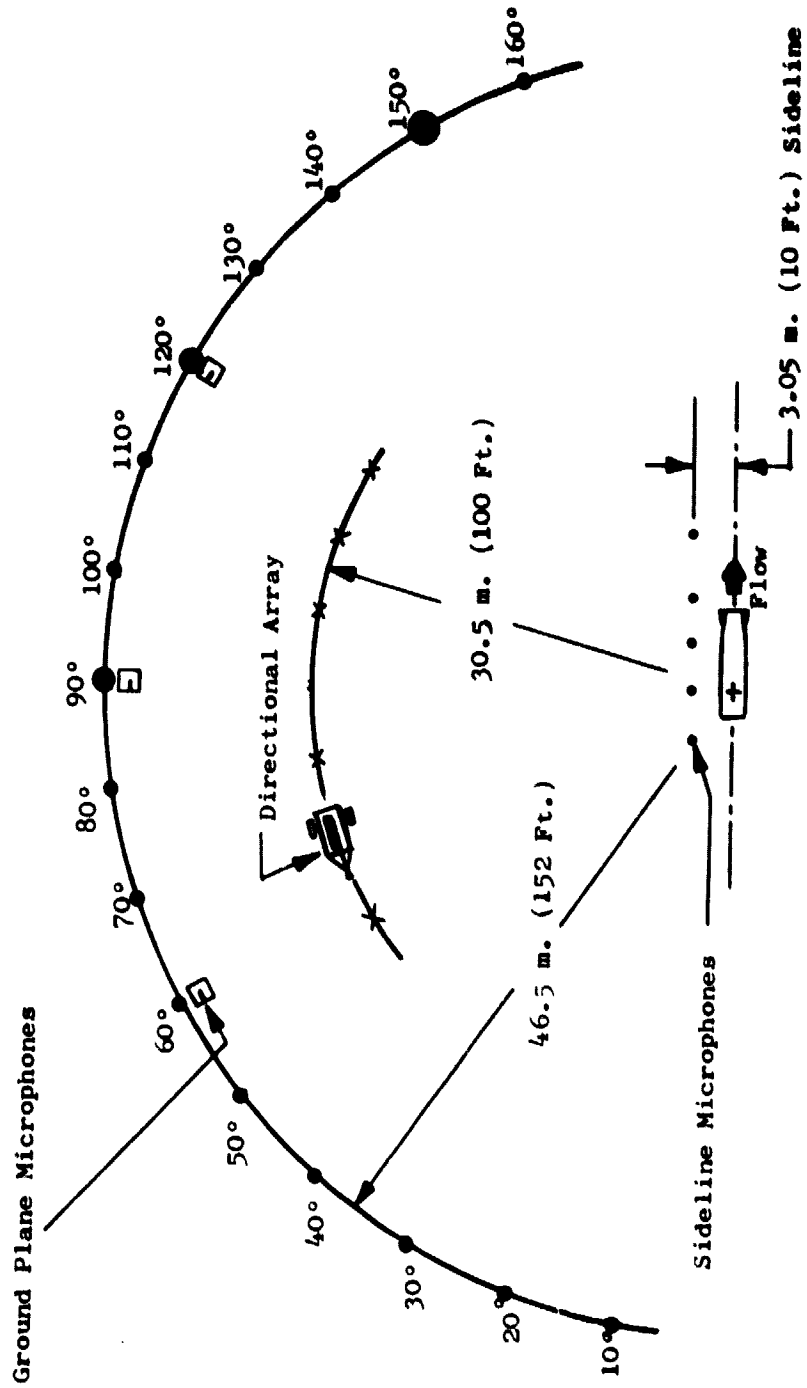
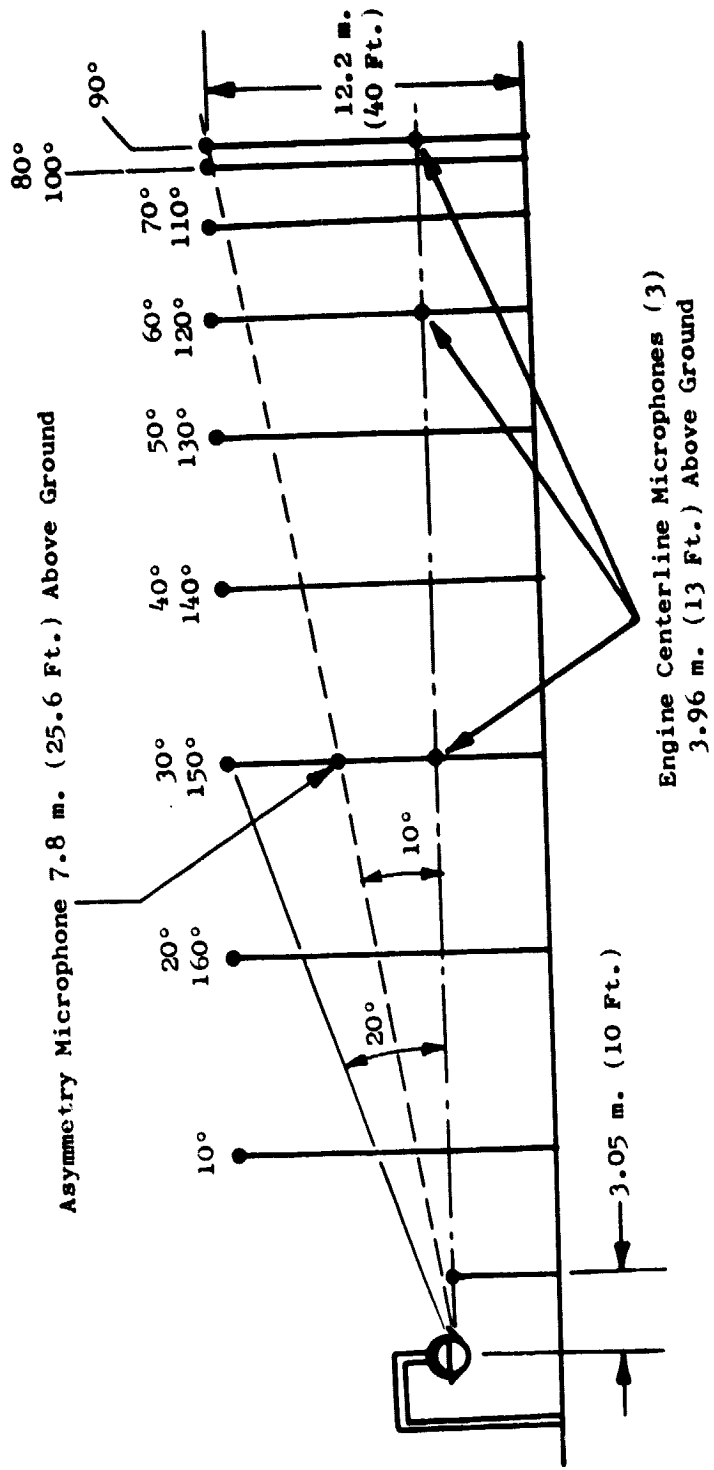Figure 9. Sound Field Acoustic Instrumentation - Top View.

21

Figure 10. Sound Field Acoustic Instrumentation - Aft Looking Forward.

22

A schematic of the far field acoustic data acquisition system used is shown on Figure 11. The system is used for obtaining data from 50 Hz through the 20 kHz 1/3-octave center frequency band.

The microphone types utilized for far field data acquisition are the Bruel and Kjaer (B&K) 4133 and B&K 4134 1.27 cm (1/2 inch) condenser microphones with the 4134 microphones utilized for the ground plane measurements. For near field measurements, B&K 4136 0.64 cm (1/4 inch) microphones, with grid cap installation, were used. Microphone orientation for the 4133's was 0° incidence and 90° incidence for the 4134's and 4136's.

All microphone systems utilized the B&K 2615 cathode follower and B&K 2801 power supply with the 50 ohm output option to provide a flat response through the 20 kHz region of interest.

All data were recorded using two Sangamo Sabre IV FM tape systems operated at a tape speed of 76 cm/sec (30 ips).

The overall frequency response of the acquisition and reduction system was determined for each channel by recording a pink noise signal through the cathode follower with playback and processing through the data reduction system. These corrections were then included in the data processing to account for flatness deviations in system response.

### 4.1.2  In-Duct Kulites

Internal acoustic instrumentation for these tests consisted of Kulites flush-mounted on the flowpath walls and probe-mounted Kulites which could be immersed into the flow. All in-duct instrumentation are shown in Figure 12. A schematic of the Kulite data acquisition system is given in Figure 13.

The probes used in the fan duct had either two or three flush-mounted Kulite sensors on them. The probe used in the "D" nozzle surveys had two elements and was water-cooled to permit immersion in the hot exhaust. These multiple-element probes, as reported previously in Reference 6, are known as sound separation probes and permit discrimination between broadband sound from turbulence in duct probe measurements. All probes were traversible radially to provide data across the duct.

### 4.2  REDUCTION

Off-line reduction of the recorded data was performed using an automated 1/3-octave reduction system, shown schematically on Figure 14. The recorded data were played back on a CEC 3700B, 28-track system.

All 1/3-octave analyses were performed using a General Radio 1921 1/3-octave analyzer. A normal integration time of 32 seconds was used to provide adequate sampling of the low frequency portion of the data signal. The data frequency range for the QCSEE OTW test series was 50 Hz through 20 kHz.
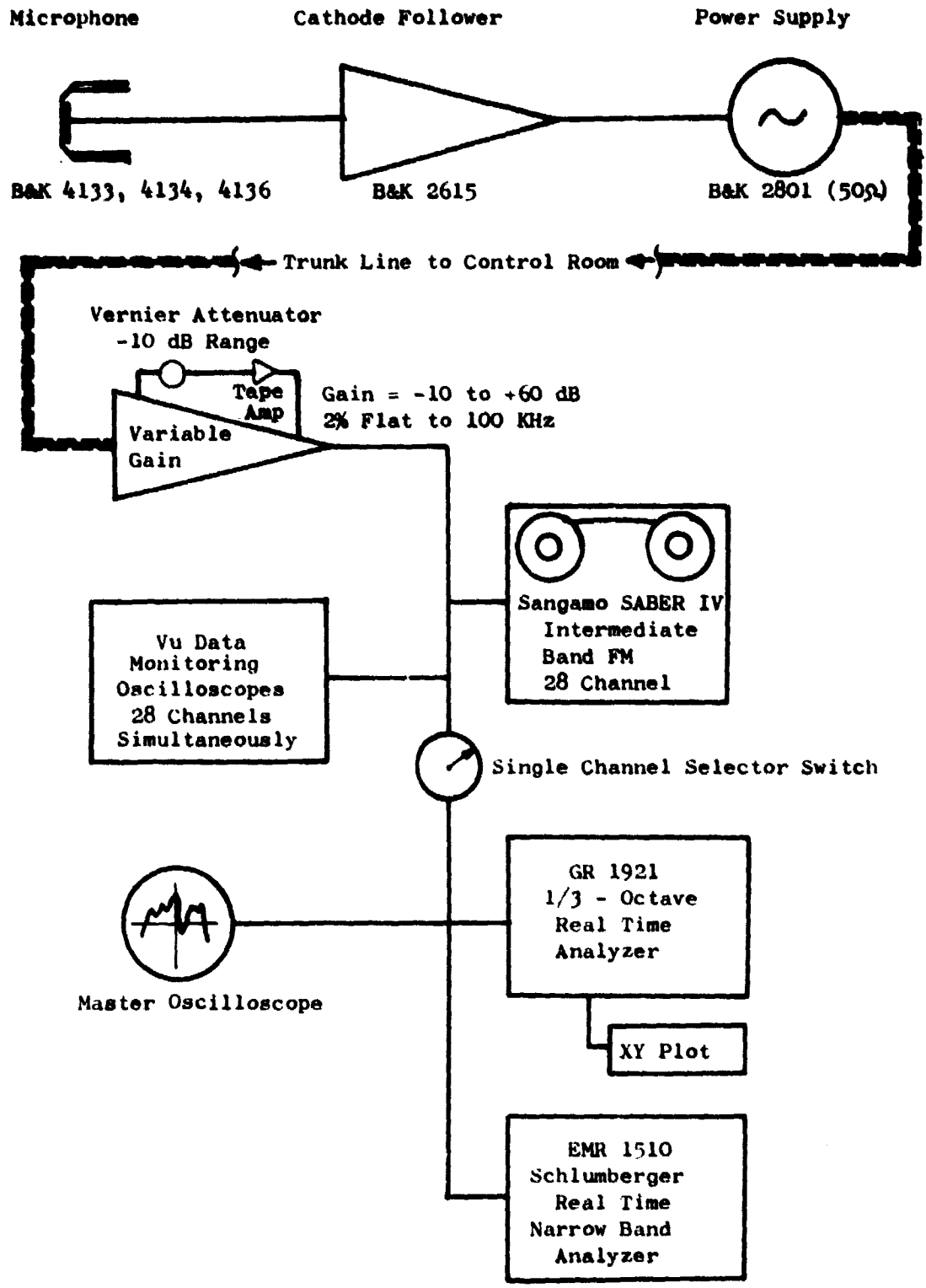
23

Microphone                Cathode Follower              Power Supply

B&K 4133, 4134, 4136          B&K 2615               B&K 2801 (50Ω)

Trunk Line to Control Room

Vernier Attenuator
-10 dB Range

Tape Amp

Variable Gain

Gain = -10 to +60 dB
2% Flat to 100 KHz

Sangamo SABER IV
Intermediate
Band FM
28 Channel

Vu Data
Monitoring
Oscilloscopes
28 Channels
Simultaneously

Single Channel Selector Switch

GR 1921
1/3 - Octave
Real Time
Analyzer

Master Oscilloscope

XY Plot

EMR 1510
Schlumberger
Real Time
Narrow Band
Analyzer

Figure 11.  Acoustic Microphone Data Acquisition System.

24

Exhaust Nozzle Probe
Immersion Survey Planes

Position 1

Position 2

Position 3

Position 4

10.2 cm (4 in.)

50.8 cm (20 in.)

Station 376.8

Station 378.8

X Probe Kulites

● Wall Kulites

Station 204.5

Station 204.5

Station 157.0

Station 157.0

Station 109.8

Suppressed Configurations

Baseline Configuration
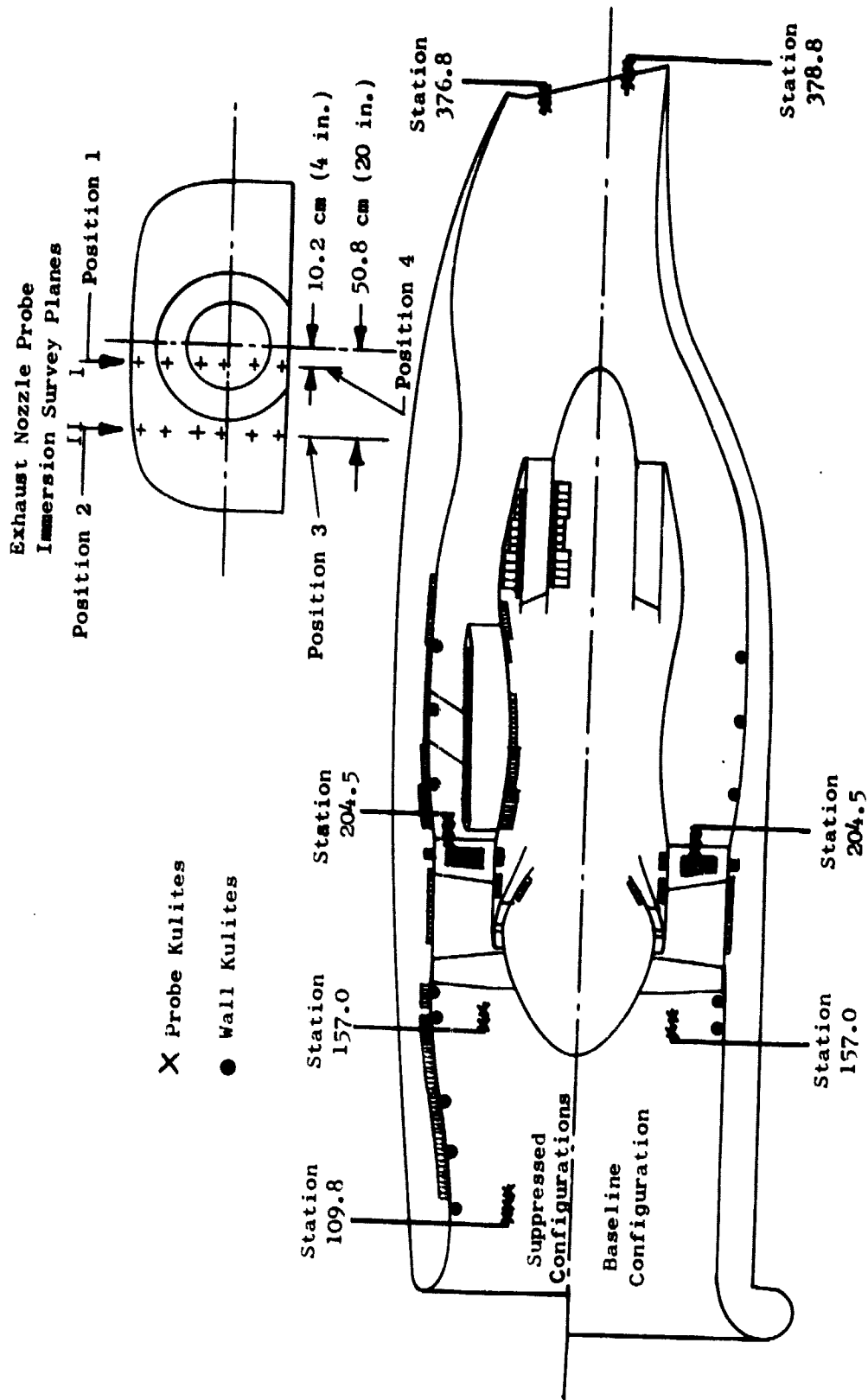
Figure 12. In-Duct Acoustic Instrumentation.

25
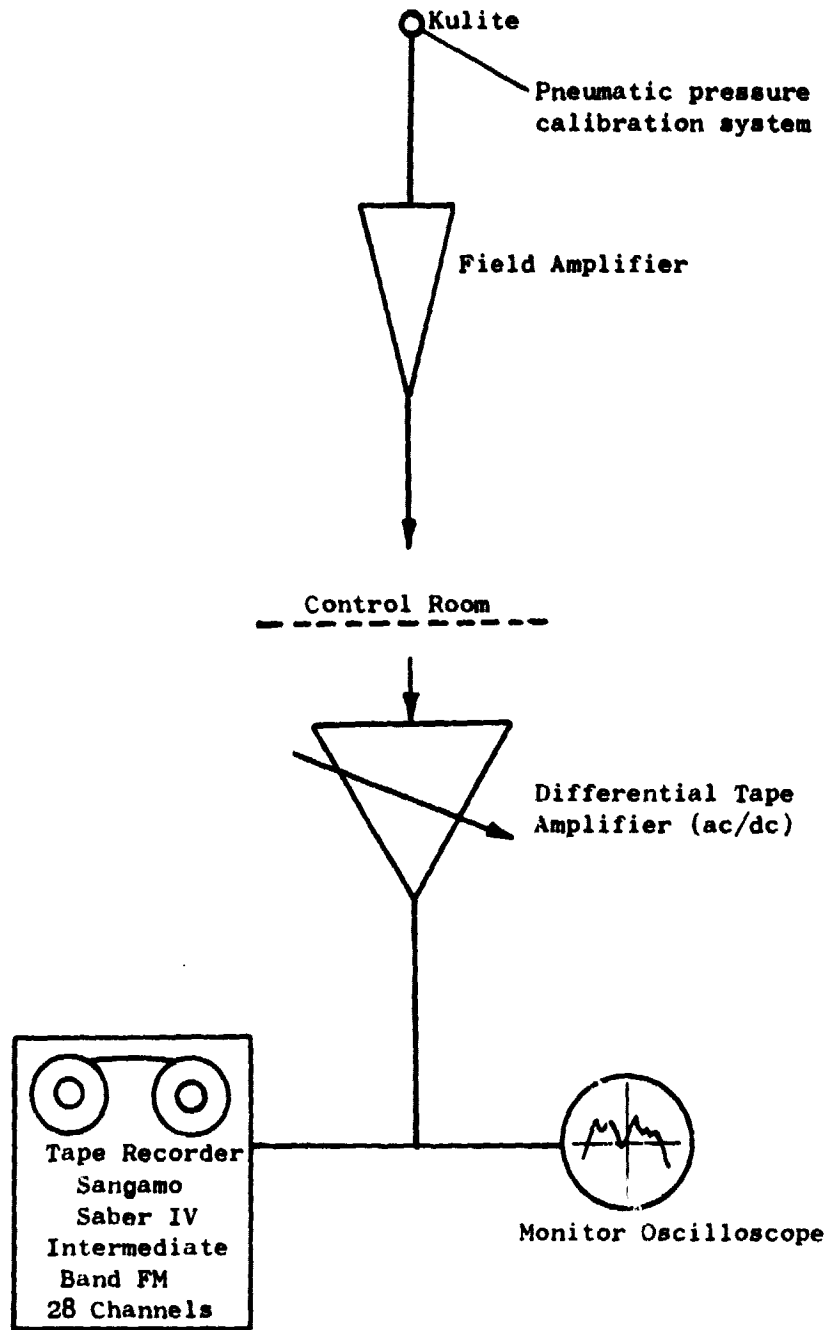
Figure 13. Kulite Data Acquisition.

- Time Code Comparator Starts Integration on G.R. Analyzer
- Tape Automatically Shuttles to Restart on Each Recording Channel
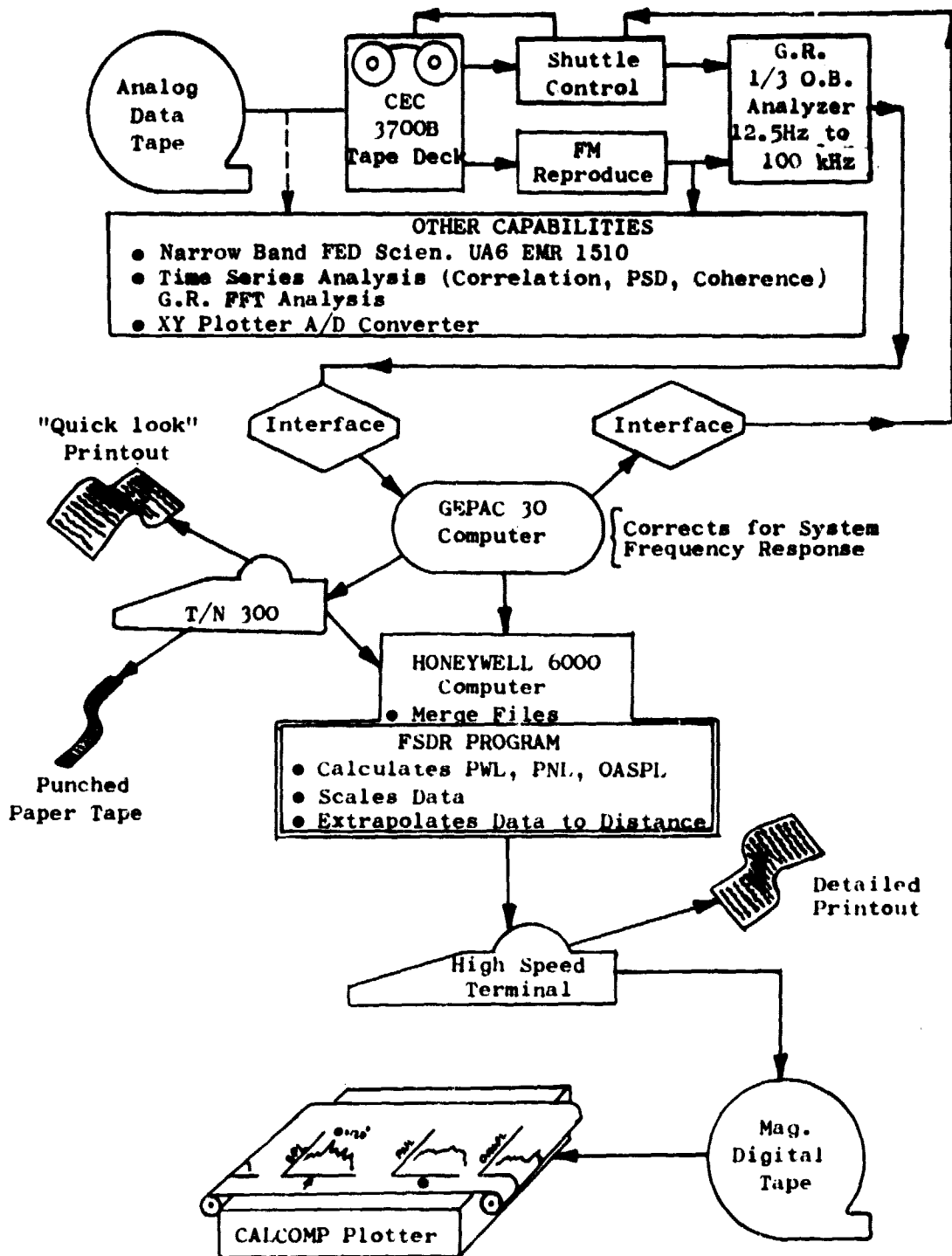


Figure 14. General Electric Acoustic Data Reduction System.

27

Each data channel is passed through an interface to the GEPAC 30 computer, where data are corrected for frequency response of the acquisition and reduction system and for microphone-head response. A "quick-look" display of results is provided by means of a Terminet 300 console with data transferred and stored in the Honeywell 6000 system via a direct time sharing link. An alternate to this method provides these data on punched paper tape for subsequent input to the 6000 system, allowing 1/3-octave processing during periods when the 6000 system is inaccessible. Processing in the 6000 system is performed via the Full-Scale Data Reduction (FSDR) program, where calculations are performed correcting data for atmospheric attenuation in accordance with Reference 7 and extra ground attenuation as prescribed in Appendix of Reference 1 with all data output corrected to 298 K (77° F)/70% relative humidity standard day. Additional calculations, including data scaling, extrapolations, perceived noise level (PNL), overall sound pressure level (OASPL), and sound power level (PWL) also are performed. As an option, the output of FSDR is written to digital magnetic tape for subsequent processing or data plotting via Calcomp plotter routines.

Other data reduction techniques also are available. Constant bandwidth narow band spectra were reduced on the Federal Scientific UA6. Complex time series analysis such as cross correlation, cross power spectral density (PSD), coherence functions and probability density can be processed through the General Padio/Time Data System, a computer-based system incorporating analysis techniques in both the time and frequency domains.

## 5.0 FORWARD THRUST ACOUSTIC RESULTS

The bulk of the testing on the OTW engine was devoted to measuring and understanding forward thrust noise levels. Approximately 160 data points were taken on the four forward thrust configurations. Inlet radiated and exhaust radiated noise will be considered first. Then engine noise levels and their relationship to the QCSEE noise goals will be discussed.

Analysis of the data in the inlet- and exhaust-radiated components means that the measured jet noise levels must be removed in some instances to see a true component effect. The reader is referred to Appendix A of this volume where the removal of jet noise is discussed in some detail. It will be noted in the text where jet noise has been removed.

## 5.1 INLET-RADIATED NOISE LEVELS

Analysis of the inlet-radiated noise is divided into two main categories - source noise levels and the suppression achieved.

### 5.1.1 Baseline Source Noise Levels

The baseline inlet configuration for the OTW engine utilized a hard wall bellmouth. The 28-bladed, fixed-pitch fan had a vane blade ratio of 1.18 and a rotor-stator spacing of 1.93 true rotor tip chords. Its design tip speed was 350 m/sec (1150 ft/sec). There were fan frame treatment and treated vanes installed on this configuration.

#### 5.1.1.1 Source Noise Characteristics

As part of the engine design procedure, prior to testing the OTW engines, estimates (Reference 2) were made of the noise levels for all the engine constituents, not just inlet radiated noise. These estimates utilized model test data and empirical correlations from previous engine tests. Figures 15 and 16 compare the actual measured levels of 60° to predicted total levels at takeoff and approach conditions. Predicted constituents are shown for reference. At takeoff, the measured engine data at 60° indicates the presence of multiple pure tones (MPT's) in the spectra at 1000 Hz. In the lower frequencies, the measured engine data differs from the predicted spectra because of ground reflection nulls and reinforcements. The pre-dicted spectra levels are free field. With these exceptions there is very good agreement between measured and predicted engine data at 60°.

Inlet-radiated MPT's at takeoff are clearly evident in the 30°, 60°, and 80° narrow band spectra, as shown in Figure 17.

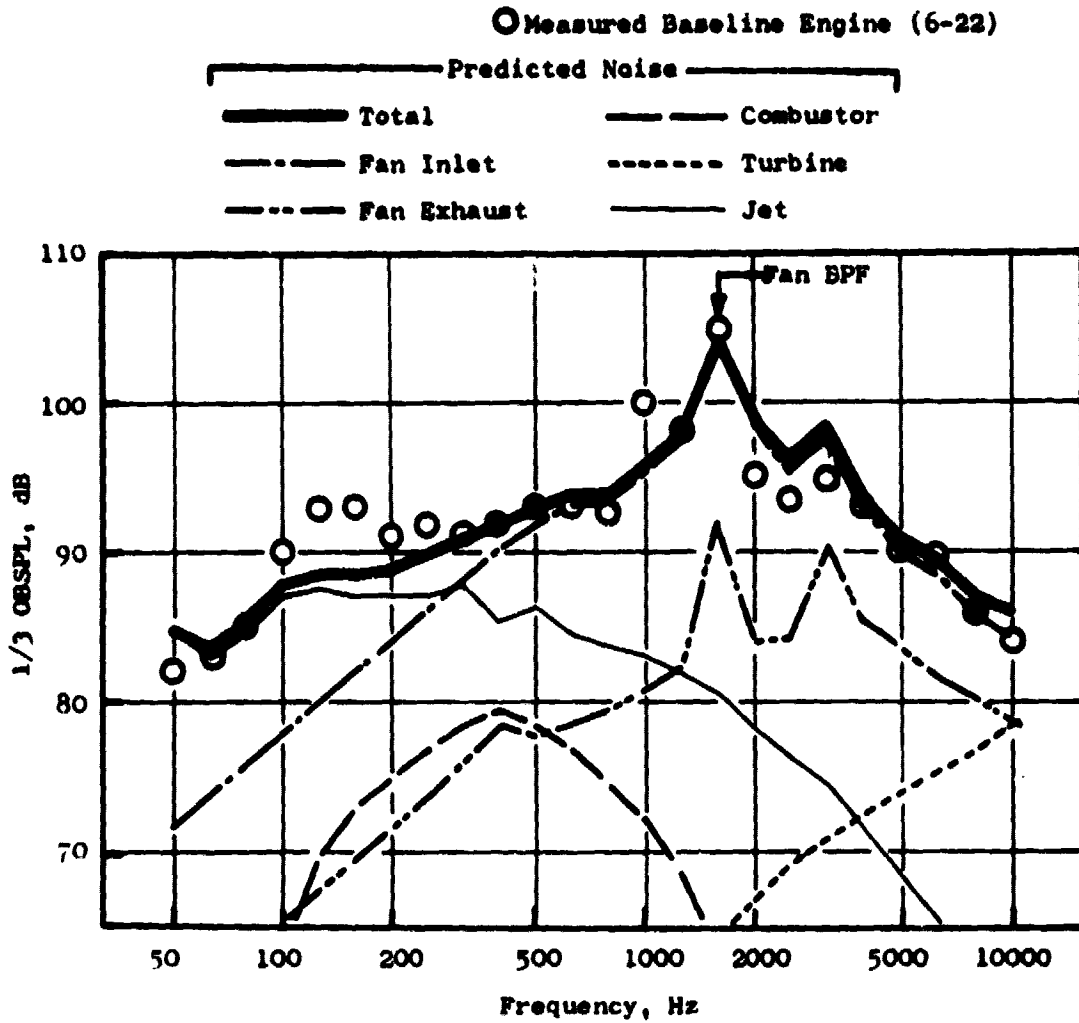- Takeoff Power
- 60° Acoustic Angle
- 46.5 m. (152 Ft.) Arc

○ Measured Baseline Engine (6-22)

Predicted Noise

| | |
|---|---|
| ▬▬ Total | ▬ ▬ Combustor |
| ▬·▬ Fan Inlet | ▪▪▪▪ Turbine |
| ▬··▬ Fan Exhaust | ▬▬ Jet |

Figure 15. Measured and Predicted 60° Baseline Noise at Takeoff.

- Approach Power
- 60° Acoustic Angle
- 46.5 m. (152 Ft.) Arc

○ Measured Baseline Engine (6-20)
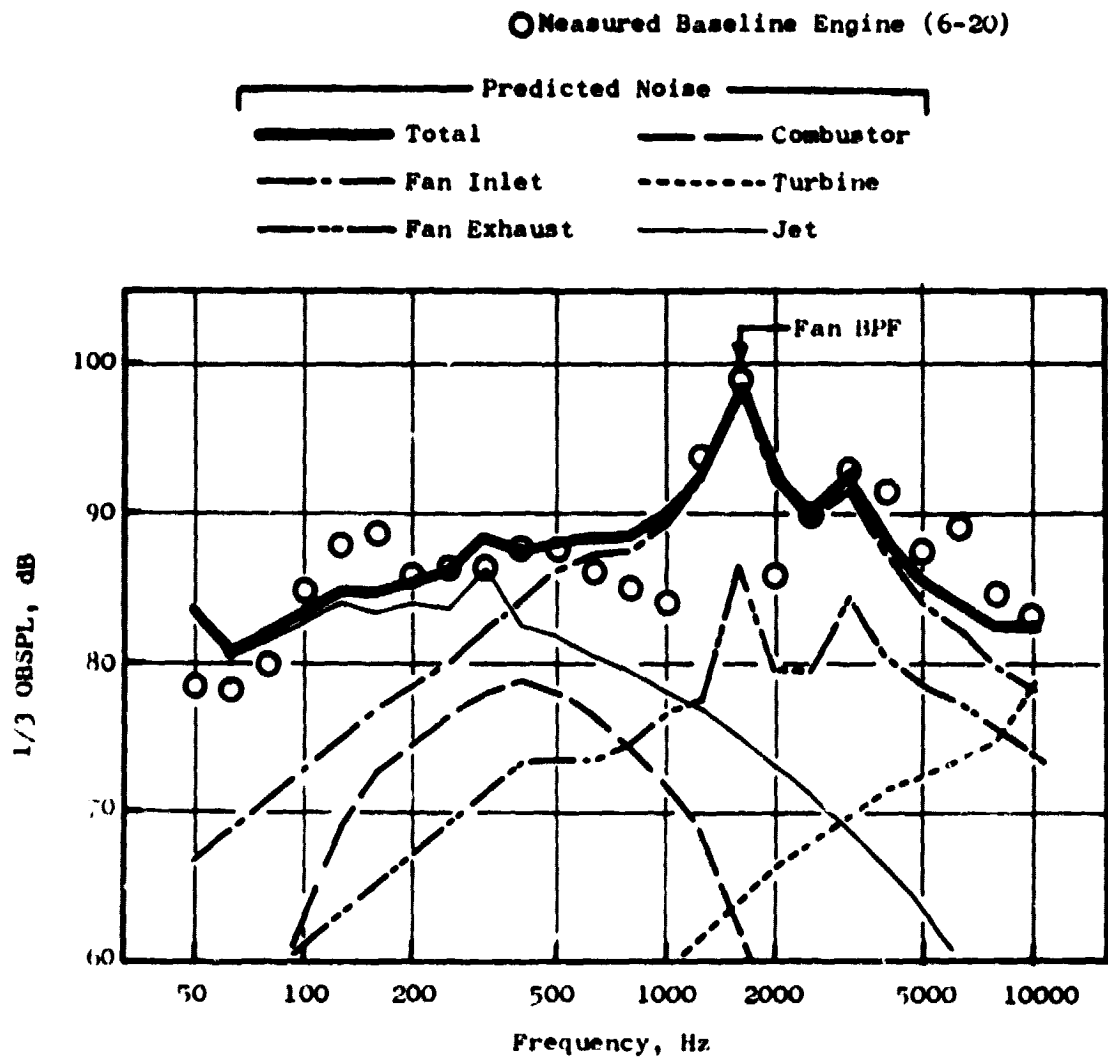
Predicted Noise

Total ──────── Combustor

Fan Inlet ──── Turbine

Fan Exhaust ──── Jet

Figure 16. Measured and Predicted 60° Baseline Noise at Approach.

- Baseline Bellmouth
- Reading 6-22
- 46.5 m (152 Ft.) Arc
- Takeoff Power
- 20 Hz Bandwidth

- 30° Acoustic Angle

10 dB

- 60° Acoustic Angle

10 dB

- 80° Acoustic Angle

10 dB
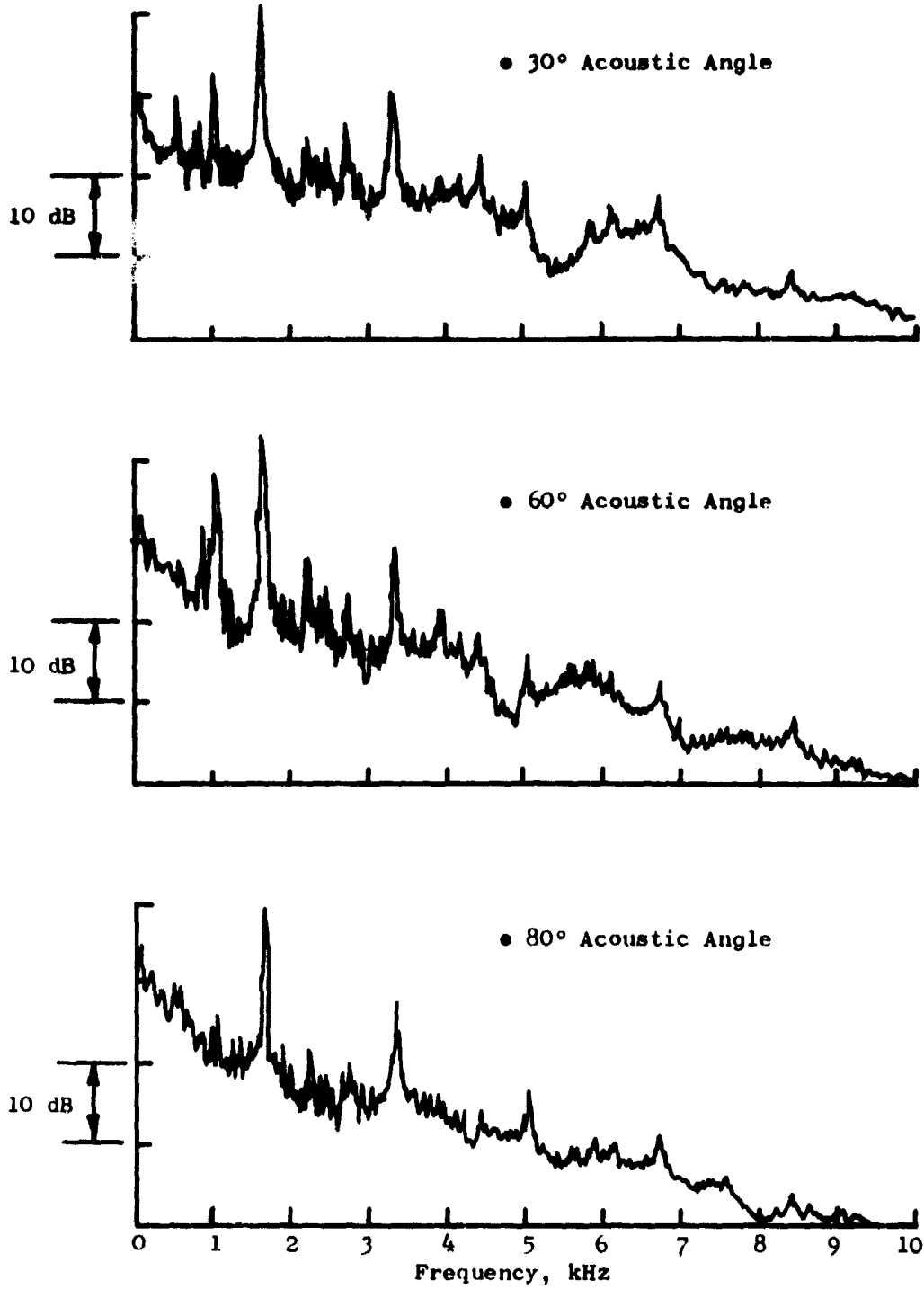
Frequency, kHz

Figure 17. Baseline Narrow Band Inlet Spectra at Takeoff.

A directivity plot of the 1/3-octave band which contains the blade passing frequency (BPF) is shown in Figure 18 for takeoff and approach. These curves indicate that the inlet radiated noise levels are higher than the exhaust-radiated noise. Figures 19 and 20 compare the relative levels of engine constituents at takeoff and approach, respectively, using directional array results. These clearly indicate that at 60° and 80° in the forward quadrant, the BPF baseline noise SPL's are inlet radiated and are at least 10 dB above exhaust-radiated noise for the 60° angle.

To further understand the source noise characteristics of the OTW engine, a probability density analysis (using digital fast Fourier transform analysis) was performed on the BPF signal received in the far field. Figure 21 indicates that the takeoff BPF tone signal at 60° and 80° has a random amplitude probability distribution. The approach noise BPF tone signal as shown in Figure 22 shows the same characteristics. This analysis indicates that a random mechanism such as rotor-turbulence-generated noise may be the source of the inlet-radiated BPF tone noise on the OTW engine.

### 5.1.1.2  Ground Vortex Destroyer

Model tests have indicated that the ground vortex associated with static tests of engines can raise the noise levels as much as 5 PNdB (Reference 8). To simulate in-flight conditions where turbulence from a ground vortex would not be present, the ground vortex should be suppressed during static tests.

One means of suppressing the ground vortex during static tests is to create an artificial headwind which prevents the stagnation streamline from touching the ground. This concept was tested on the QCSEE OTW engine during testing of the baseline configuration. A bank of three fans shown schematically in Figure 23 was used to create an artificial head wind of approximately 12 m/sec (40 ft/sec).

In order to visualize the ground vortex and the effect of the fans upon it, the pad in front of the engine was flooded with water. Observations were made at several engine speeds. The ground vortex was observed to dissipate when the fans were blowing. However, acoustic results indicated no change in the far field noise signature of the engine. Results for 30° and 60° are presented in Figure 24 at a speed near approach power. The probability density analysis in the preceding section indicates that the inlet-radiated fan noise may be controlled by a rotor-turbulence interaction mechanism. The turbulence is caused by not only the ground vortex but also atmospheric turbulence associated with the earth's boundary layer. It appears that the latter type of turbulence is the controlling mechanism. Accordingly, the vortex fans were not used in subsequent tests.

### 5.1.1.3  Comparison to Other Engines

Fan inlet-radiated noise comparisons between different fans can be made as a function of tip speed. A comparison of design tip speeds from several
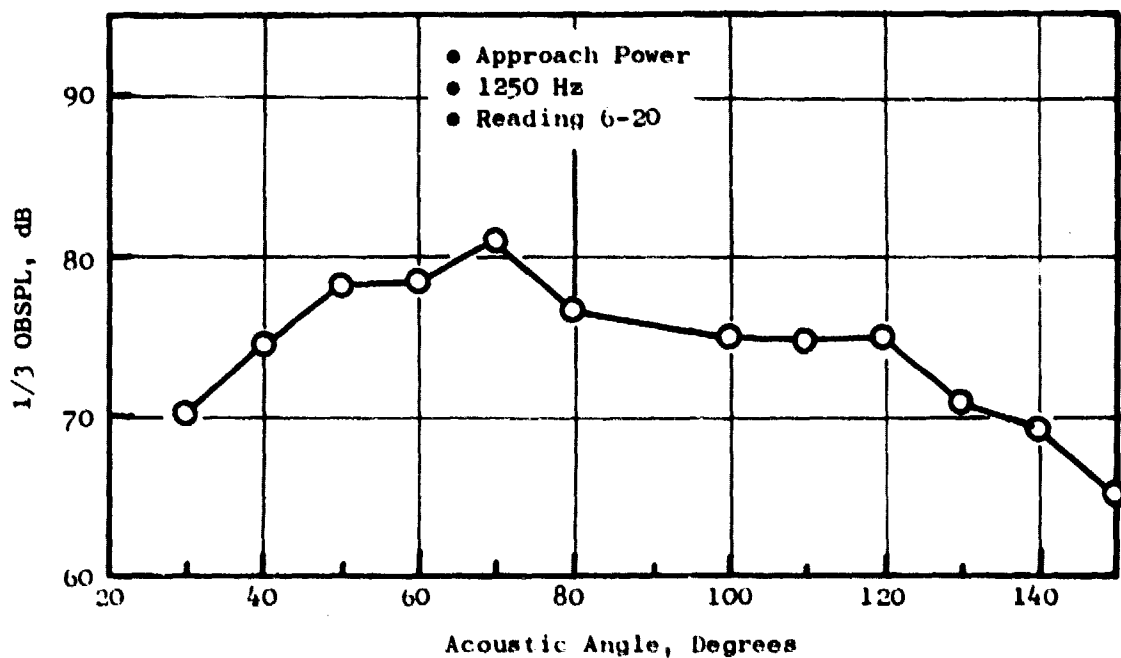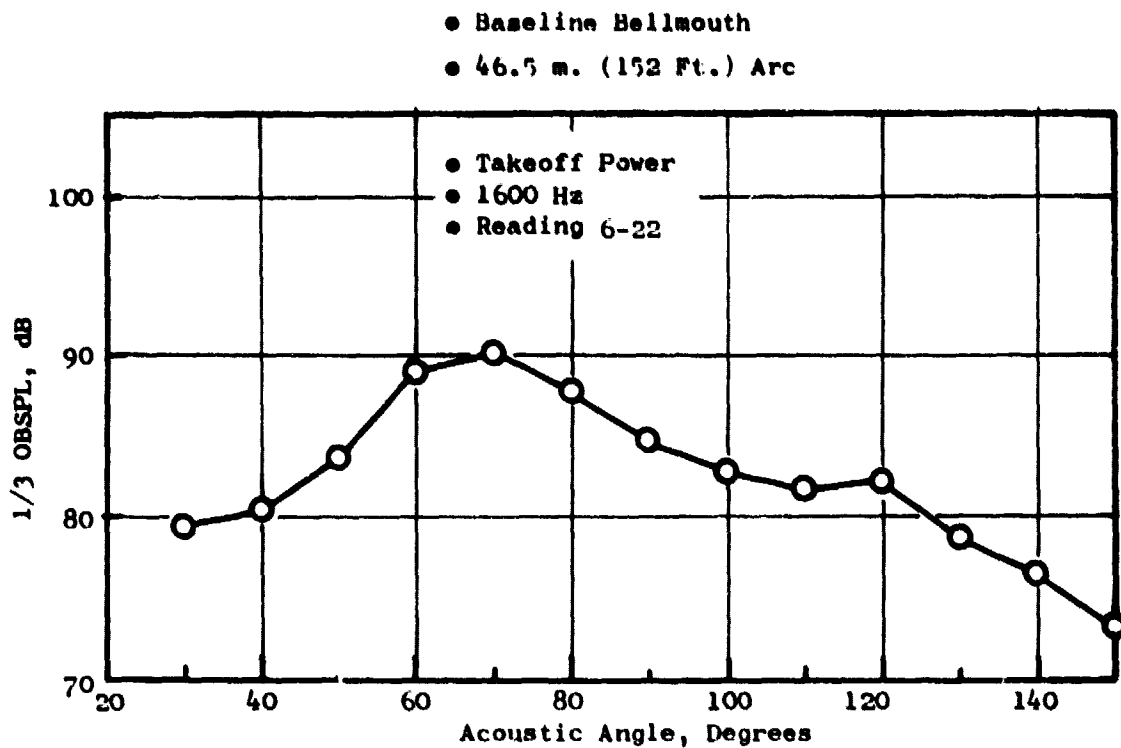
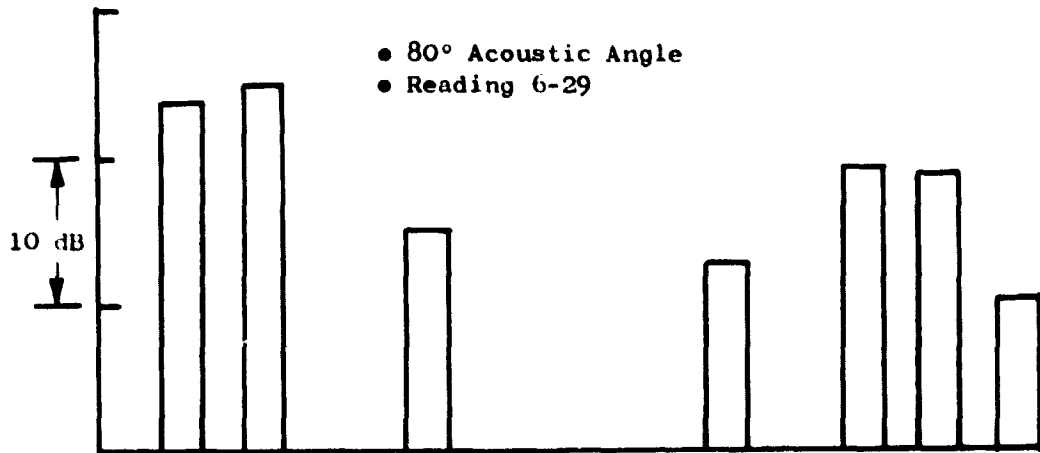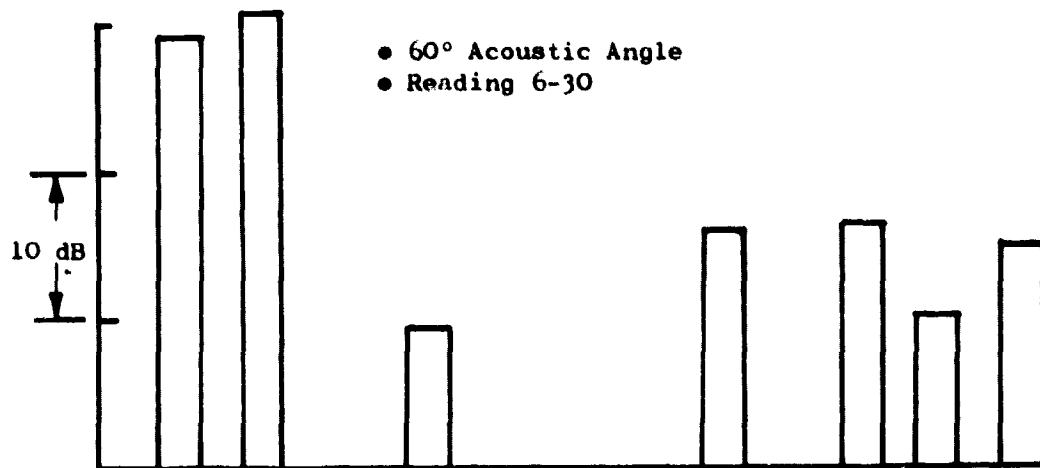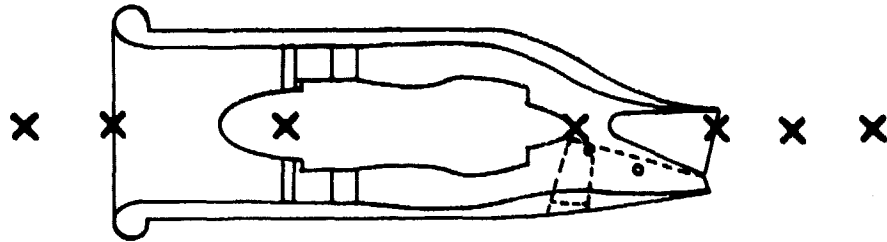Figure 18. Baseline BPF SPL Directivity at Takeoff and Approach.

Figure 19. Directional Array Baseline BPF SPL's at Takeoff for 60° and 80°.

- Baseline Bellmouth
- Approach Power
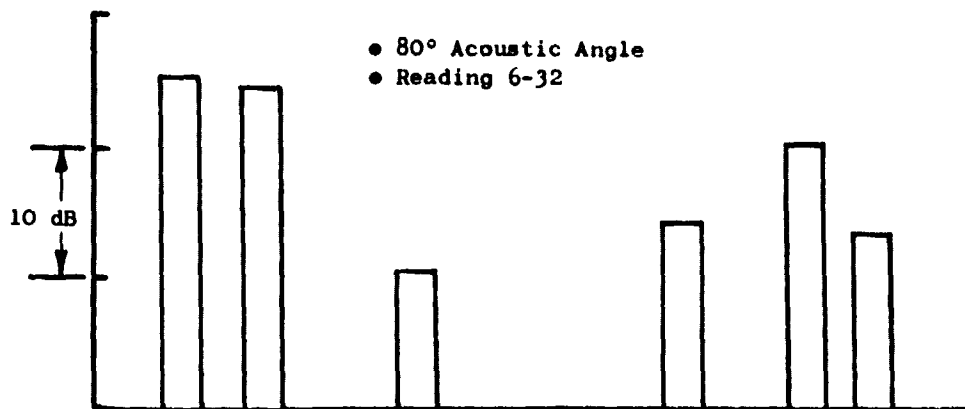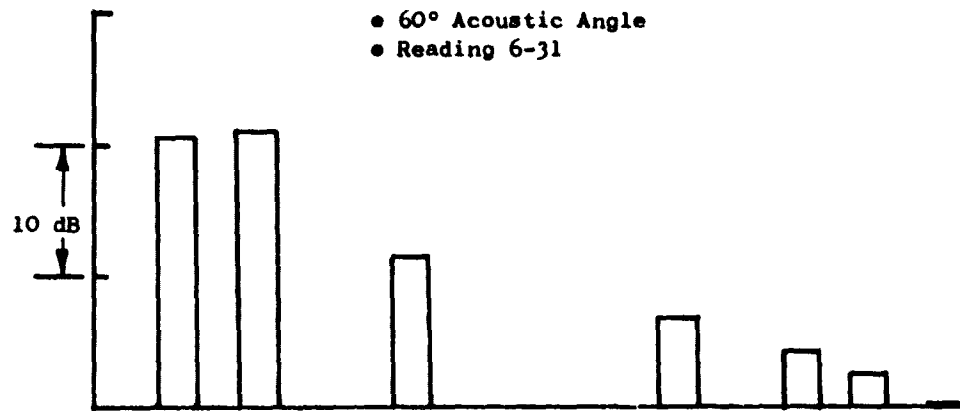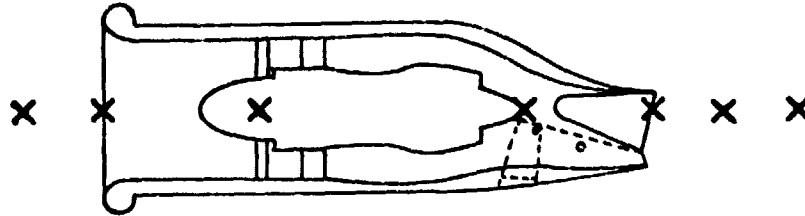- 1600 Hz  1/3 Octave Band SPL (Contains BPF)
- 30.5 m. (100 Ft.) Arc

- 60° Acoustic Angle
- Reading 6-31

10 dB

- 80° Acoustic Angle
- Reading 6-32

10 dB

Figure 20.   Directional Array Baseline BPF SPL's at
Approach for 60° and 80°.

- Baseline Bellmouth
- Takeoff Power
- Reading 6-22
- 20 Hz Bandwidth

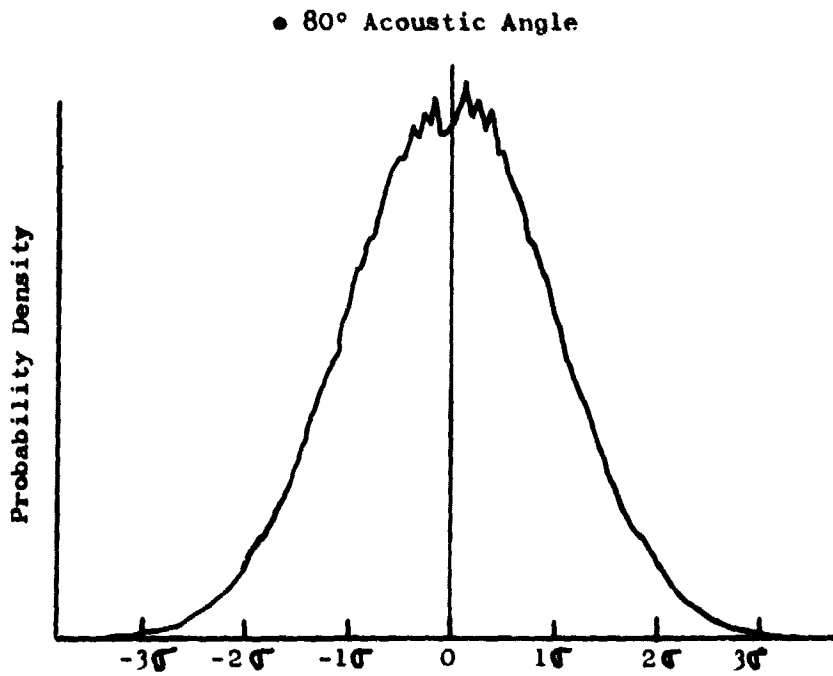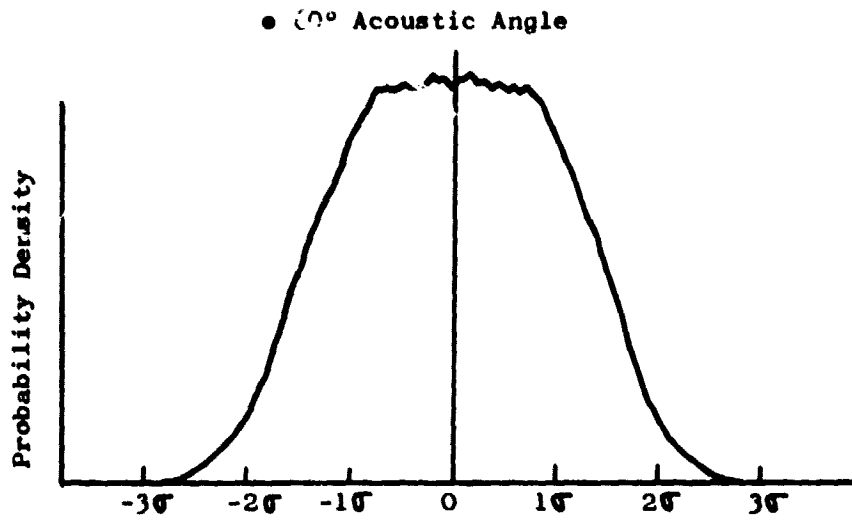- 0° Acoustic Angle



- 80° Acoustic Angle



Figure 21. Baseline Inlet-Radiated Source Noise
Characteristic at Takeoff.

- Baseline Bellmouth
- Approach Power
- Reading 6-20
- 20 Hz Bandwidth

- 60° Acoustic Angle

Probability Density

-3σ   -2σ   -1σ   0   1σ   2σ   3σ

- 80° Acoustic Angle

Probability Density
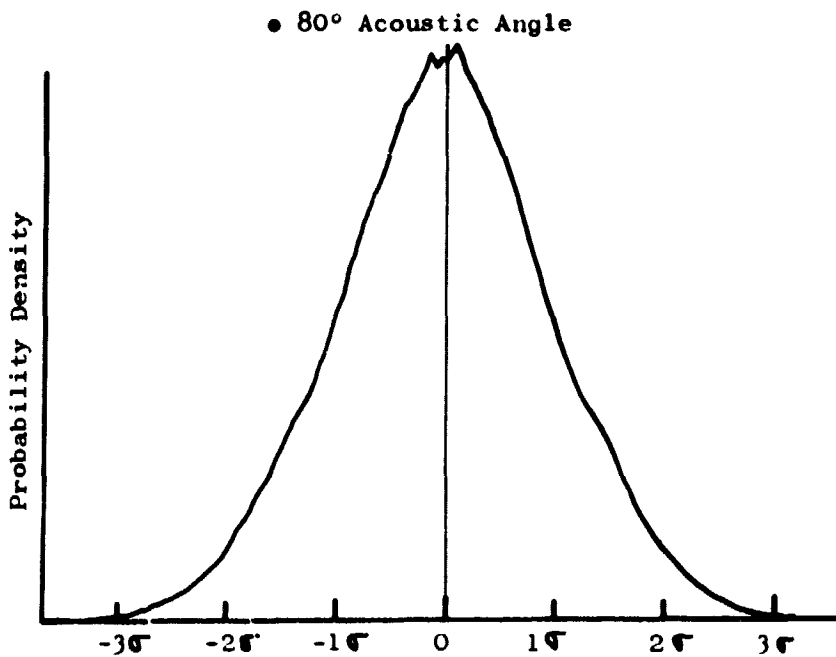
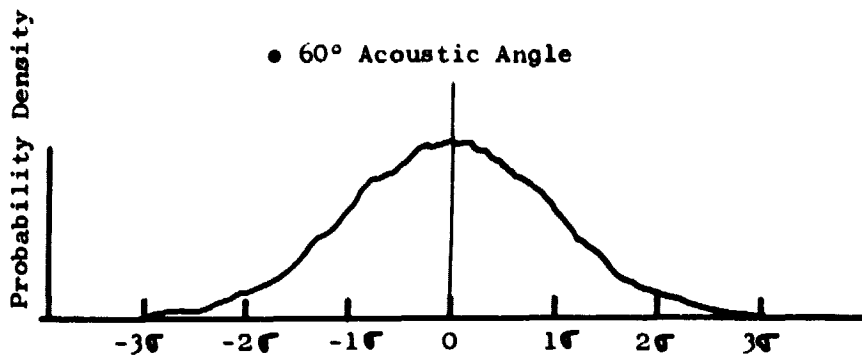-3σ   -2σ   -1σ   0   1σ   2σ   3σ

Figure 22.   Baseline Inlet-Radiated Source Noise
Characteristic at Approach.

1.07 m (42 inch) DIAMETER FAN
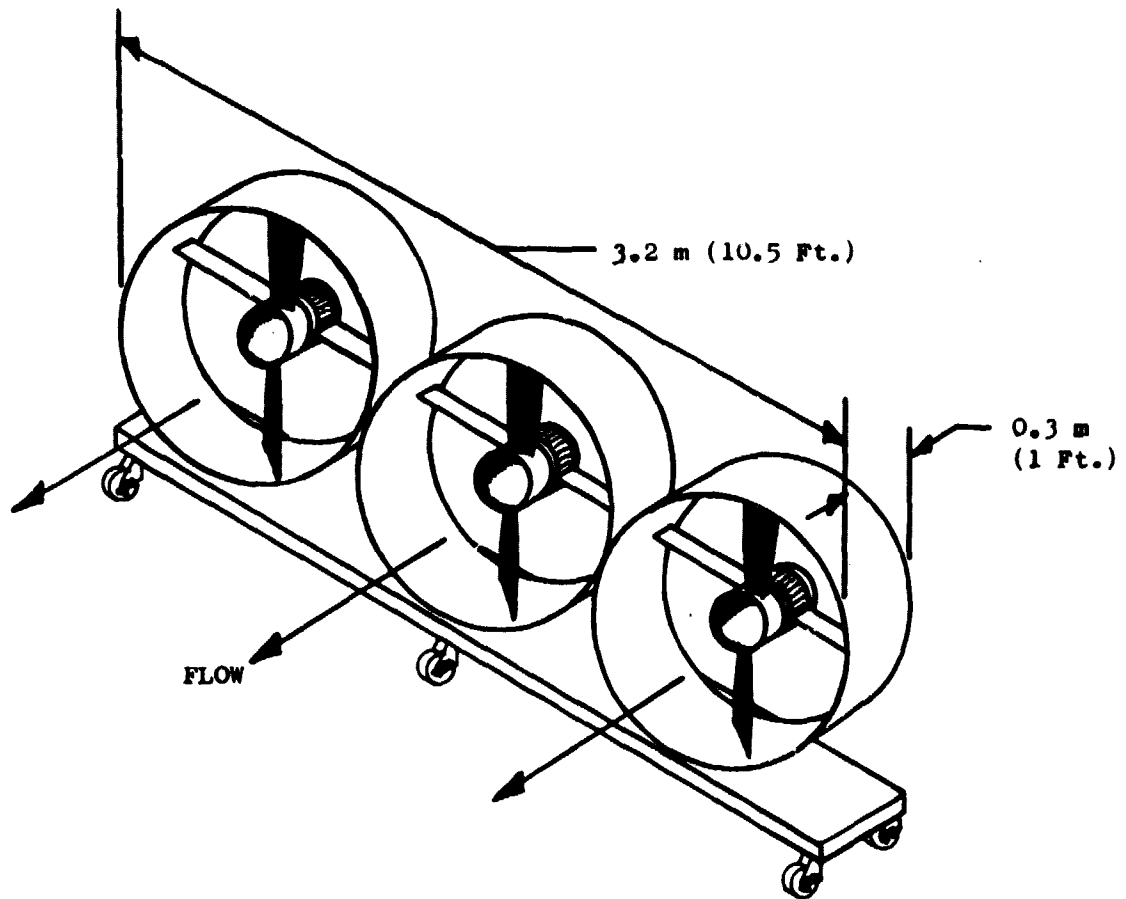
HARTZEL PROPELLER FAN CO.

MODEL NO.  N-40-AKR



3.2 m (10.5 Ft.)

0.3 m
(1 Ft.)

FLOW

Figure 23.  Ground Vortex-Destroying Fans.

- Baseline Bellmouth
- 81.4% Corrected Fan Speed
- 46.5 m. (152 Ft.) Arc

| Reading | Vortex Fans |
|---------|-------------|
| O 6-10 | On |
| □ 6-11 | Off |

- 30° Acoustic Angle
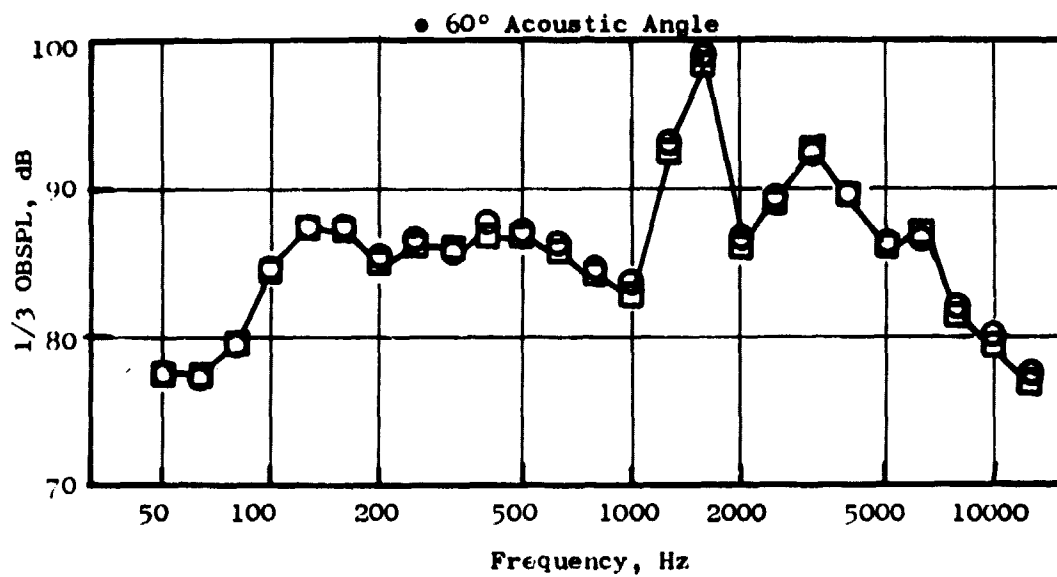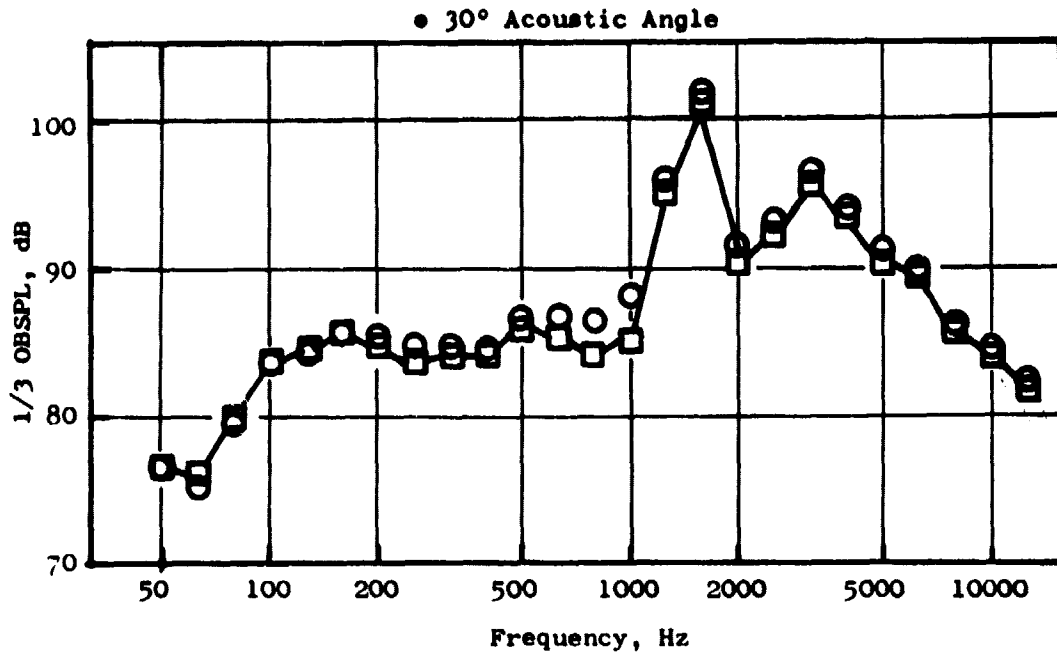
- 60° Acoustic Angle

Figure 24. Effect of Ground Vortex Elimination on Inlet Radiated Noise.

40

fans of approximately the same diameter is made in Figure 25. Included in these comparisons are Quiet Engine Fans A and C (References 9 and 10) and several of the NASA Quiet Fans. The OTW's tip speed is higher than all the fans except QEP C. A comparison of engine PNL's from these fans is presented in Figure 26. All fans are approximately the same diameter so no size correction was used. The OTW is quieter than QEP C as expected since QEP C has a much higher tip speed. QEP A and the OTW have about the same levels while the OTW is quieter than QF1, QF3, and QF5 which have about the same tip speed. Both the QF6 and QF9 fans are quieter than the QTW; however, this is expected because their tip speed is considerably less.

It appears that the OTW engine inlet-radiated noise levels compare favorably with other fans having about the same tip speed.

## 5.1.2  Inlet Suppression

OTW design studies (References 2 and 3) indicated that inlet suppression levels of 13.5 and 10.4 PNdB, respectively, were required at takeoff and approach to meet the system noise goals.

Acoustic suppression for the OTW inlet at approach was achieved with bulk absorber treatment on the wall. At takeoff, both wall treatment and high throat Mach number acceleration effect were used to provide suppression. Details of the inlet treatment selection and design are discussed in References 2 and 3. A schematic of the inlet is presented in Figure 27 along with the in-duct acoustic instrumentation.

### 5.1.2.1  Far Field Results

The overall performance of the inlet is shown in Figure 28, which compares far field PNL's at three acoustic angles (30°, 60°, and 80°) as a function of throat Mach number. At 0.79 throat Mach number for which the inlet was designed, the suppression achieved at 30°, 60°, and 80° is 12, 10, and 7.5 PNdB, respectively. These suppressions are for the measured engine data. At 60°, calculating the inlet suppression with the jet noise removed results in 14 PNdB inlet suppression.

Although it would appear from Figure 28 that there is less suppression at 80°, it may be that exhaust-radiated noise is contributing to the spectra seen in the far field at 80°.

Comparison plots of the BPF SPL as a function of throat Mach number are shown in Figure 29. Here at 0.79 throat Mach number, 30° and 60° data indicate about 19 dB suppression while at 80° the suppression is only about 14 dB. Directional array results for the BPF at takeoff are presented in Figure 30. At 60° the exhaust components are at least 10 dB below the components from the inlet. However, at 80°, the exhaust-radiated BPF is less than 3 dB below the inlet radiated signal. Therefore, at 80°, inlet suppression will be masked by exhaust radiated noise.
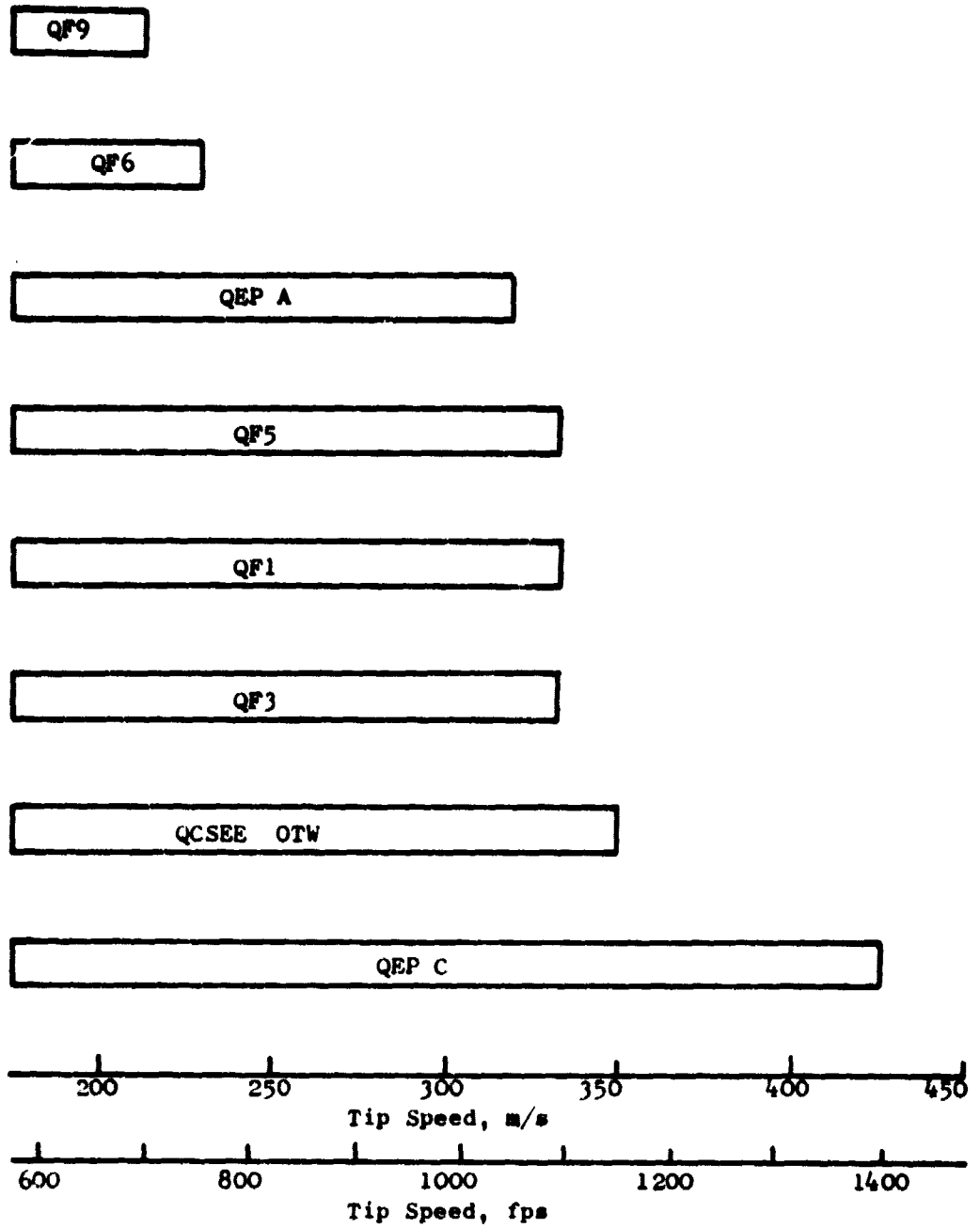
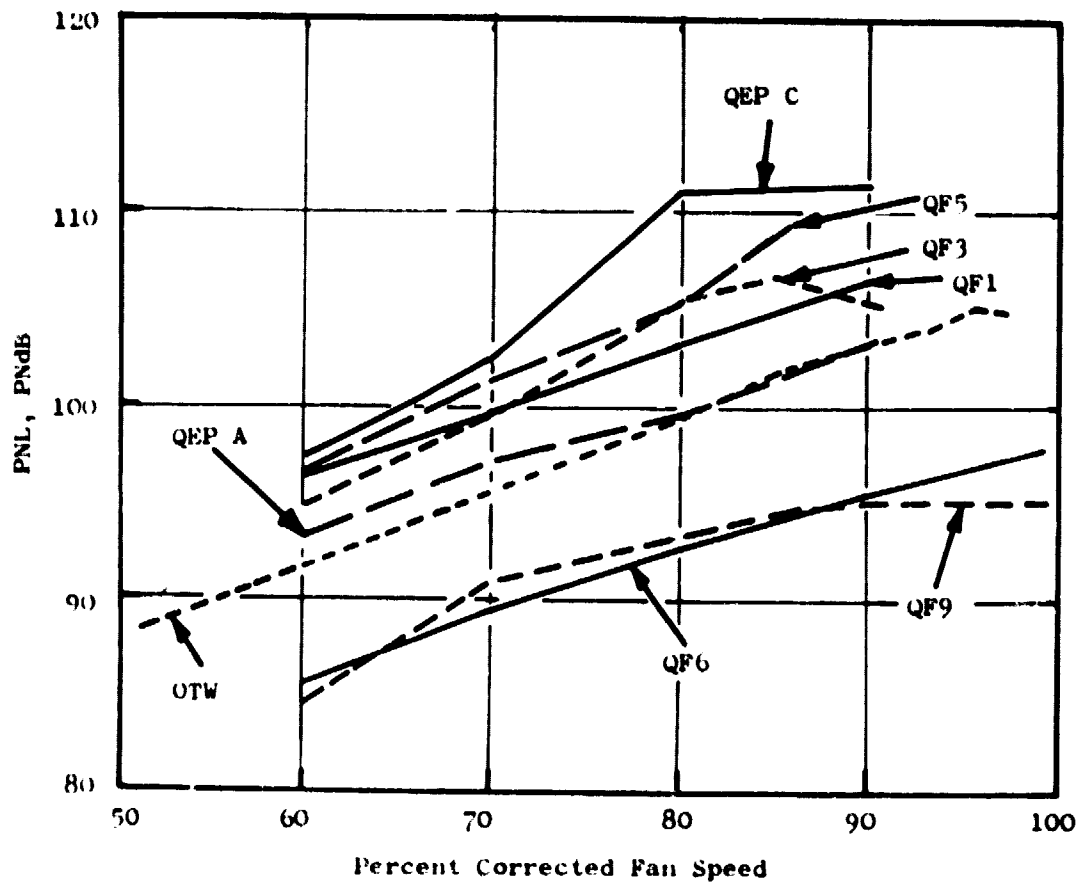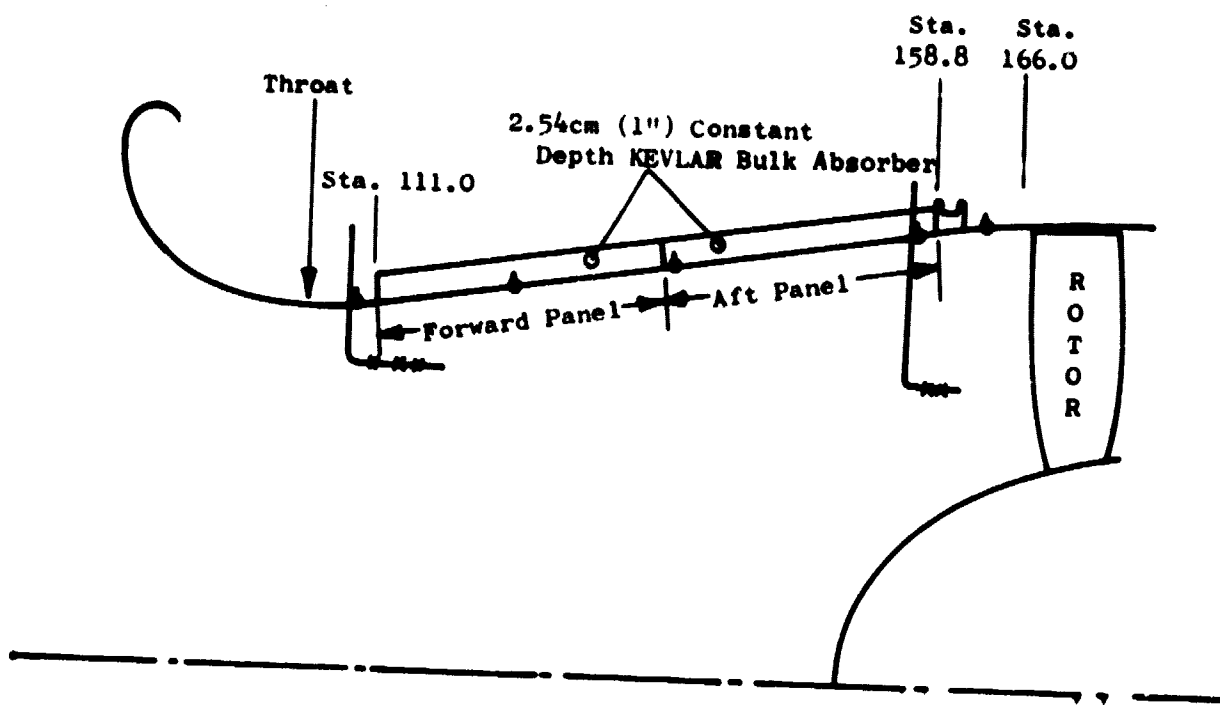Figure 25. Tip Speed Comparison of Several Fans.

● 152.4 m. (500 Ft.) Sideline



Figure 26. Comparison of Inlet Radiated Noise from Several Fans.

**✻ Probe Kulites**

**♦ Wall Kulites**



|  | Faceplate Thickness | Porosity | Hole Size |
|---|---|---|---|
| Forward Panel | 1.27mm(.05") | 14% | 1.59mm(.0625") |
| Aft Panel | 1.27mm(.05") | 22% | 1.59mm(.0625") |

Figure 27. Bulk Absorber Fan Inlet Treatment Design.

• 152.4 m (500 Ft.) Sideline

| Symbol Representation | Inlet | Test |
|---|---|---|
| Open - 11.5° Side Door Angle | ◯ Bellmouth | 6 |
| Solid - 25° Side Door Angle | ☐ Hybrid | 12 |
| Flagged - Jet Noise Removed | ◇ Hard Wall Accel. | 13 |
| | △ Hybrid | 14 |

• 30° Acoustic Angle
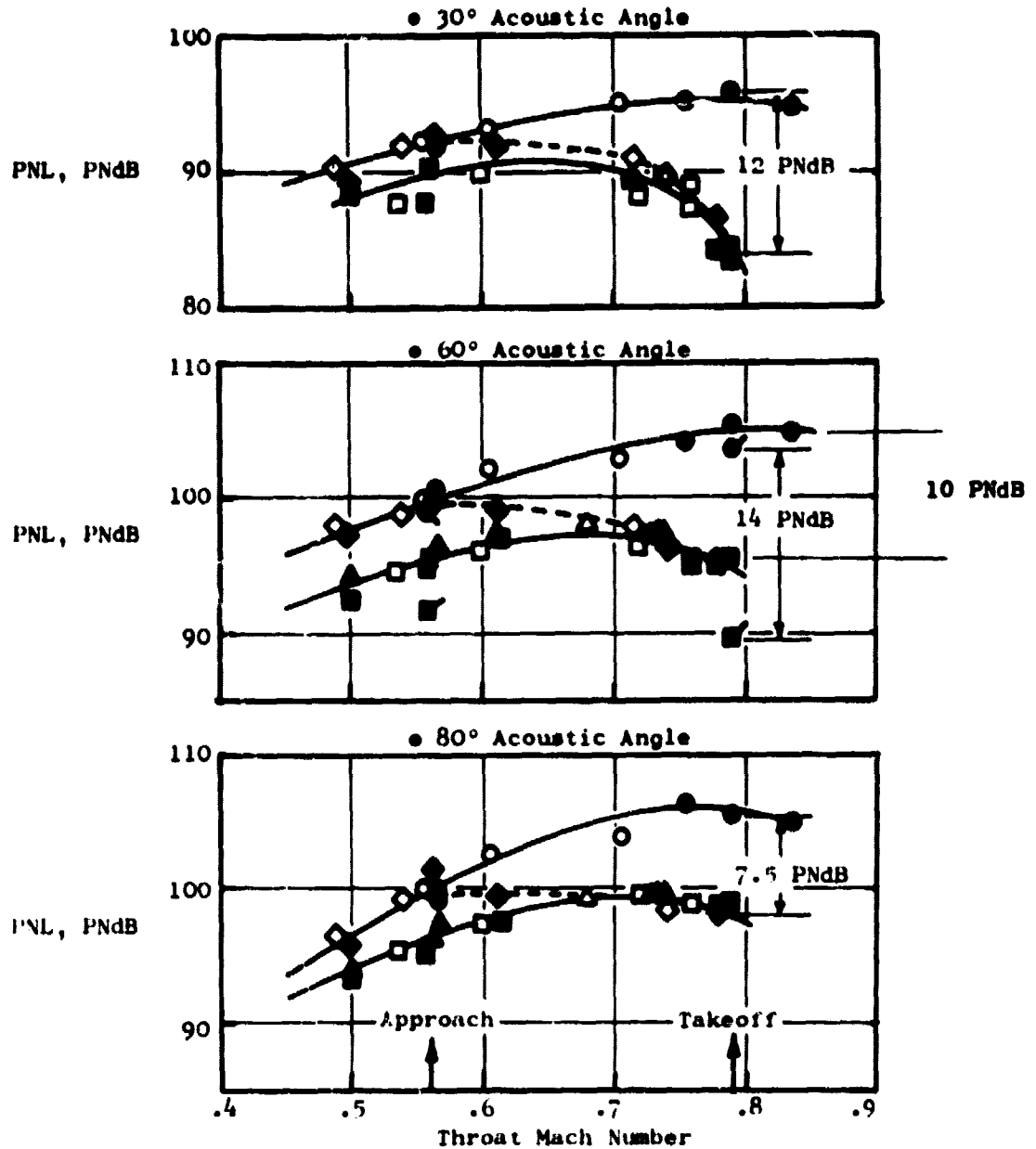
• 60° Acoustic Angle

• 80° Acoustic Angle

PNL, PNdB

Throat Mach Number

Figure 28. Inlet Radiated Noise Suppression.

● 152.4 m (500 Ft.) Sideline

Symbol Representation

Open - 11.5° Side Door Angle
Solid - 22° Side Door Angle

| Inlet | | Test |
|-------|---|------|
| O | Bellmouth | 6 |
| □ | Hybrid | 12 |
| ◇ | Hard Wall Accel. | 13 |
| △ | Hybrid | 14 |

● 30° Acoustic Angle

BPF SPL, dB

● 60° Acoustic Angle

BPF SPL, dB

● 80° Acoustic Angle

BPF SPL, dB

Approach          Takeoff
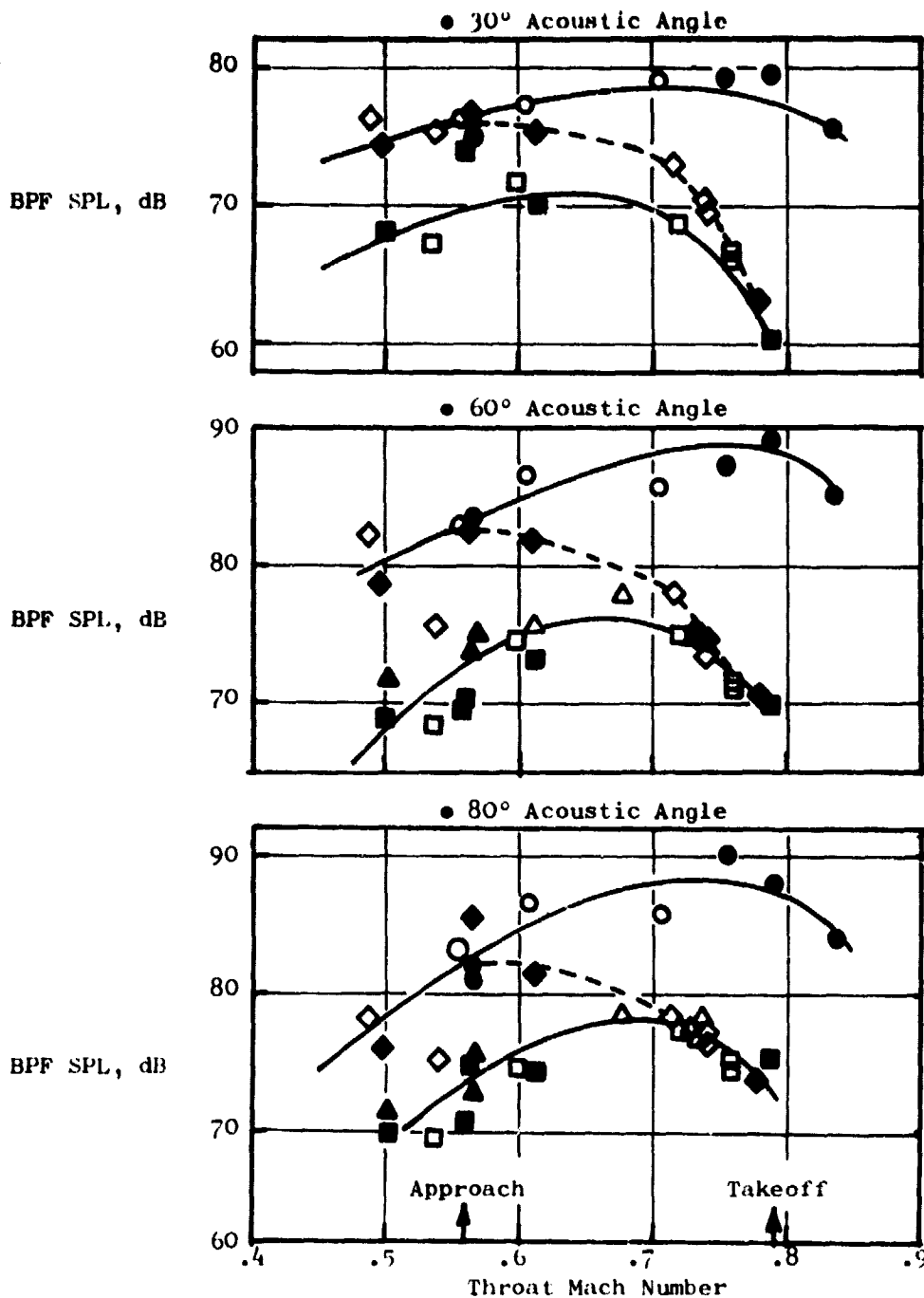
Throat Mach Number

Figure 29.   Inlet BPF Suppression.

46

- Fully Suppressed
- Takeoff Power
- 1600 Hz 1/3 Octave Band SPL (Contains BPF)
- 30.5 m (100 Ft.) Arc

- 60° Acoustic Angle
- Reading 12-33

10 dB

- 80° Acoustic Angle
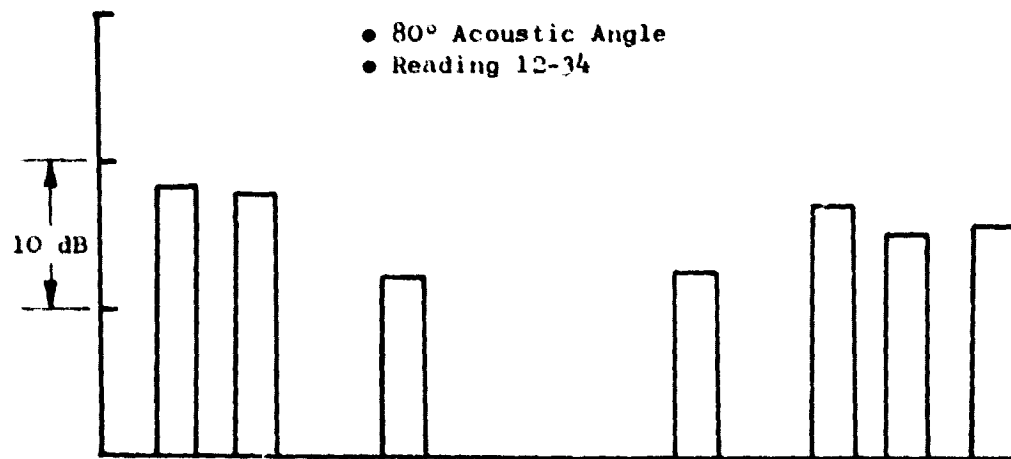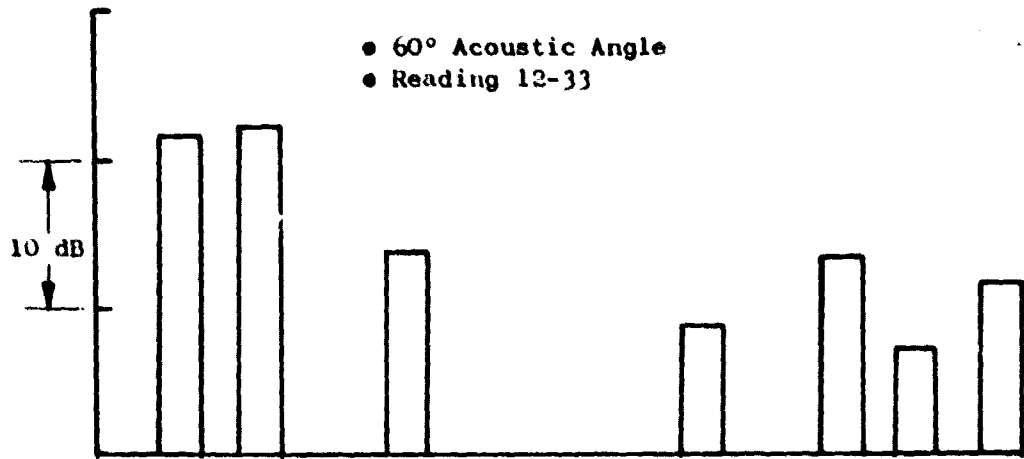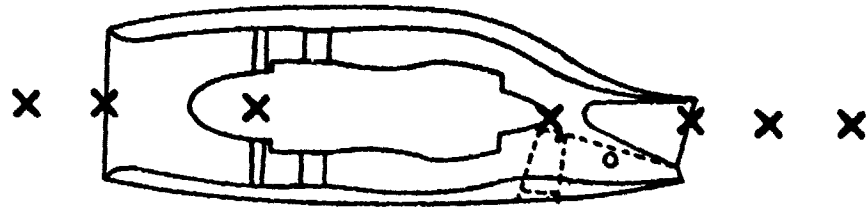- Reading 12-34

10 dB

Figure 30. Hybrid Inlet Directional Array Results for the Fan BPF.

It is evident from Figure 28 that the treatment in the inlet did not produce any significant suppression on a PNL basis at high-throat Mach numbers. Figure 31 shows the engine takeoff spectra at 60°. The inlet treatment resulted in about 1 dB increase in suppression at high frequencies. The suppression spectra at takeoff due to the accelerating or high-throat Mach number inlet is shown in Figure 32. It is compared to acceleration suppression spectra acquired during tests of a scale model fan (Reference 11). The scale model fan had a BPF of 1000 Hz and its suppression spectra with the hard wall accelerating inlet was shifted so that the BPF suppression occurred at the OTW BPF of approximately 1600 Hz. Higher BPF suppression is evident with the OTW inlet as is suppression of MPT's at 1000 Hz. Similar suppression results are presented in Figure 33 for the hybrid inlet. It also is compared to suppression results from the model tests of Reference 11. BPF multiple pure tone (MPT) suppressions are evident. This engine spectra results in inlet suppression of 14 PNdB which is slighly higher than the 13.5 PNdB estimated prior to the engine test (Reference ?).

At approach in Figure 28 where the throat Mach number is about 0.56, PNL suppression for the engine data is 2 to 5 PNdB. At 60°, with the jet noise removed from the spectra, inlet suppression is approximately 7 PNdB. This is less than predicted by 3.5 PNdB. Spectral comparison of the 60° SPL's at approach are presented in Figure 34. At frequencies near the BPF and above, the hard wall accelerating inlet SPL's are the same as the baseline bellmouth. This is not unexpected since there is no acceleration effect at this low throat Mach number.

An interesting observation can be made from Figure 34. At frequencies below the BPF from about 250 Hz to 1000 Hz, the hard wall accelerating inlet SPL's and the hybrid inlet SPL's are the same. If the noise in this region were inlet radiated, then one would expect the hard wall accelerating inlet SPL's to be the same level as the baseline bellmouth. If the noise from 250 to 1000 Hz were exhaust radiated, then one might expect the hard wall accelerating and hybrid inlet configurations to be identical since they both have the same full exhaust suppression. This means that the baseline levels in these frequencies are core-related, not fan, noise.

### 5.1.2.2  In-Duct Instrumentation Results

Instrumentation in the inlet included wall Kulites and immersible Kulite probes. These are shown schematically in Figure 27. Probe data were taken at approach and near takeoff conditions.

At approach in Figure 35, the BPF SPL profiles are skewed at both the throat and fan face with higher levels near the outer wall.

The BPF PWL change due to the treatment is 5 to 7 dB. This difference is about what is seen in Figure 29 at the BPF.

At high power, near takeoff, the probe profiles for the BPF are presented in Figure 36. The profile at the throat is very flat. At the throat, the

48

- 95% Corrected Fan Speed
  (Nominal)
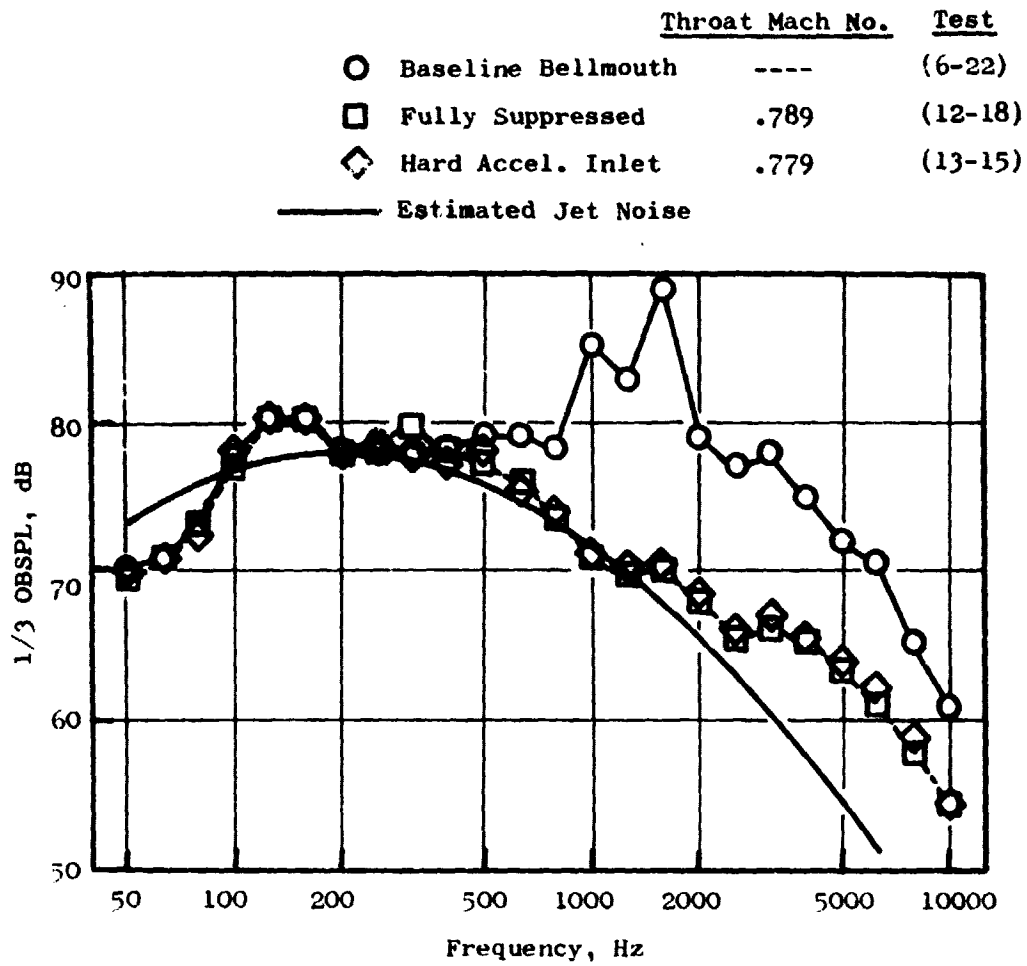- 152.4 m (500 Ft.) Sideline
- 25° Side Door Angle
- 60° Acoustic Angle

| | | Throat Mach No. | Test |
|---|---|---|---|
| O | Baseline Bellmouth | ---- | (6-22) |
| □ | Fully Suppressed | .789 | (12-18) |
| ◇ | Hard Accel. Inlet | .779 | (13-15) |
| —— | Estimated Jet Noise | | |



Figure 31. Takeoff Spectra at 60°.

- 60° Acoustic Angle
- Throat Mach No. = .79

——— OTW

- - - - Model Suppression (Reference 11)
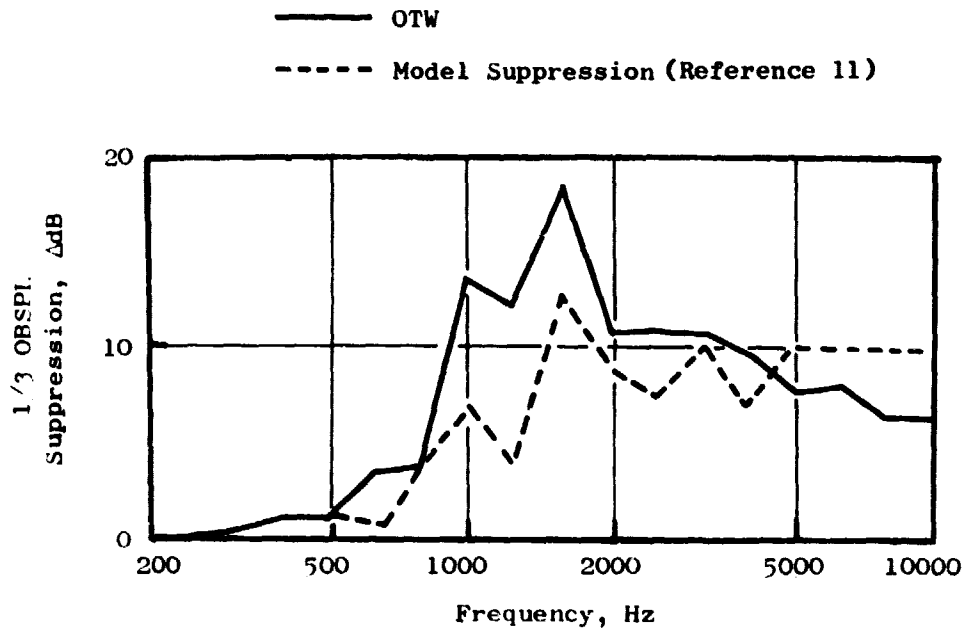


Figure 32. Hard Wall Accelerating Inlet Suppression.

● 60° Acoustic Angle

● Throat Mach No. = .79

——————— OTW

— — — — Model Suppression (Reference 11)


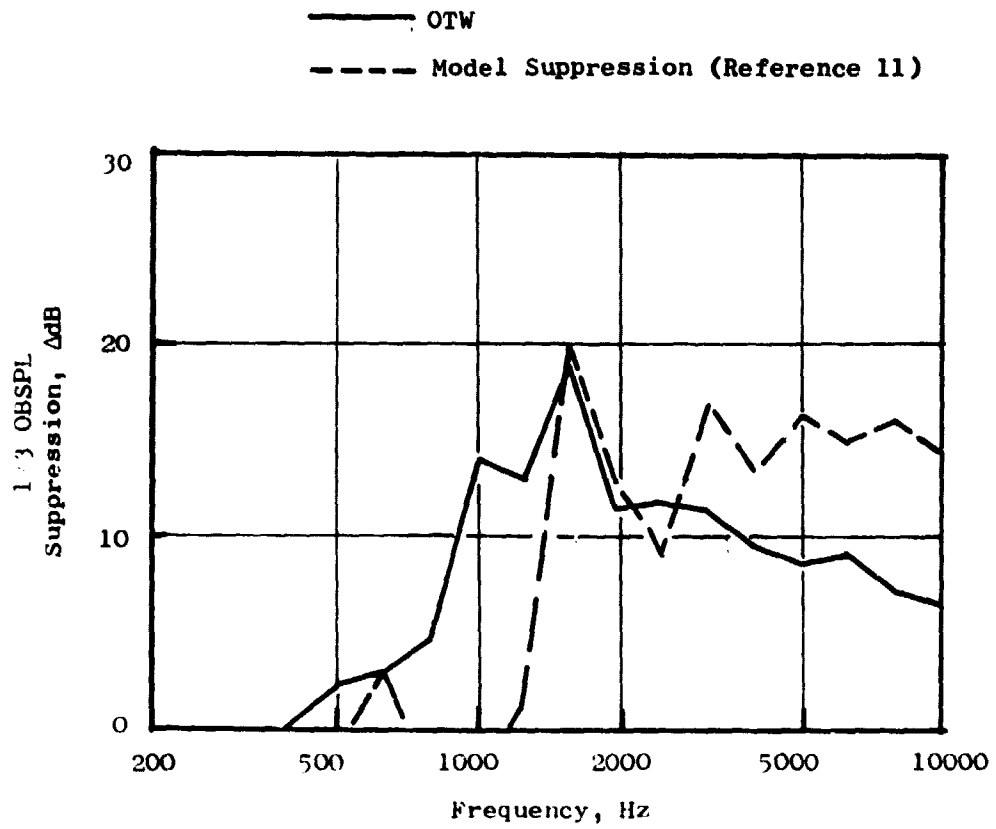
Figure 33. Hybrid Inlet Suppression.

- 81% Corrected Fan Speed
- 152.4 m (500 Ft.) Sideline
- 25° Side Door Angle
- 60° Acoustic Angle

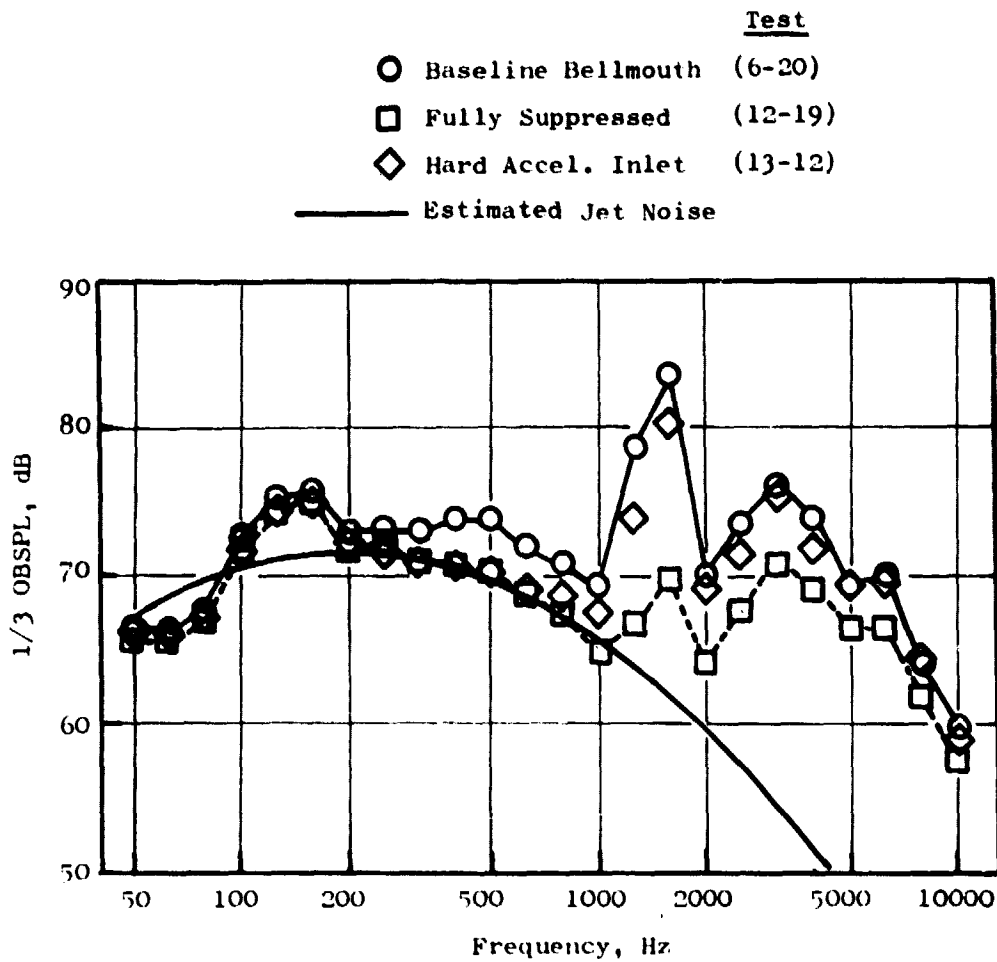|  |  | Test |
|---|---|---|
| O | Baseline Bellmouth | (6-20) |
| □ | Fully Suppressed | (12-19) |
| ◇ | Hard Accel. Inlet | (13-12) |
| —— | Estimated Jet Noise | |

Figure 34. Approach Spectra at 60°.

52

- Approach Power
- 1600 Hz 1/3 Octave Band SPL (Contains BPF)
- 25° Side Door Angle

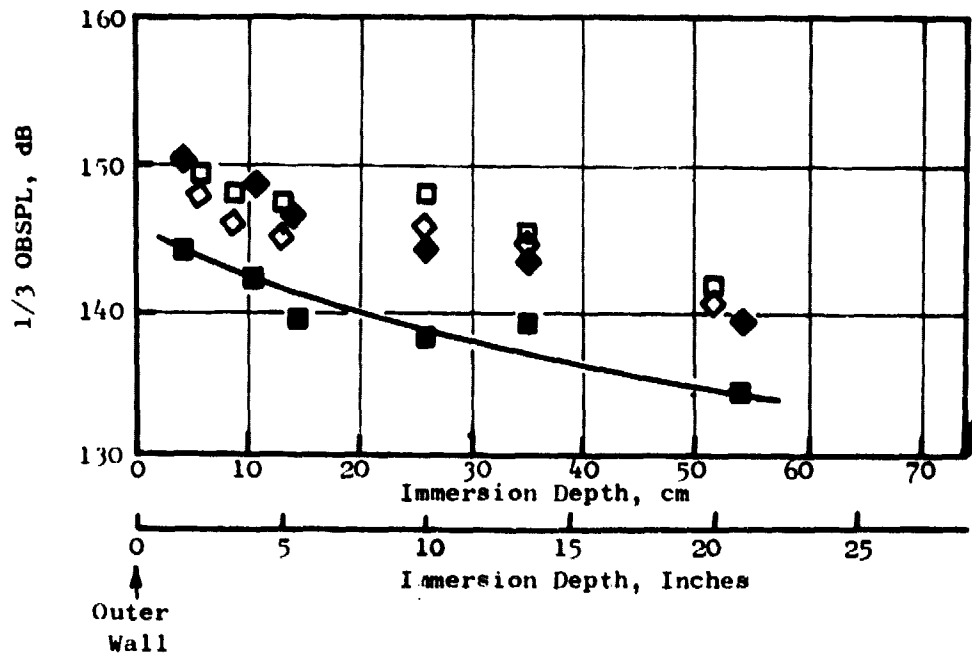| Probe | Configuration |
|---|---|
| □ Fan Face | Fully Suppressed |
| ◇ Fan Face | Hard Wall Accel. |
| ■ Inlet Throat | Fully Suppressed |
| ◆ Inlet Throat | Hard Wall Accel. |



Figure 35. Approach Inlet Probe Profiles.

53

- 95% Corrected Fan Speed (Nominal)
- 1600 Hz 1/3 Octave Band SPL (Contains BPF)
- 11.5° Side Door Angle

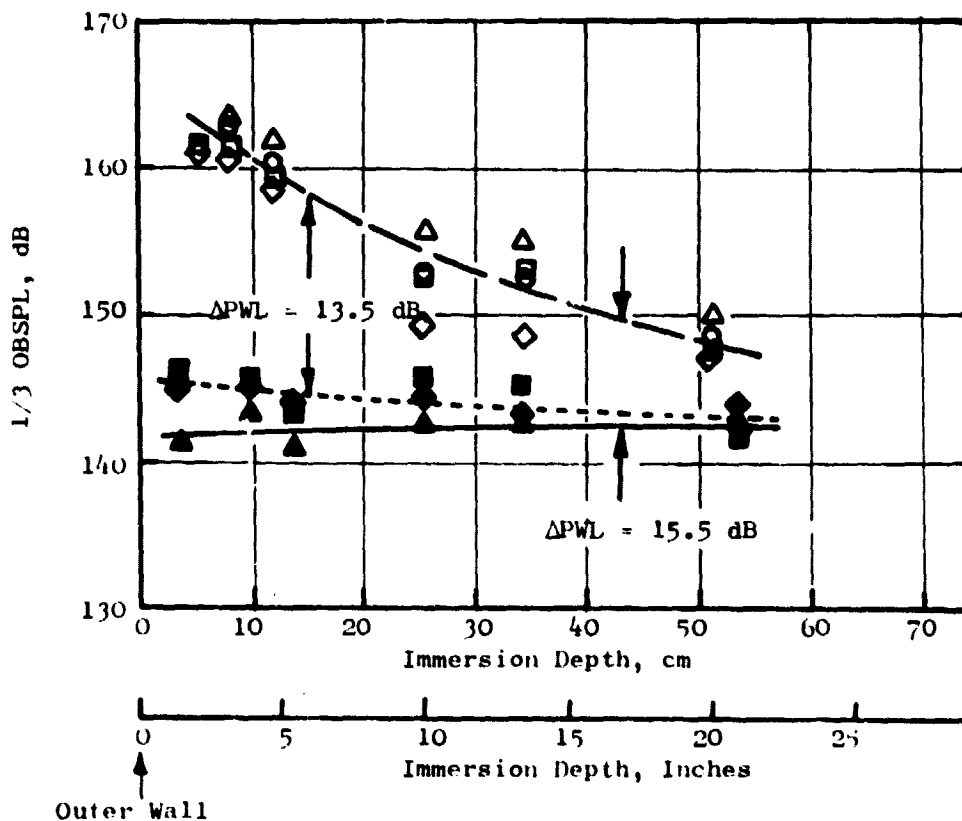| Probe | Configuration | Test |
|-------|--------------|------|
| O Fan Face | Baseline Bellmouth | (6-67) |
| □ Fan Face | Fully Suppressed | (12-45) |
| ◇ Fan Face | Hard Wall Accel. | (13-25) |
| △ Fan Face | Hybrid | (14-199) |
| ■ Inlet Throat | Fully Suppressed | (12-44) |
| ◆ Inlet Throat | Hard Wall Accel. | (13-24) |
| ▲ Inlet Throat | Hybrid | (14-200) |



Figure 36. Takeoff Inlet Probe Profiles.

54

hard wall accelerating inlet at about 0.74 throat Mach number has higher levels than the hybrid at nearly the same throat Mach number. This indicates suppression due to treatment. At 0.79 throat Mach number, the hybrid inlet has even lower levels. The PWL difference between the fan face and throat probe at 0.79 throat Mach number is 15.5 dB. This value compares favorably with the SPL difference observed in Figure 29 in the far field.

The decay pattern of the BPF SPL along the outer wall is shown in Figure 37 as indicated by the wall Kulites. Both takeoff and approach are shown here. At approach the hard wall accelerating-inlet SPL's do not decay significantly; however, the hybrid inlet BPF gets attenuated by the treatment. At a throat Mach number of 0.7 to 0.73, the decay seen is about the same for both the hard wall accelerating inlet and the hybrid inlet.


## 5.2 EXHAUST-RADIATED NOISE

The OTW engine has a "D"-shaped exhaust nozzle, through which exhaust radiated fan noise, combustor noise, turbine noise, and jet noise passes. The test program investigating exhaust-radiated noise was structured to evaluate suppression of fan, core, and turbine noise. Baseline levels were measured on a configuration which had hard walls in the fan and core flow-paths; however, the fan frame was treated as were the outlet guide vanes. Suppression of all sources was measured on the fully suppressed configuration. A partial level of suppression was achieved by removing the fan duct splitter and by replacing the core/turbine treatment with hard panels.

This section of the report will analyze and report on the results achieved with the exhaust suppression.


### 5.2.1  Baseline Source Noise Levels

#### 5.2.1.1  Source Noise Characteristics

Prior to testing of the OTW engine, estimates were made of the exhaust-radiated baseline levels for takeoff and approach. Figures 38 and 39 compare the measured levels with pretest total noise predictions at  both takeoff and approach.  The measured levels at frequencies above the BPF are lower than predicted.  At frequencies below the BPF there is good agreement. There is an apparent disagreement at 100 and 125 Hz; however, that is attributed to a ground reflection reinforcement which has not been removed from the measured data.  The jet noise levels used in the prediction are free field.

The OTW engine has a rotor-OGV spacing of 1.93 true rotor tip chords. This wide spacing was chosen to lower rotor-stator interaction noise. The probability density plots of the BPF tone in Figure 40 for both takeoff and approach at the maximum aft angle, indicate that the BPF fan noise amplitude distribution is primarily random. This means that the rotor-turbulence interaction noise source is probably controlling the far field levels rather than the cut-on rotor-stator tone!

- 20 Hz Bandwidth
- Inlet Wall Kulite Data
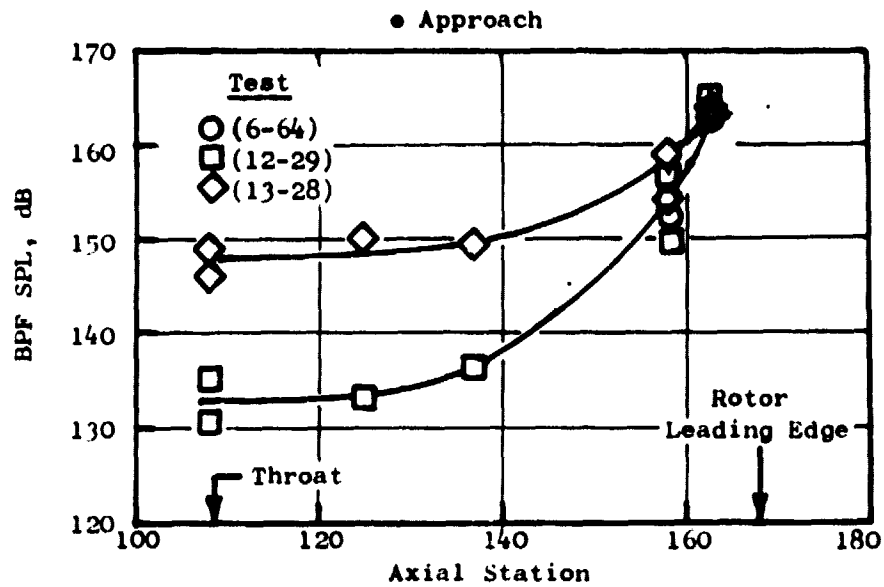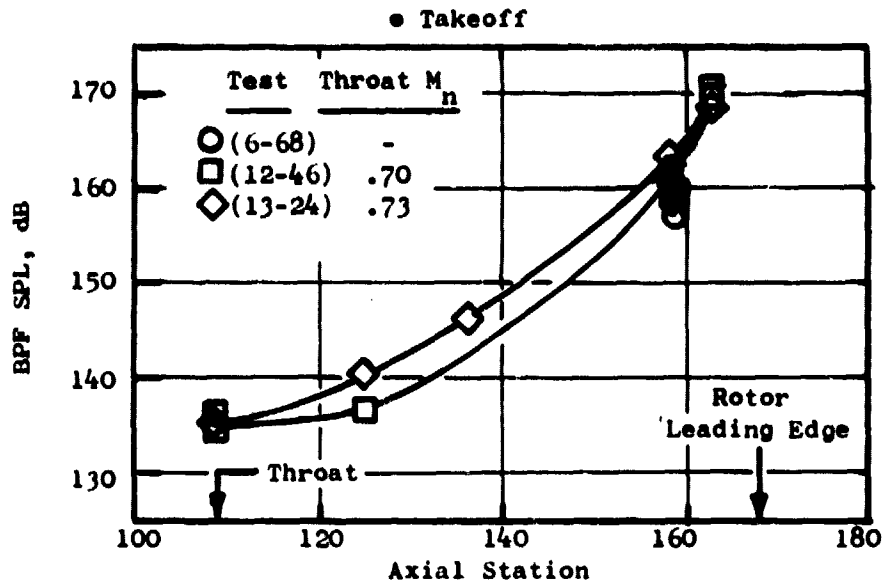
○ Baseline Bellmouth
□ Fully Suppressed
◇ Hard Wall Accel.

- Takeoff



- Approach



Figure 37.  Inlet Wall BPF Attenuation.

56

- Takeoff Power
- 120° Acoustic Angle
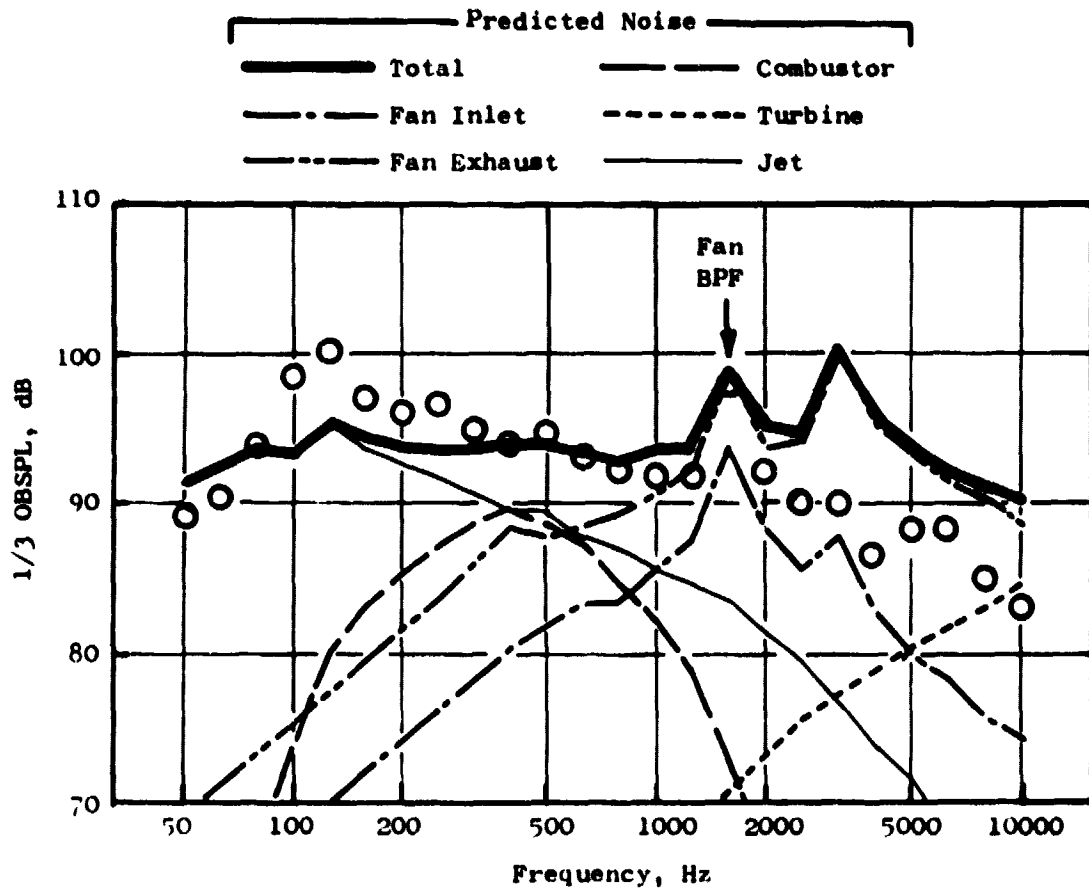- 46.5 m (152 Ft.) Arc

◯ Measured Baseline Engine (6-22)

Predicted Noise

━━ Total          ━ ━ Combustor
━·━ Fan Inlet     ━ ━ ━ Turbine
━··━ Fan Exhaust  ━━━ Jet

Figure 38.  Measured and Predicted 120° Baseline Spectra at Takeoff.
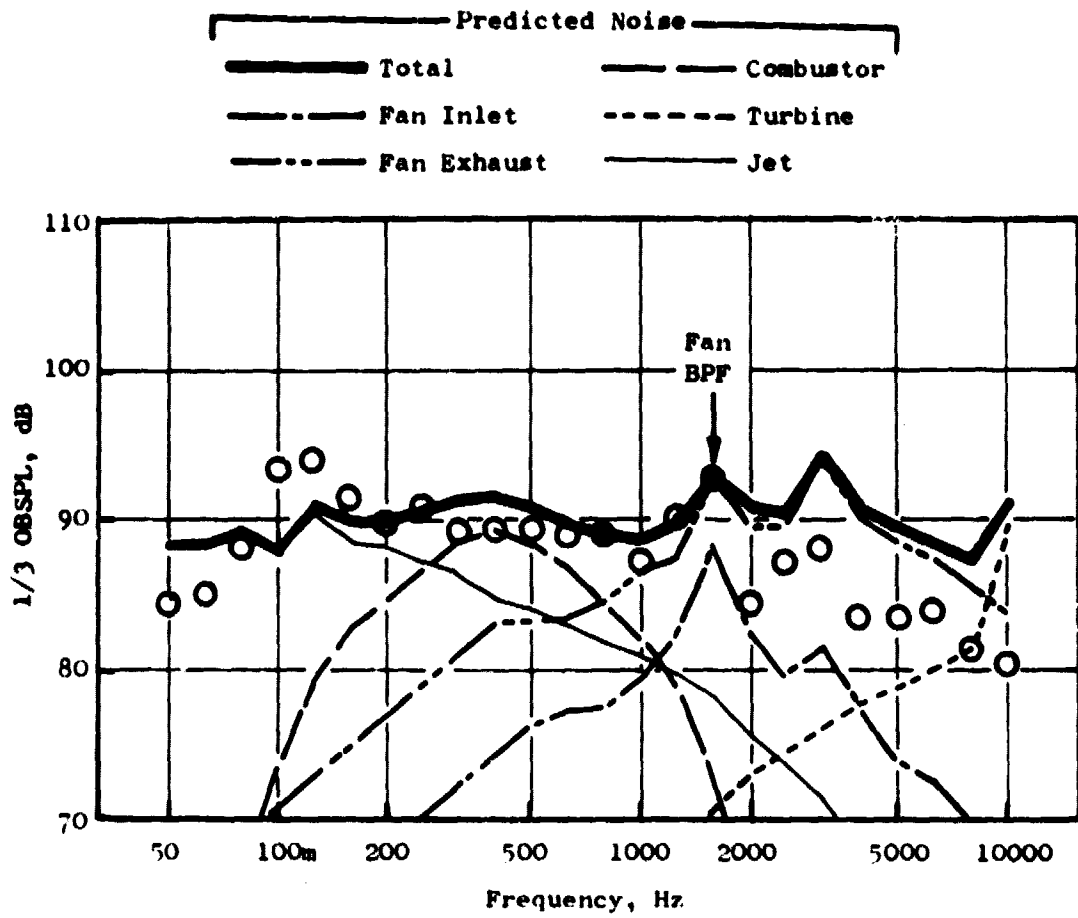
Figure 39. Measured and Predicted 120° Baseline Spectra at Approach.
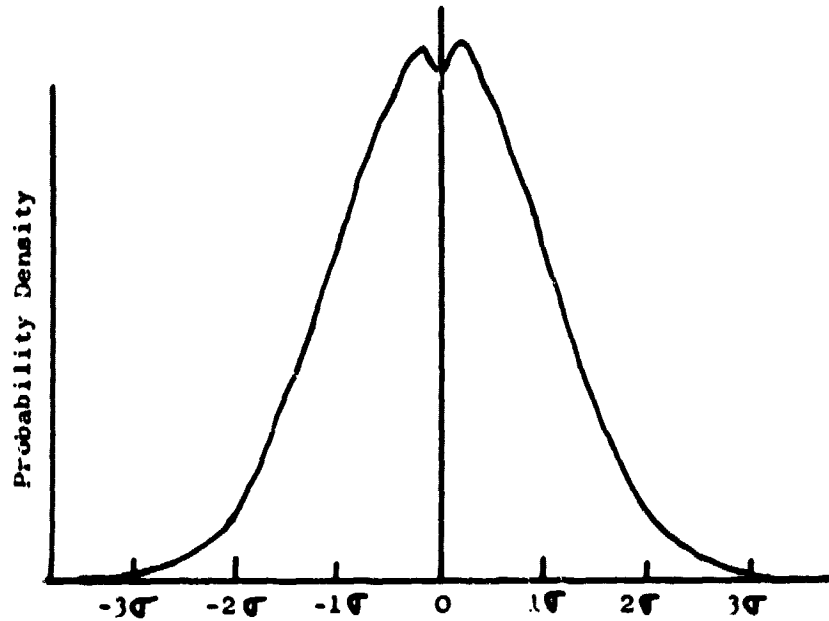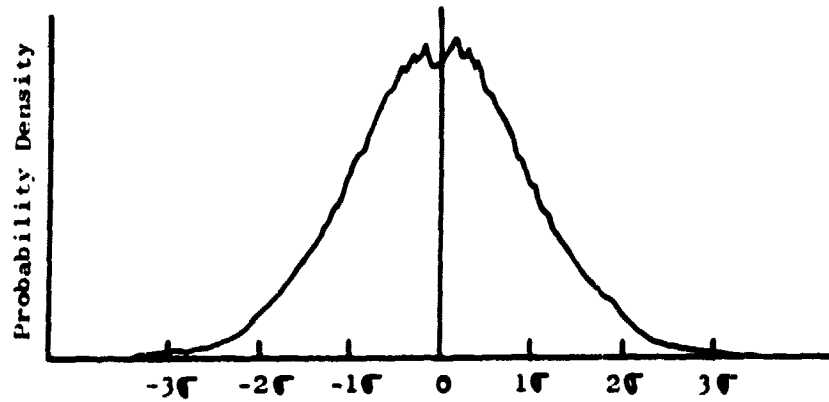
Figure 40. Baseline Aft-Radiated Source Noise Characteristics.

Directional array results for the BPF of the baseline configuration, in Figure 41, indicate that takeoff inlet-radiated noise is about equal to exhaust-radiated noise at 100°. At 110° and 120° the BPF is dominated by exhaust-radiated noise. Similar results are shown for approach in Figure 42. Here the inlet-radiated BPF component at 100° and 110° is down about 5 dB from the exhaust-radiated BPF, while at 120° the BPF is clearly from exhaust-radiated noise.

### 5.2.1.2  Comparison to Other Engines

Aft-radiated fan noise comparisons can be made as a function of fan pressure ratio. Figure 43 compares takeoff fan pressure ratios of fans of similar diameters and thrust levels such as Quiet Engine Fans A and C and the NASA Quiet Fans. Such a comparison is roughly a comparison of fan loading and shows that fans such as QF6 and QF9 are more lightly loaded than QF5.

The OTW aft noise levels are compared to other fans (without adjusting for size or fan pressure ratio) in Figure 44. On such a basis the OTW noise levels are higher than QF6 and QF9 as one would expect from fan pressure ratio or loading consideration. OTW levels are lower than the other higher pressure ratio fans. This indicates that the OTW exhaust-radiated baseline fan levels are generally as one would expect when compared to other fans of about the same diameter and thrust.

### 5.2.2  Exhaust Suppression

A schematic of the fan treatment is shown in Figure 45. The core exhaust treatment design shown in Figure 46 consisted of a stacked treatment design which incorporated high frequency turbine treatment and low frequency core suppression. On the fully suppressed configuration (test number 12) all of the fan and core suppression was installed. On the partially suppressed configuration (test number 14), the core was hard wall and the 1.02 m (40 in.) acoustic splitter was removed.

### 5.2.2.1  Far Field Results

Far field PNL's at three aft angles are compared as a function of fan speed in Figure 47. The indicated suppression of the fully suppressed engine compared to the baseline is on the order of 3 to 4 PNdB. However, at takeoff and approach, where jet noise has been removed, the PNL suppressions are 5 and 6 PNdB, respectively. These observed suppressions are about half of the anticipated total exhaust suppressions (Reference 2) of 11 and 11.6 PNdB. Figures 48 to 50 compare 120° SPL spectra for the baseline and fully suppressed engine at approach, takeoff, and at 95 percent fan speed with 11.5° side door. Superimposed on these spectra are jet noise spectra scaled from Reference 12. These comparisons indicate that suppression levels at low frequencies are masked by jet noise and therefore unknown. At the BPF, jet noise does not completely mask the fully suppressed BPF. At high frequencies of 4 to 10 kHz there is little or no suppression observed.

60

- Takeoff Power
- 1600 Hz 1/3 Octave Band SPL (Contains BPF)
- 30.5 m (100 Ft.) Arc
- Baseline Engine

- 100° Acoustic Angle
- Reading 6-28

- 110° Acoustic Angle
- Reading 6-27
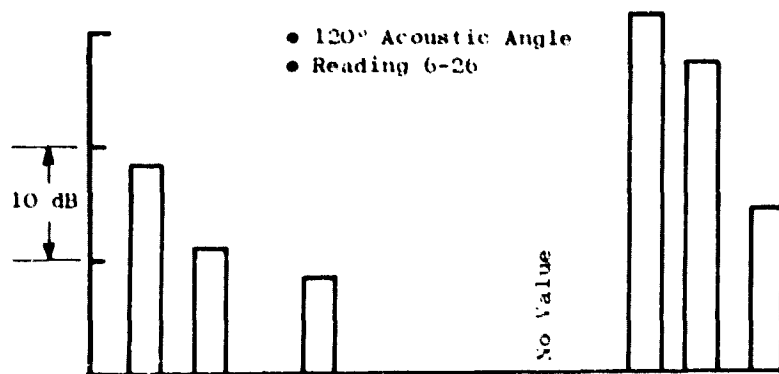
- 120° Acoustic Angle
- Reading 6-26
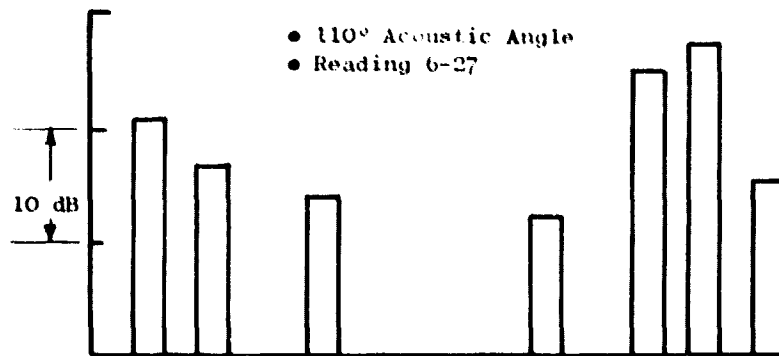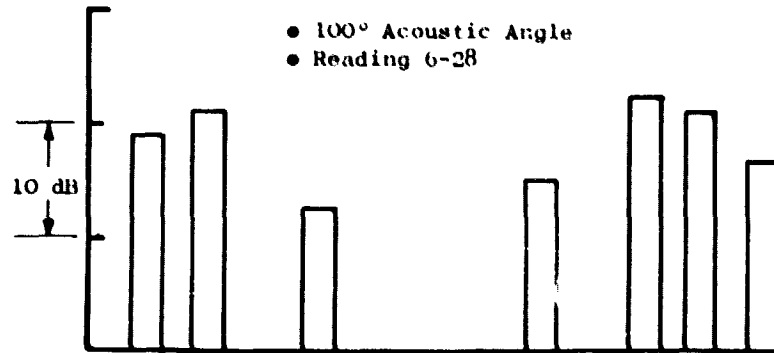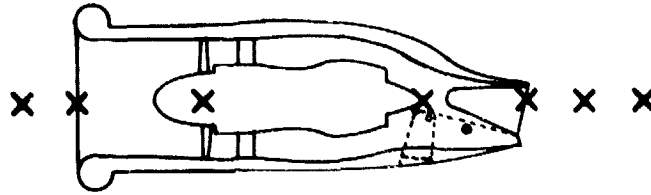
Figure 41.   Directional Array Baseline BPF SPL's at
Takeoff for 100°, 110°, and 120°.

- Baseline Engine
- Approach Power
- 1600 Hz 1/3 Octave Band SPL (Contains BPF)
- 30.5 m (100 Ft.) Arc

- 100° Acoustic Angle
- Reading 6-33

- 110° Acoustic Angle
- Reading 6-34
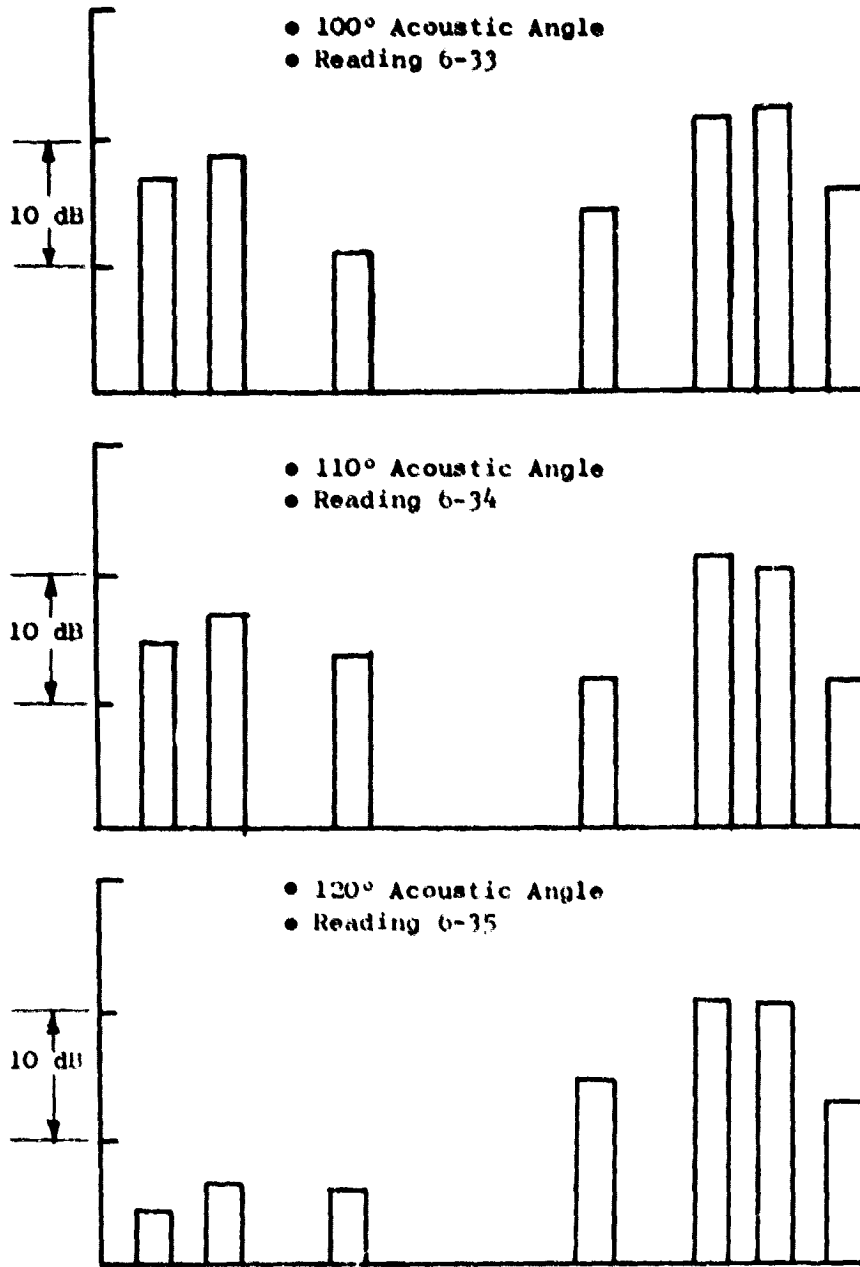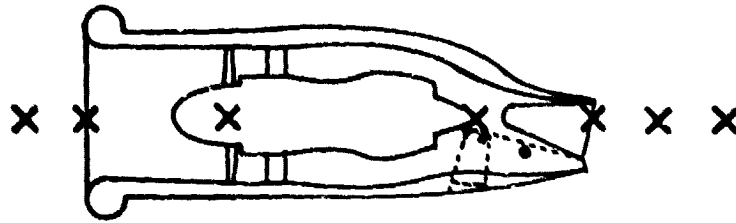
- 120° Acoustic Angle
- Reading 6-35

Figure 42.   Directional Array Baseline BPF SPL's at Approach
for 100°, 110°, and 120°.
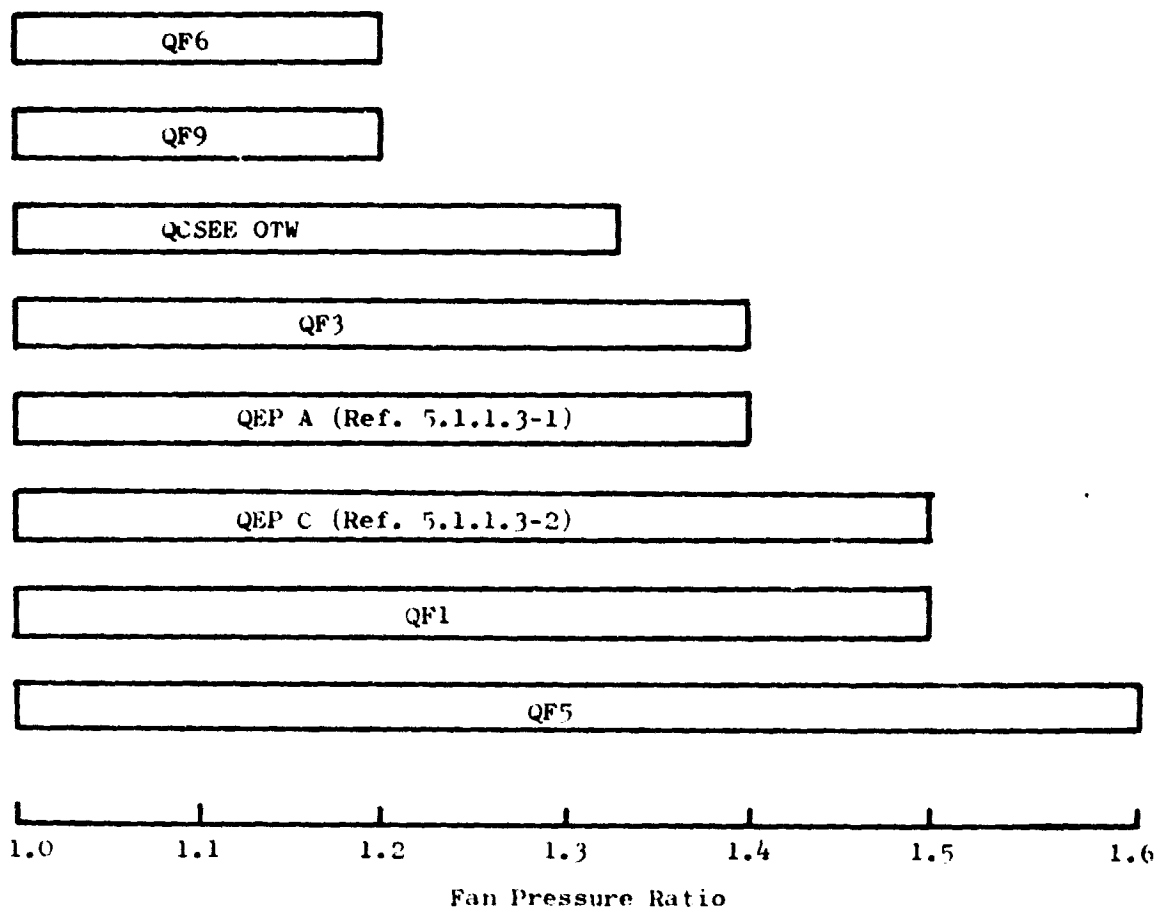
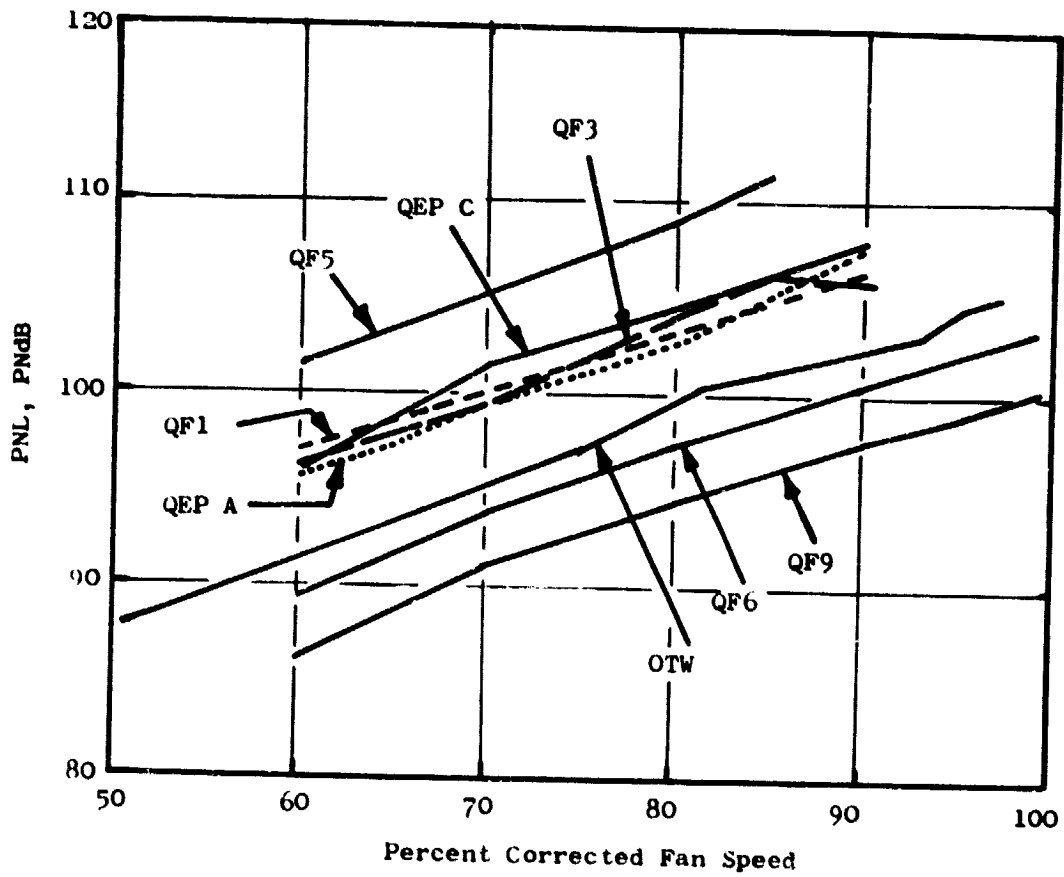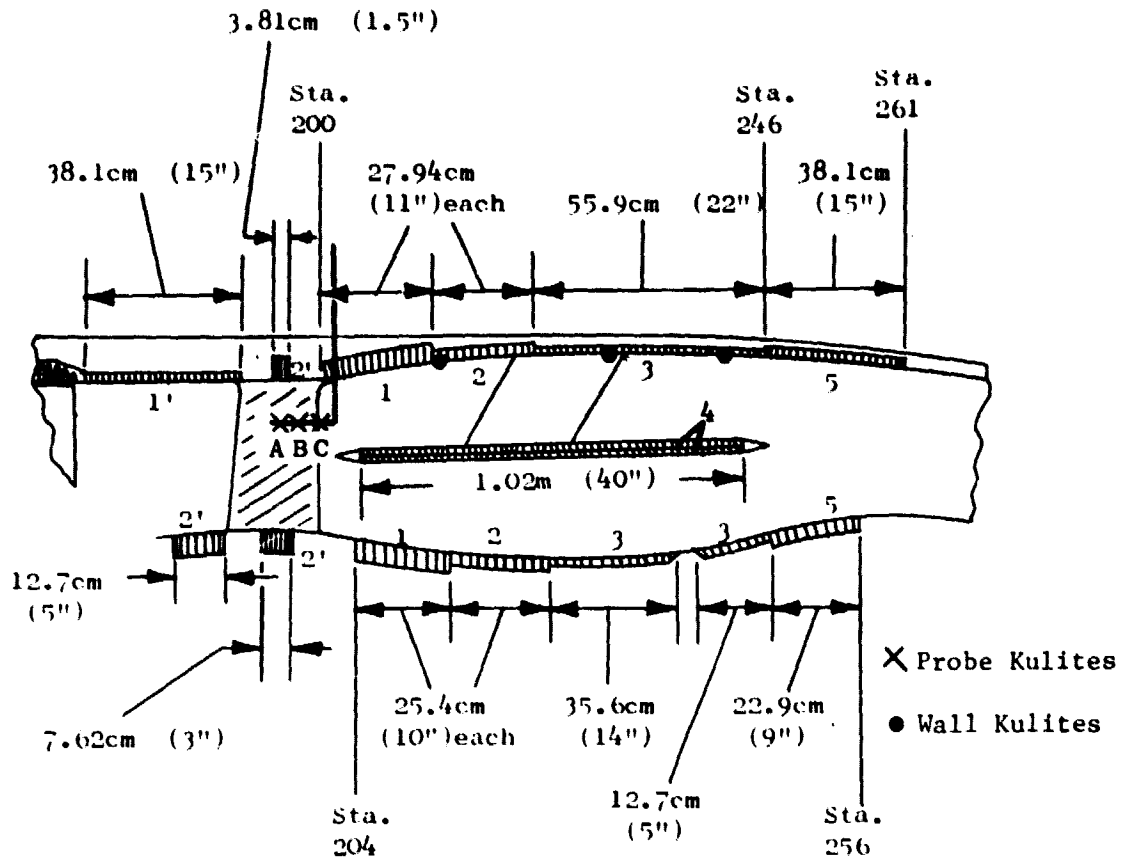Figure 43. Comparison of QCSEE OTW Fan Pressure Ratio With Other Fans.

Figure 44. Comparison of QCSEE OTW Aft Radiated PNL's With Other Engines.

3.81cm  (1.5")

38.1cm  (15")

27.94cm (11")each

55.9cm  (22")

38.1cm (15")

Sta. 200

Sta. 246

Sta. 261

1'

2'

A B C

1

2

3

4

5

1.02m  (40")

12.7cm (5")

2'

2'

25.4cm (10")each

35.6cm (14")

22.9cm (9")

7.02cm  (3")

2

3

3

5

12.7cm (5")

Sta. 204

Sta. 256

X Probe Kulites

● Wall Kulites

| | Depth | Porosity | Hole Size | Faceplate Thickness | Tuning Frequency |
|---|---|---|---|---|---|
| **Fan Frame Treatment:** | | | | | |
| Section 1' | 1.90 cm (0.75 in.) | 10% | 0.1589 cm (0.0625 in.) | 0.0889 cm (0.035 in.) | 1600 Hz |
| Section 2' | 5.08 cm (2 in.) | 10% | 0.1589 cm (0.0625 in.) | 0.0889 cm (0.035 in.) | 1000 Hz |
| Treated Vanes | 0.76 cm (0.3 in.) | 10% | 0.1589 cm (0.0625 in.) | 0.127 cm (0.05 in.) | 4000 Hz |
| **Fan Exhaust Treatment:** | | | | | |
| Section 1 | 5.08 cm (2 in.) | 22% | 0.1589 cm (0.0625 in.) | 0.1016 cm (0.040 in.) | 1250 Hz |
| Section 2 | 2.54 cm (1 in.) | 15.5% | 0.1589 cm (0.0625 in.) | 0.1016 cm (0.040 in.) | 2000 Hz |
| Section 3 | 1.90 cm (0.75 in.) | 15.5% | 0.1589 cm (0.0625 in.) | 0.1016 cm (0.040 in.) | 2500 Hz |
| Section 4 | 1.27 cm (0.5 in.) | 11.5% | 0.198 cm (0.078 in.) | 0.2032 cm (0.080 in.) | 2500 Hz |
| Section 5 | 2.54 cm (1 in.) | 15.5% | 0.1589 cm (0.0625 in.) | 0.1016 cm (0.040 in.) | 1600 Hz |

Figure 45.   Fan Exhaust Duct Treatment Design.

65
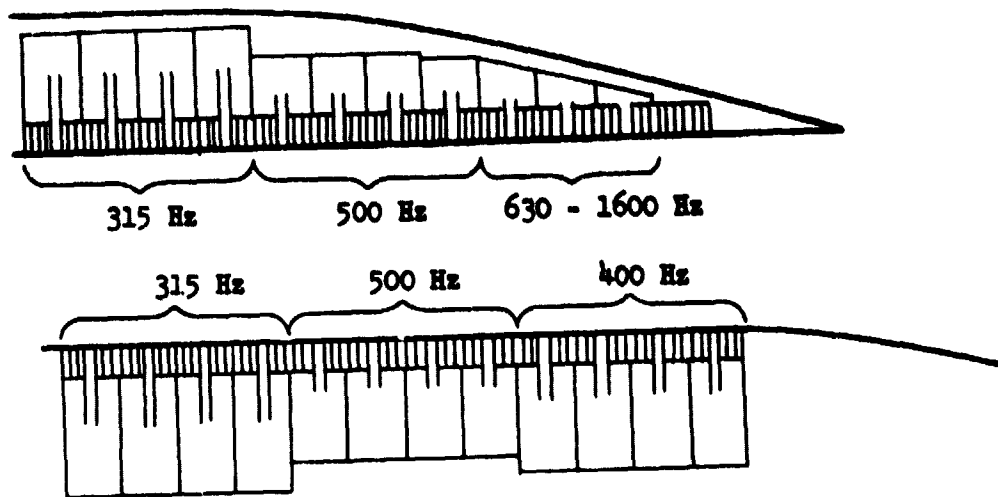
|  | Combustor | | | | | | Turbine |
|  | Inner Wall | | | Outer Wall | | | Both Walls |
|---|---|---|---|---|---|---|---|
| Tuning Frequency, Hz | 315 | 400 | 500 | 315 | 500 | 630 - 1600 | 3150 |
| Neck Length, cm<br>(Faceplate Thick.)(in ) | 6.99<br>(2.75) | 5.72<br>(2.25) | 4.45<br>(1.75) | 6.99<br>(2.75) | 4.45<br>(1.75) | 3.56 - 2.54<br>(1.4)-(1.0) | .08128<br>(.032) |
| Cavity Depth, cm<br>(in ) | 10.2<br>(4.0) | 8.89<br>(3.5) | 7.62<br>(3.0) | 7.62<br>(3.0) | 4.32<br>&5.08<br>(1.7)<br>&(2) | 4.06 - .51<br>(1.6)-(.2) | 1.905<br>(.75) |
| Porosity | 10% | 10% | 10% | 7% | 7% | 7% | 10% |
| Treatment Length cm<br>(in) | 20.32<br>(8.0) | 20.32<br>(8.0) | 20.32<br>(8.0) | 20.32<br>(8.0) | 15.24<br>&5.08<br>(6.0)<br>&(2.0) | 20.32<br>(8.0) | 60.96<br>(24.0) |
| Hole Diameter, cm<br>(in ) | 1.52<br>(.6) | 1.52<br>(.6) | 1.52<br>(.6) | 1.52<br>((.6) | 1.52<br>(.6) | 1.52<br>(.6) | .1575<br>(.062) |

Figure 46. Core Exhaust Treatment Design.

- 152.4 m (500 Ft.) Sideline

○ Baseline Bellmouth
□ Fully Suppressed
△ Partially Suppressed

Open Symbols = 11.5° Side Door Angle
Solid Symbols = 25° Side Door Angle
Flagged Symbols = Jet Noise Removed
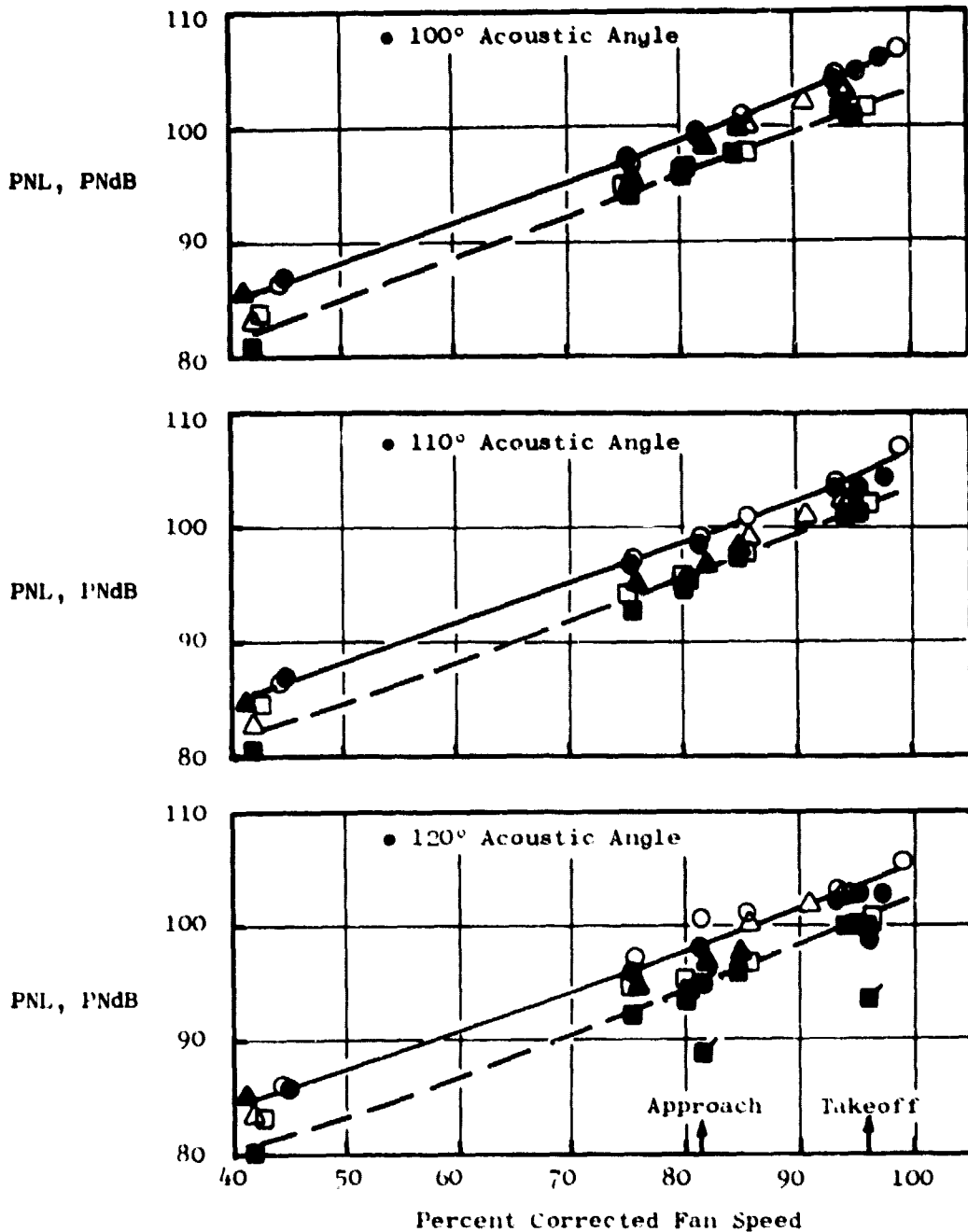
Figure 47. Aft Radiated PNL Comparison as a Function of Fan Speed.

67

- 81% Corrected Fan Speed
- 152.4 m (500 Ft.) Sideline
- 25° Side Door Angle
- 120° Acoustic Angle

○  Baseline Bellmouth     (6-20)
□  Fully Suppressed       (12-19)
──── Estimated Jet Noise

Figure 48.  Approach Spectra at 120°.

- 95% Corrected Fan Speed
- 152.4 m (500 Ft.) Sideline
- 25°Side Door Angle
- 120° Acoustic Angle

O Baseline Bellmouth (6-22)
☐ Fully Suppressed (12-18)
◇ Hard Accel. Inlet (13-15)
———— Estimated Jet Noise

Figure 49. Takeoff Spectra at 120°.

- 95% Corrected Fan Speed
- 152.4 m (500 Ft.) Sideline
- 11.5° Side Door Angle
- 120° Acoustic Angle

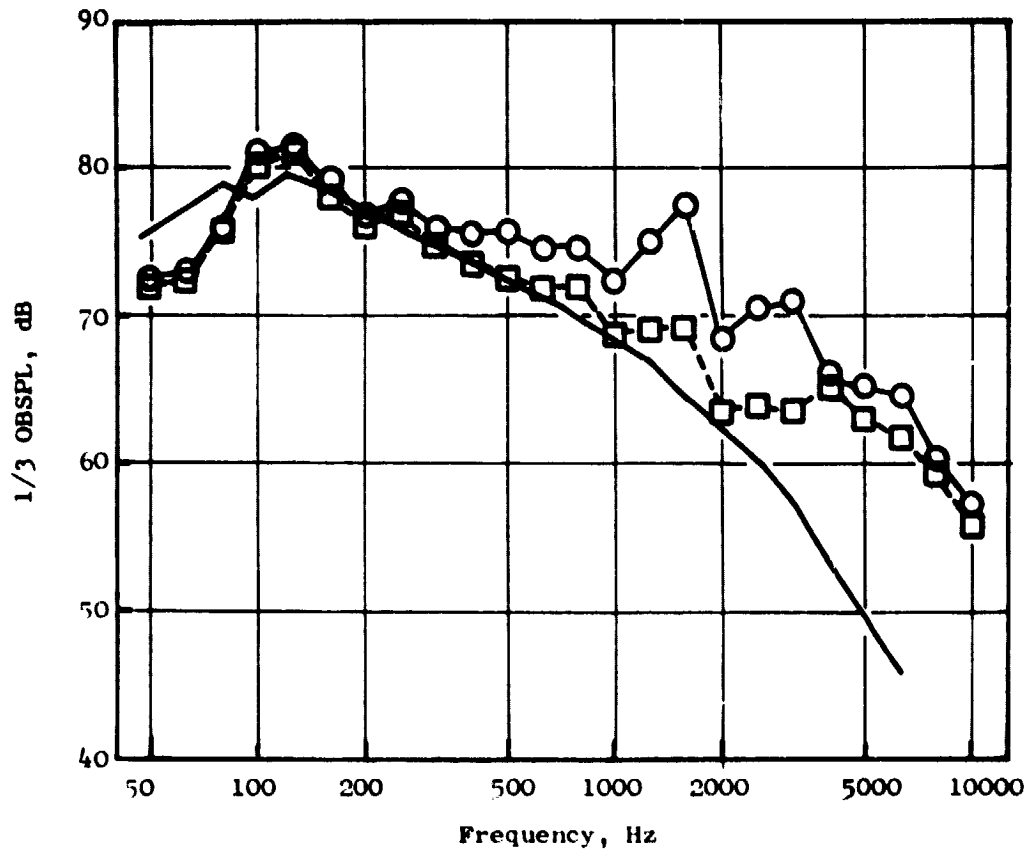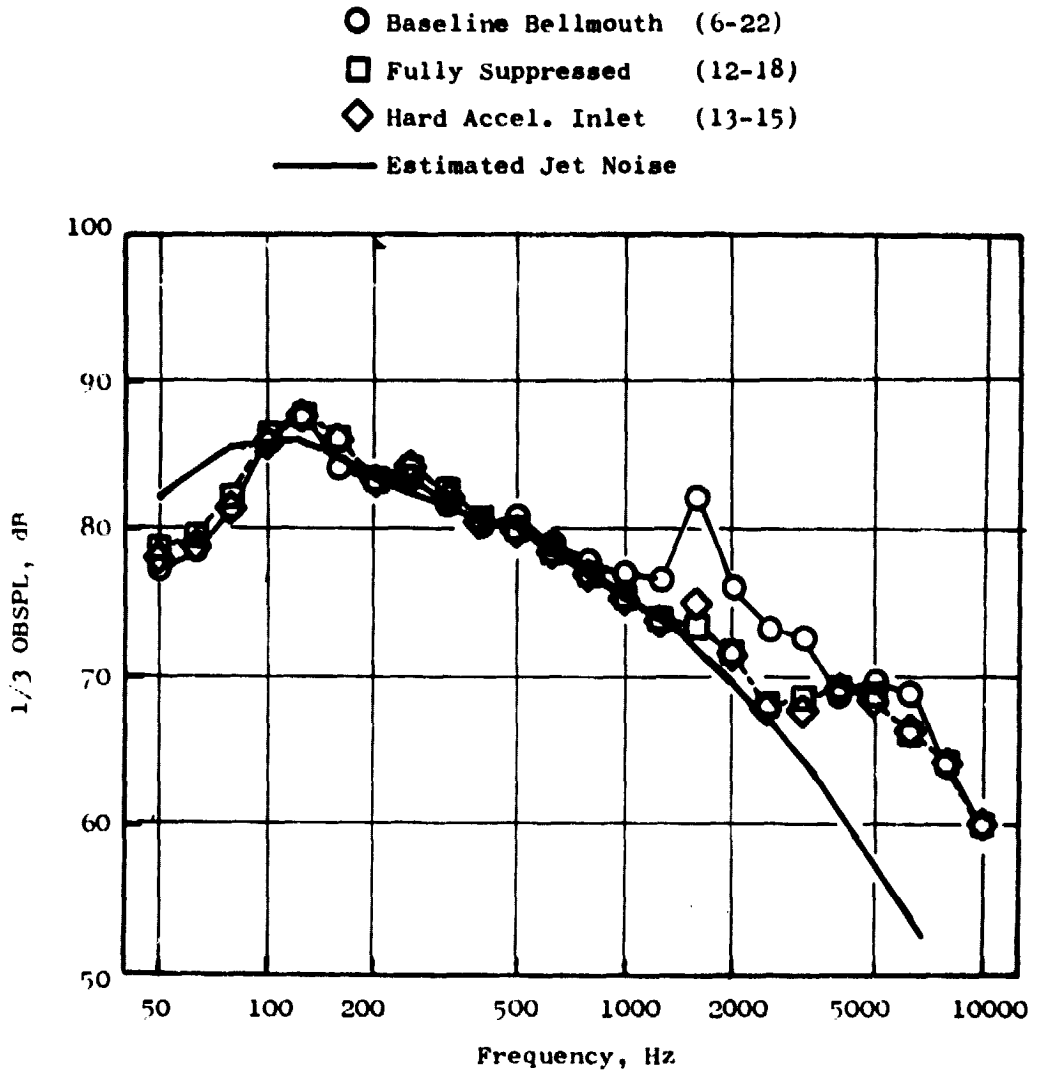○ Baseline Bellmouth    (6-16)

□ Fully Suppressed      (12-10)

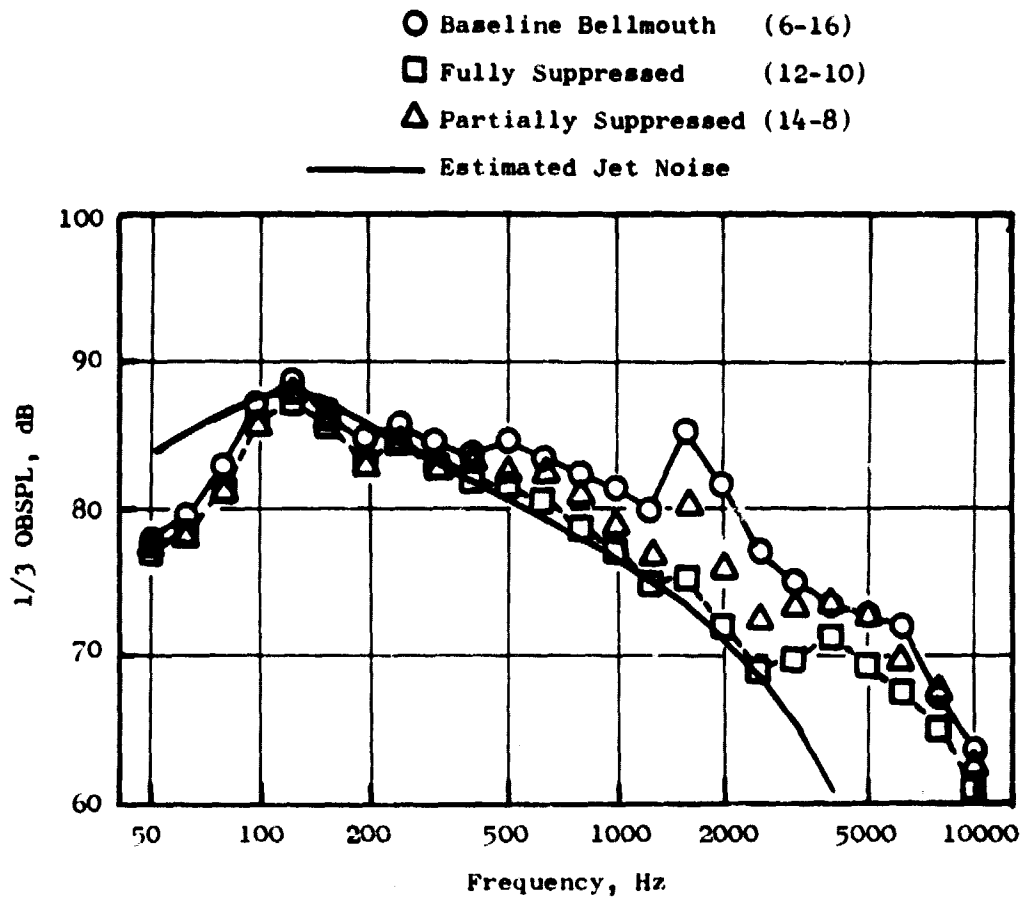△ Partially Suppressed (14-8)

——— Estimated Jet Noise

Figure 50.   95% Corrected Fan Speed, 11.5° Side Door Angle Spectra at 120°.

Narrowband spectra as presented in Figure 51 show that the fully suppressed spectra still has a BPF and harmonics which have not been completely suppressed.

Figure 52 compares the measured suppression spectra (corrected for jet noise) to predicted exhaust suppression. Measured suppression was obtained from both 11.5° and 25° side door positions at near 95 percent corrected fan speed. The 25° side door data begin at 1600 Hz due to jet noise masking engine noise at lower frequencies. The measured suppression from 640 Hz to 1600 Hz from the 11.5° side door data is nearly as predicted. Above 2000 Hz the suppression is 0 to 4 dB in the far field and much lower than predicted.

As a check to see if noise was reaching the far field from other sources such as the inlet or casing, directional array results were analyed for the fully suppressed configuration. At 120° in the far field, Figure 53 compares BPF and second harmonic levels from the various aiming points on the engine. The noise at the far field is exhaust radiated for these two frequency bands. The directional array could not be used for higher frequency bands because the angular separation between aiming points on the engine correspond to side lobes in the array and prevented discrimination of sources. This means that the lack of BPF and second harmonic suppression in the exhaust is not due to fan noise reaching the far field via a flanking path external to the engine. However, there might be an internal flanking path which bypasses the treatment. At this point the existance of a flanking path for the fan tones is conjecture and cannot be substantiated.

As was noted in Figure 52 there is an apparent lack of suppression evident at the high frequencies of 4000 Hz and above. Although early design studies (References 1 and 3) had indicated that treatment regenerated flow noise would not contribute significantly to engine noise levels, a reevaluation of those studies uncovered several errors in those early analyses (see Appendix B for details). Figure 54 presents calculated flow noise sound power levels (PWL) and compares them to engine PWL's. A series of Mach numbers was considered in the duct to bracket the estimated fan duct Mach number of 0.38 from Reference 4. It is apparent that treatment regenerated flow noise is of sufficient magnitude to mask the suppressed fan exhaust noise and thus the level of fan exhaust suppression achieved.

The engine tests included a configuration which had a partially suppressed exhaust. This was achieved by removing the splitter from the fully suppressed fan duct and by replacing the stacked core treatment with hard wall panels. A comparison of measured and predicted suppression at 95 percent fan speed and 11.5° side door angle is given in Figure 55. Up to 2500 Hz, there is good agreement between measured and predicted suppression. However, above 2500 Hz, the suppression falls off and is well below predicted. The splitter when comparing Figures 52 and 55, does account for some fan noise suppression.

Most of the suppression discussed has been in the frequency regions associated with fan noise. As shown in the schematic in Figure 46, much of the stacked treatment in the core is tuned to low frequencies near 400 Hz. Figure 56 compares spectra measured at approach up to 800 Hz. Jet noise

- 95% Corrected Fan Speed
- 25° Side Door Angle
- 120° Acoustic Angle
- 20 Hz Bandwidth
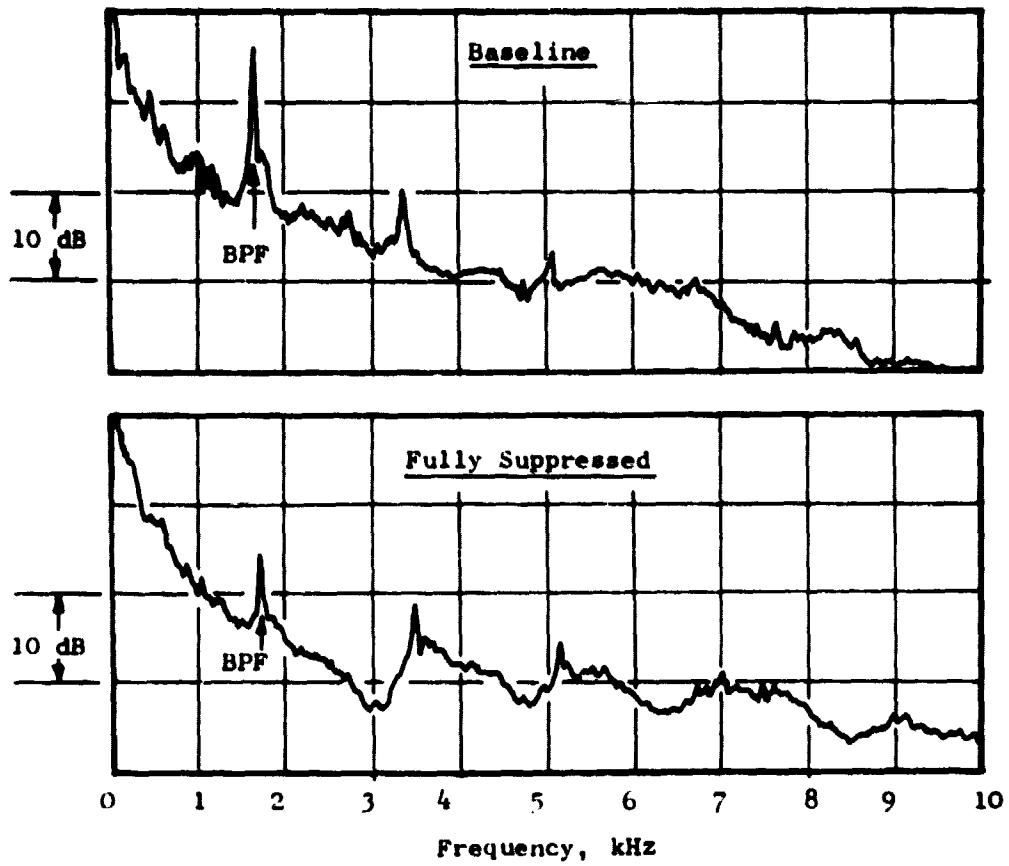


Figure 51. Exhaust Narrow Band Spectra at Takeoff.

Figure 52. Measured Takeoff Exhaust Suppression - Fully Suppressed Engine.

- Takeoff Power
- 120° Acoustic Angle
- 30.5 m (100 Ft.) Arc
- Reading 12-37



- 1600 Hz Fan BPF

10 dB

- 3150 Hz Fan Second Harmonic

10 dB
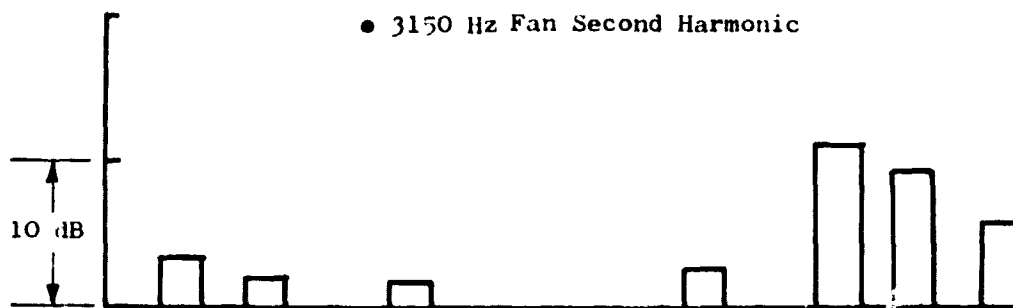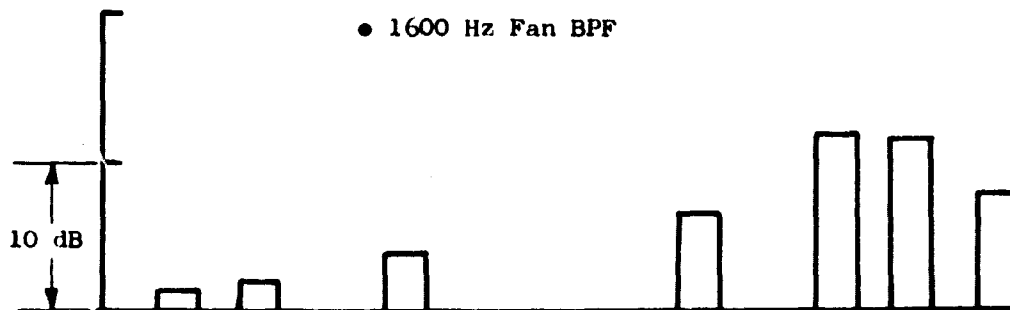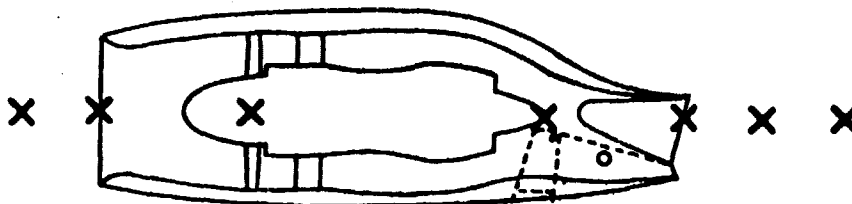
Figure 53.  Directional Array Levels at 120° - Fully Suppressed Engine.
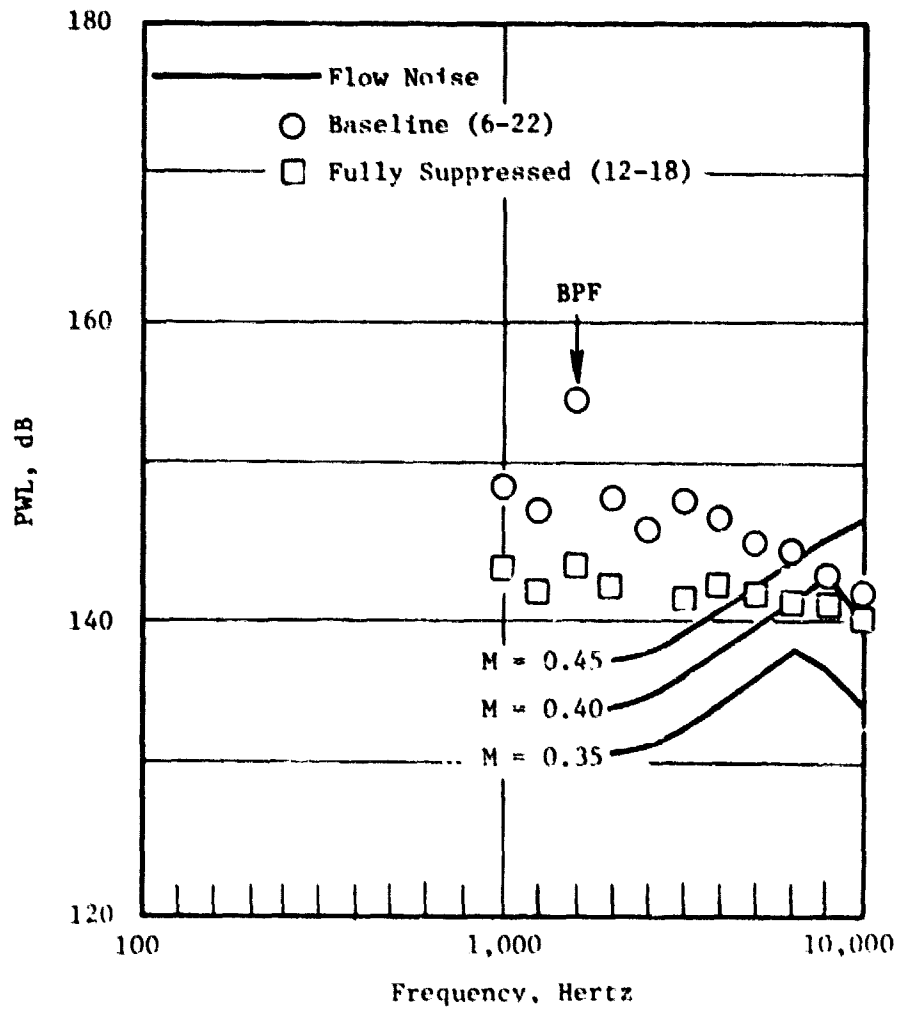
Figure 54. Comparison of Predicted Treatment Regener-
ated Flow Noise and Measured Engine Noise.

- Partially Suppressed , Test 14
- Takeoff Power
- 120° Acoustic Angle
- 152.4 m (500 Ft.) Sideline
- Relative to Baseline
- Jet Noise Removed
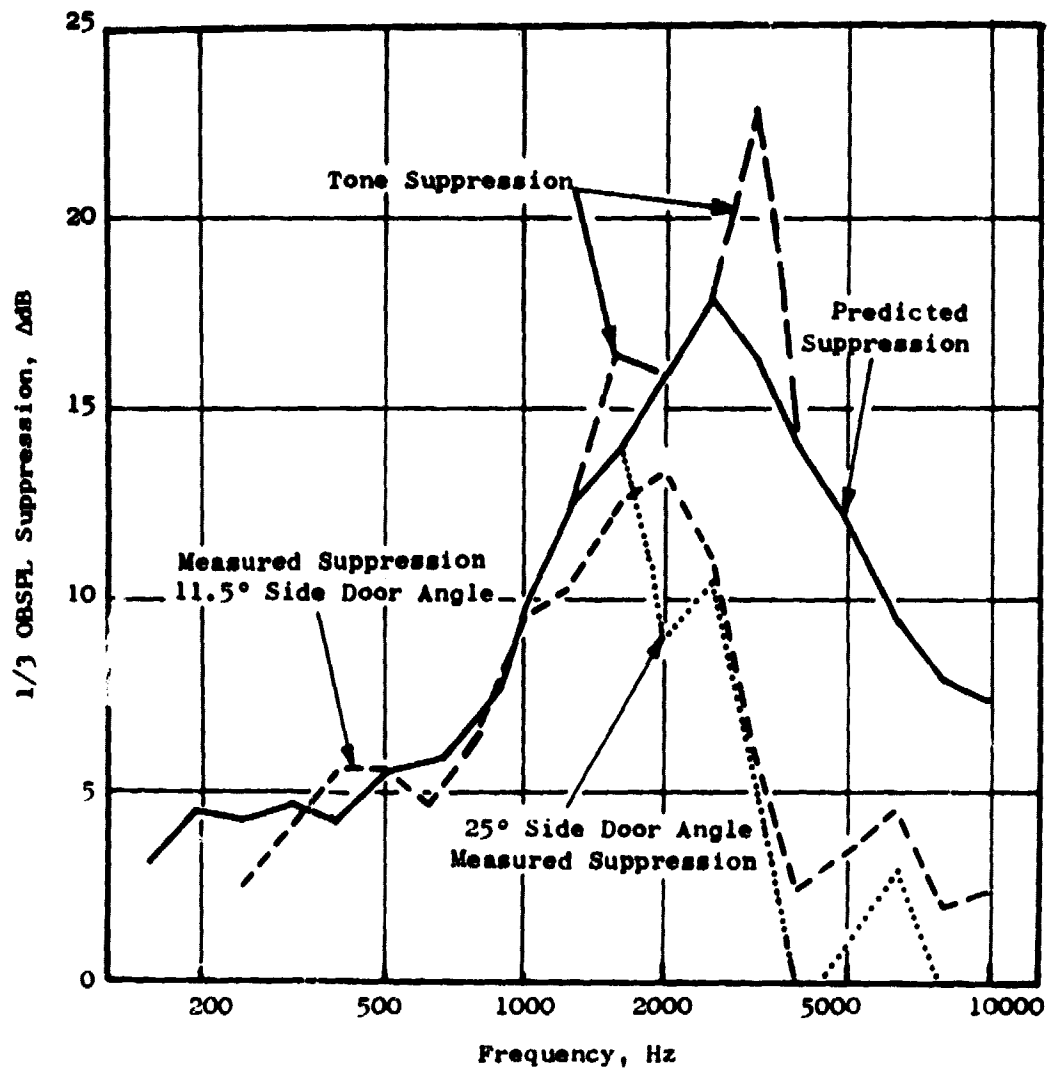- 11.5° Side Door Angle
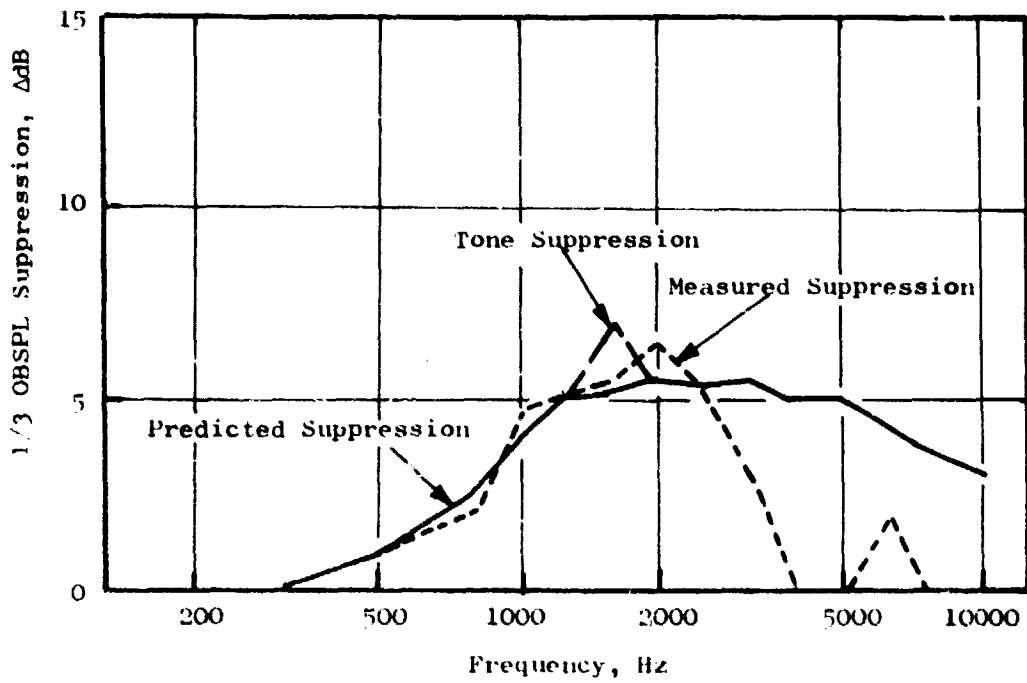


Figure 55. Measured Takeoff Exhaust Suppression – Partially Suppressed Engine.

- Approach Power
- 120° Acoustic Angle
- 152.4 m (500 Ft.) Sideline
- 25° Side Door Angle

| | | |
|---|---|---|
| O | Baseline Bellmouth | (6-20) |
| □ | Fully Suppressed | (12-19) |
| ◇ | Hard Accel. Inlet | (13-12) |
| △ | Partially Suppressed | (14-15) |
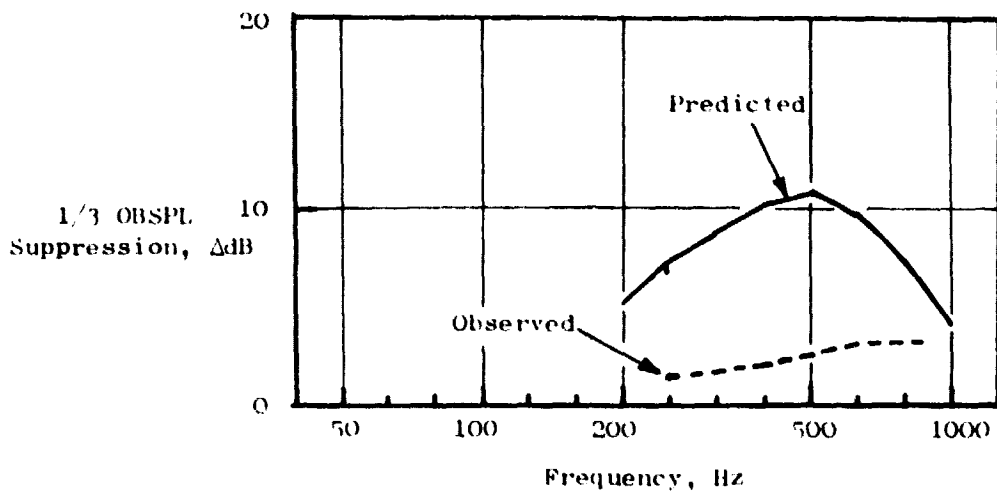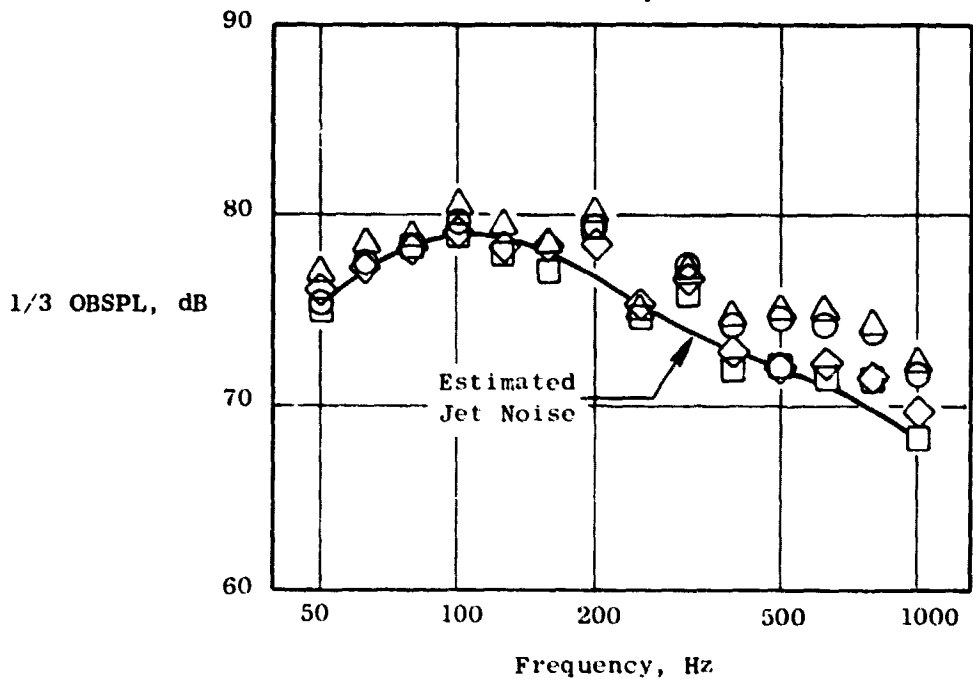


Figure 56.   Low Frequency Suppression.

levels are a floor below which suppressed core noise levels cannot be determined; however, the fact that low frequency suppression is observed from 250 to 800 Hz indicates that the core suppression is attenuating low frequency noise.

### 5.2.2.2  In-Duct Results

The in-duct kulite results were analysed to determine if the trends in the duct agreed with the far field results. Attenuation down the duct from the vane trailing edge is shown in Figure 57. At takeoff speed, the BPF and fan second harmonic attenuation is 12 to 15 dB for both configurations. BPF suppression is about the same as that observed in the far field (see Figure 52); however, the second harmonic attenuation is more than that observed in the far field. Note that the hard wall levels of the second harmonic apparently increase down the duct. Why this happens is not understood; it may be due to some kind of standing wave phenomena in the duct. At approach, the fully suppressed attenuations are slightly less than the takeoff speed case; while the partially suppressed BPF tone suppression values are 4 to 5 dB less than the fully suppressed values. Also at approach, the hard wall configuration shows an apparent attenuation down the duct for the second harmonic.

Probe surveys were taken at the exit of the "D" nozzle in two vertical planes (see Figure 12). The BPF results are shown in Figure 58 for the three exhaust configurations: baseline, fully suppressed, and partially suppressed. At survey plane number II, which is farthest from the core flow, there is about a 10 dB decrease in the BPF at both high speed and approach power. The partially suppressed levels show a decrease in suppression as one would expect and generally fall between the baseline and fully suppressed levels.

### 5.2.2.3  Modal Analysis and Suppression Prediction

During the OTW test program, in-duct radial modal measurements were performed for selected vehicle configurations in the exhaust duct of the engine. These modal measurements were then used to provide modal source characteristic definition for subsequent prediction of suppression.

Data discussed in this section are at 95 percent corrected fan speed with the 11.5° side door nozzle position and are representative of takeoff conditions.

### 5.2.2.3.1  Exhaust Duct Radial Modal Measurements

Figure 45 shows the location of the modal measurement probe in the exhaust duct of the QCSEE OTW vehicle. The modal measurement probe centerline was located just downstream of the OGV exit plane, and Element C, as shown
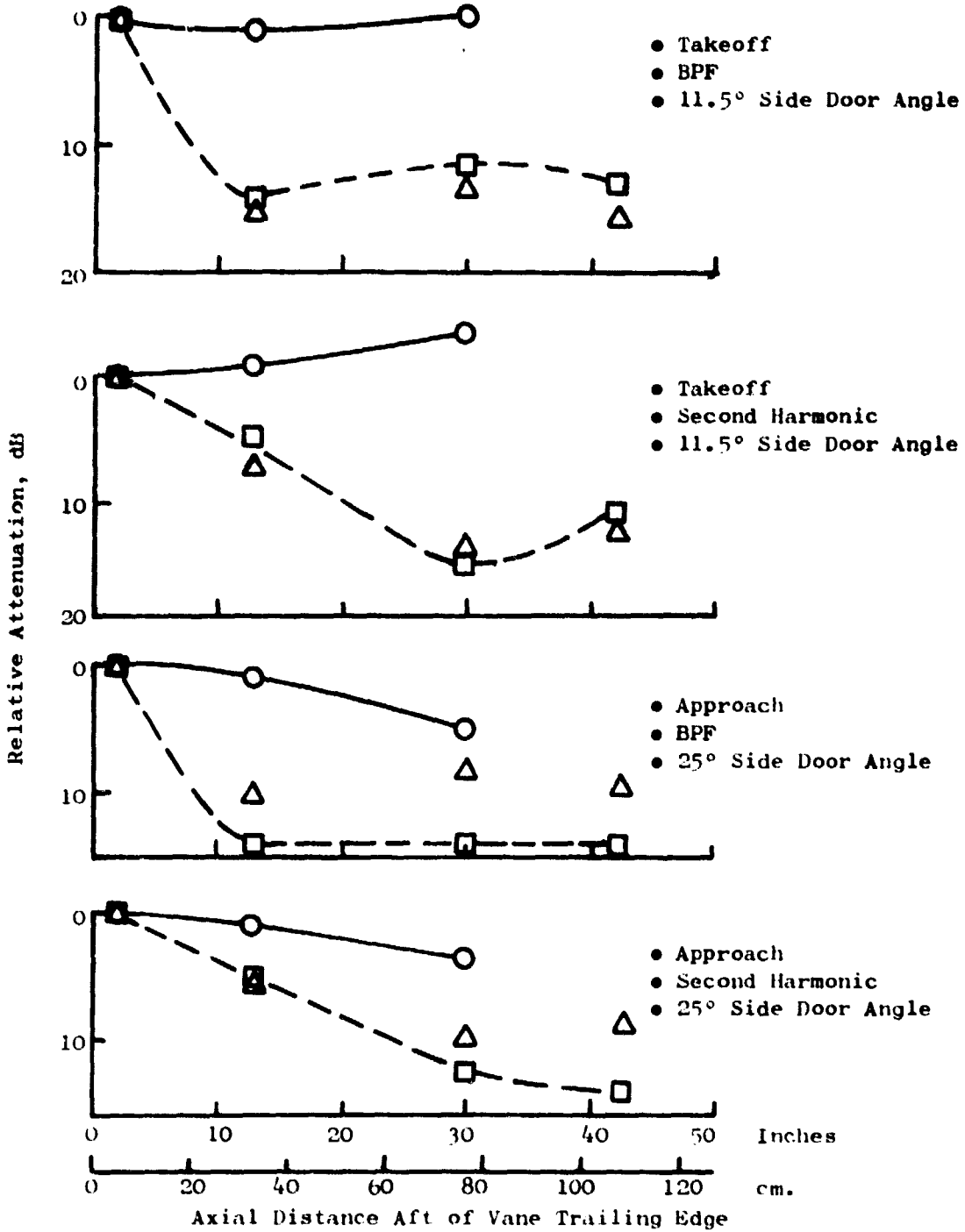
78

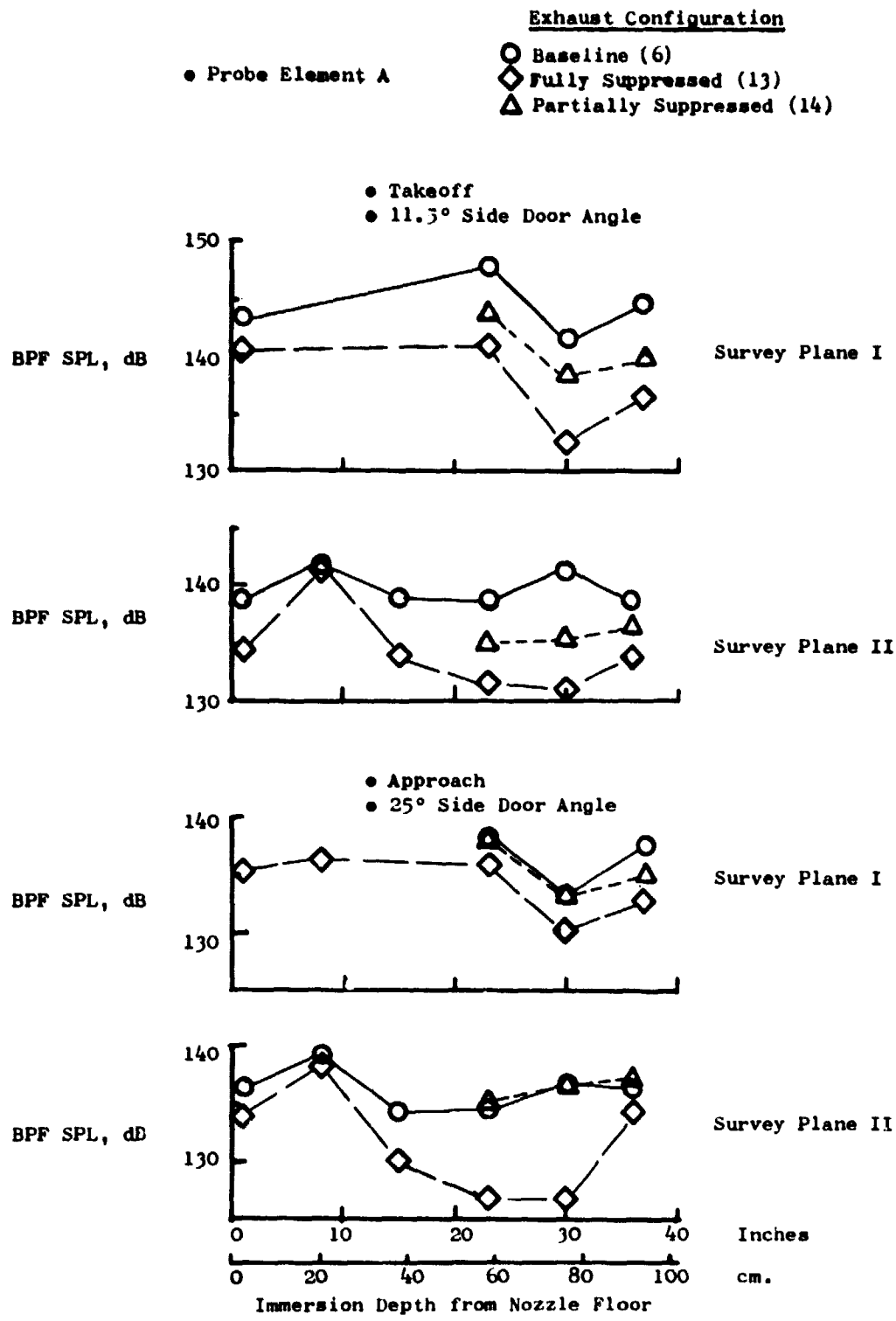Figure 57. Fan Exhaust Duct Tone Attenuation.

Figure 58. "D" Nozzle Probe Surveys.

in Figure 45 was used for the modal measurement. The wall reference Kulite was located 33.7 cm (13.25 inches) downstream of the probe sensor with an azimuthal separation of 97°.

The modal measurement data were reduced in 160 Hz narrow bands using 400 averages. The frequency bands of primary concern are 1760 Hz (blade passing), and 3360 Hz (second harmonic). Plots of the complex pressure profiles for the treated and hard wall configurations are shown in Figures 59 and 60 comparisons of the modal content are made in Figures 61 and 62 for the BPF and second harmonic.

Note the gap in the measured pressure profile from an immersion of about x/H = 0.34 to x/H = 0.56. This was due to a required vibration avoidance band for the probe. It is suspected that the lack of data in this region causes some error in the modal measurement.

The comparison of modal content for the downstream treated and hard wall cases shows very little difference in mode levels. Thus, the downstream treatment had only a small effect on the source characteristics. Based on this result, the modal content measured in the hard wall duct was used as the input to the suppression prediction program.

Figures 63 and 64 show the modal spectra (i.e., modal content measured as a function of frequency) for the hard wall and treated configurations. Note the dominance of the second order mode for both cases at blade passing frequency and the strong contributions of very high order modes at the second harmonic. In the broadband regions, the modes seem to mix with no recognizable pattern. The theoretical cut-on frequency for each mode is noted at the bottom of the plot, and a slight tendency for each mode to "blossom" in relative participation just above its cut-on point can be noted. It should be noted that the measurement is performed in the near field region of the OGV's so that one would expect to see participation of cut-off modes in the measurement even below their cut-off frequencies.

### 5.2.2.3.2 Suppression Prediction

PWL suppression predictions using the analytical techniques of Reference 13 were made for the OTW configuration which had fan exhaust wall treatment only (Configuration 14). Limitations in the prediction program prevented predicting suppression for the case with a splitter in the flowpath. For the prediction, the exhaust duct was modeled as a rectangular duct of unit width and height of 45.7 cm (18 inches).

Two series of prediction calculations were made. The first utilized the measured in-duct modal source characteristics for the first six modes while the second series assumed that only the lowest order mode was present. Treatment panel impedances were obtained from standard perforated faceplate/honeycomb single-degree-of-freedom impedance models (Reference 14) including the effect of mean flow. Results are shown in Figure 65. Assuming only lower modes are present in the duct lowers the peak suppression and results in less suppression bandwidth. The lowest order mode predicted

- Takeoff
- BPF
- 160 Hz Bandwidth
- 11.5° Side Door Angle

Exhaust Configuration

○ Baseline (6-68)
□ Fully Suppressed (12-46)
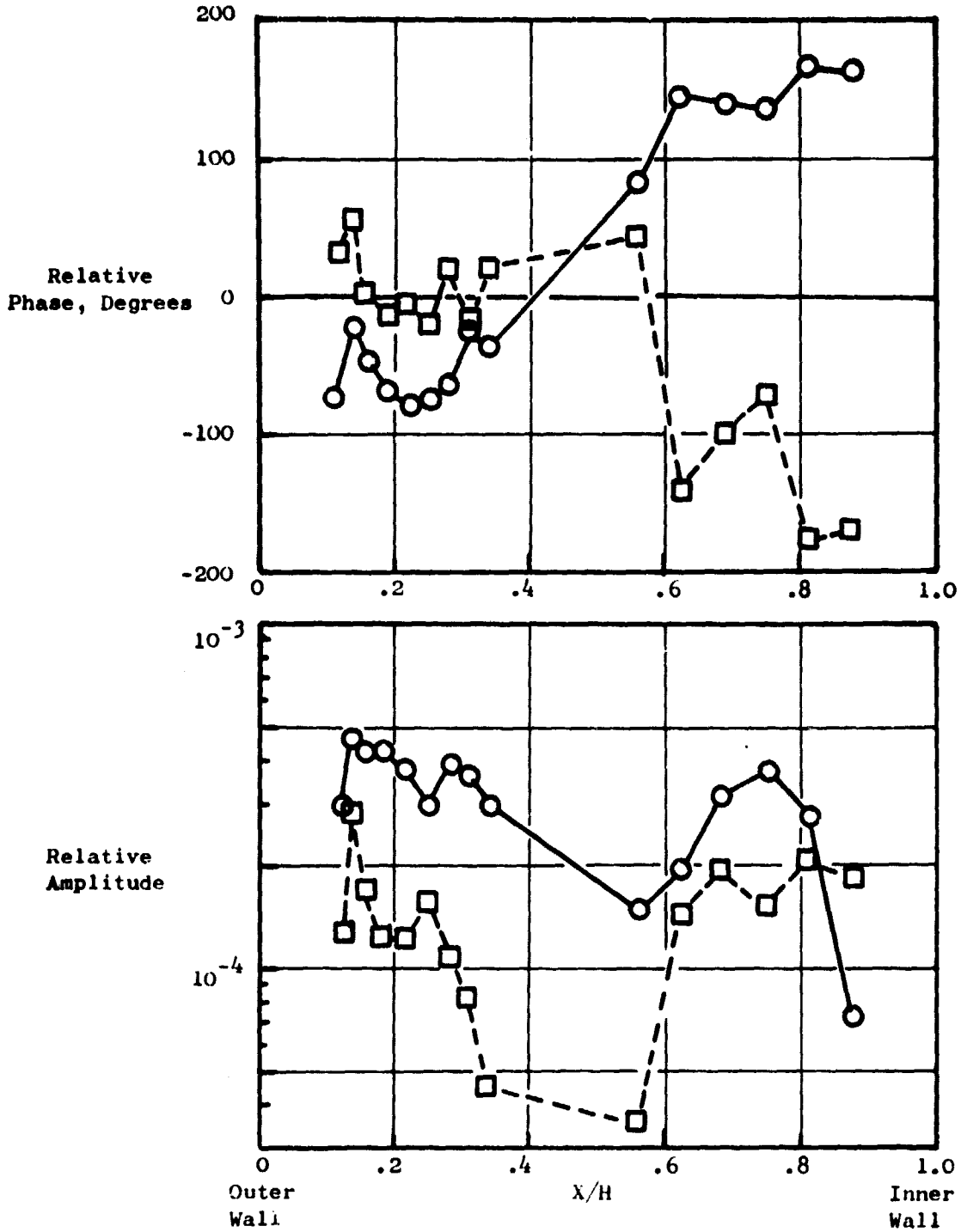
Figure 59.  BPF Complex Pressure Profiles.

82

- Takeoff
- Second Harmonic
- 160 Hz Bandwidth
- 11.5° Side Door Angle

Exhaust Configuration

○ Baseline (6-68)
□ Fully Suppressed (12-46)
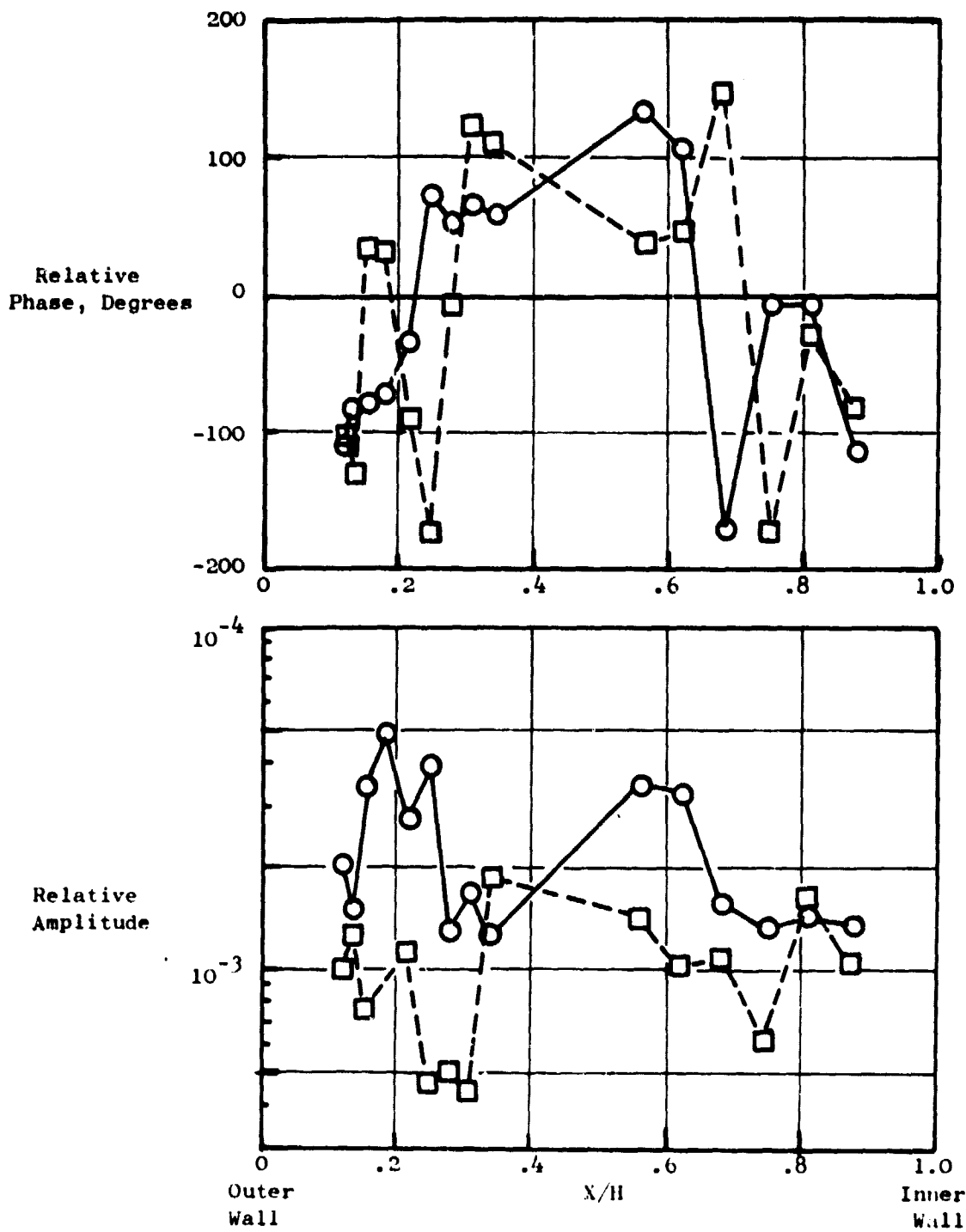
Figure 60.    Second Harmonic Complex Pressure Profiles.

- Takeoff
- BPF
- 160 Hz Bandwidth
- 11.5° Side Door Angle

Exhaust Configuration
○ Baseline (6-68)
□ Fully Suppressed (12-46)
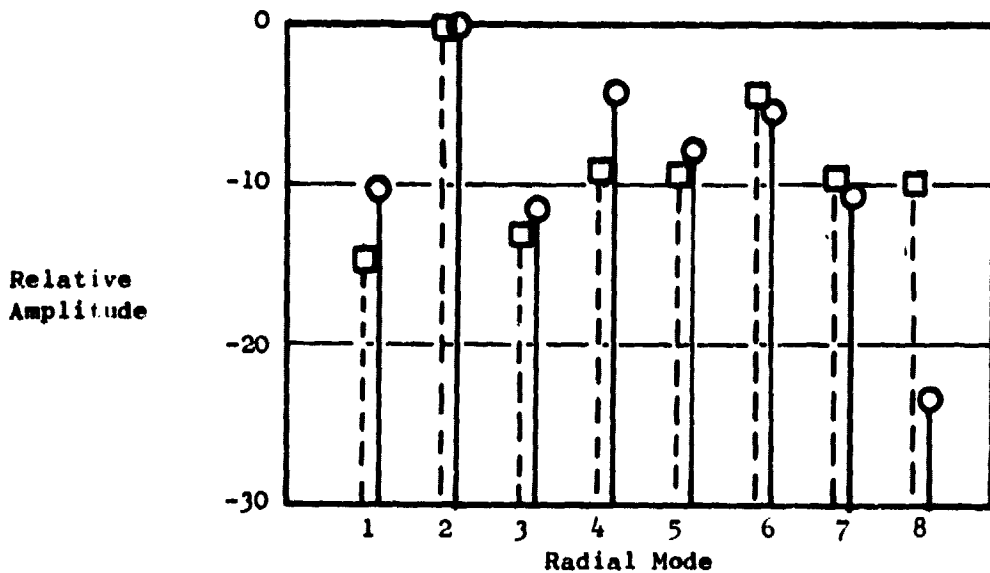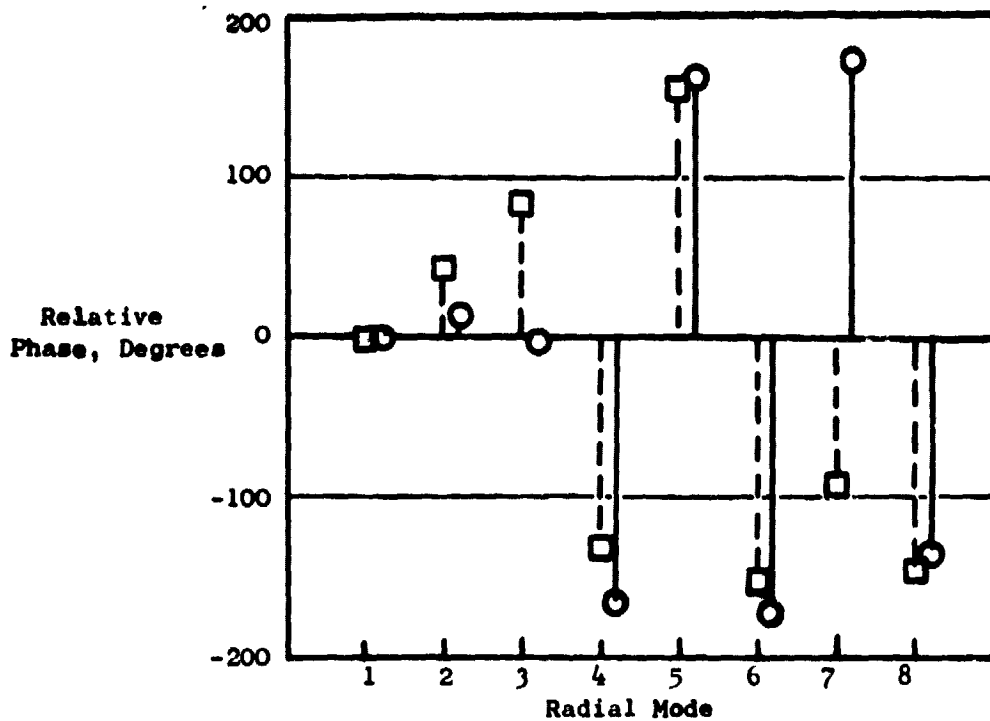
Figure 61.  BPF Modal Content.

Relative
Phase, Degrees

Radial Mode

Relative
Amplitude
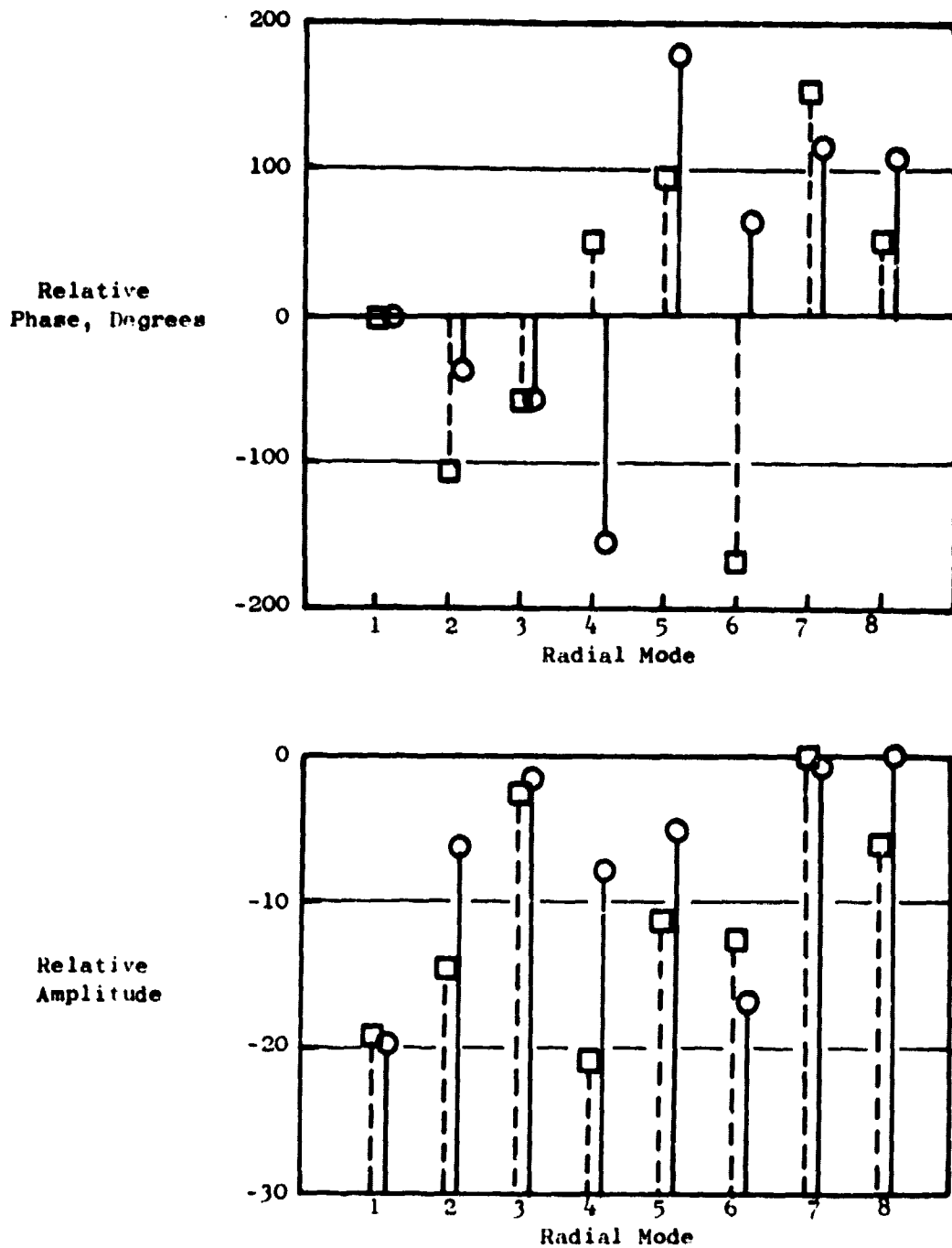
Radial Mode

Figure 62.   Second Harmonic Modal Content.
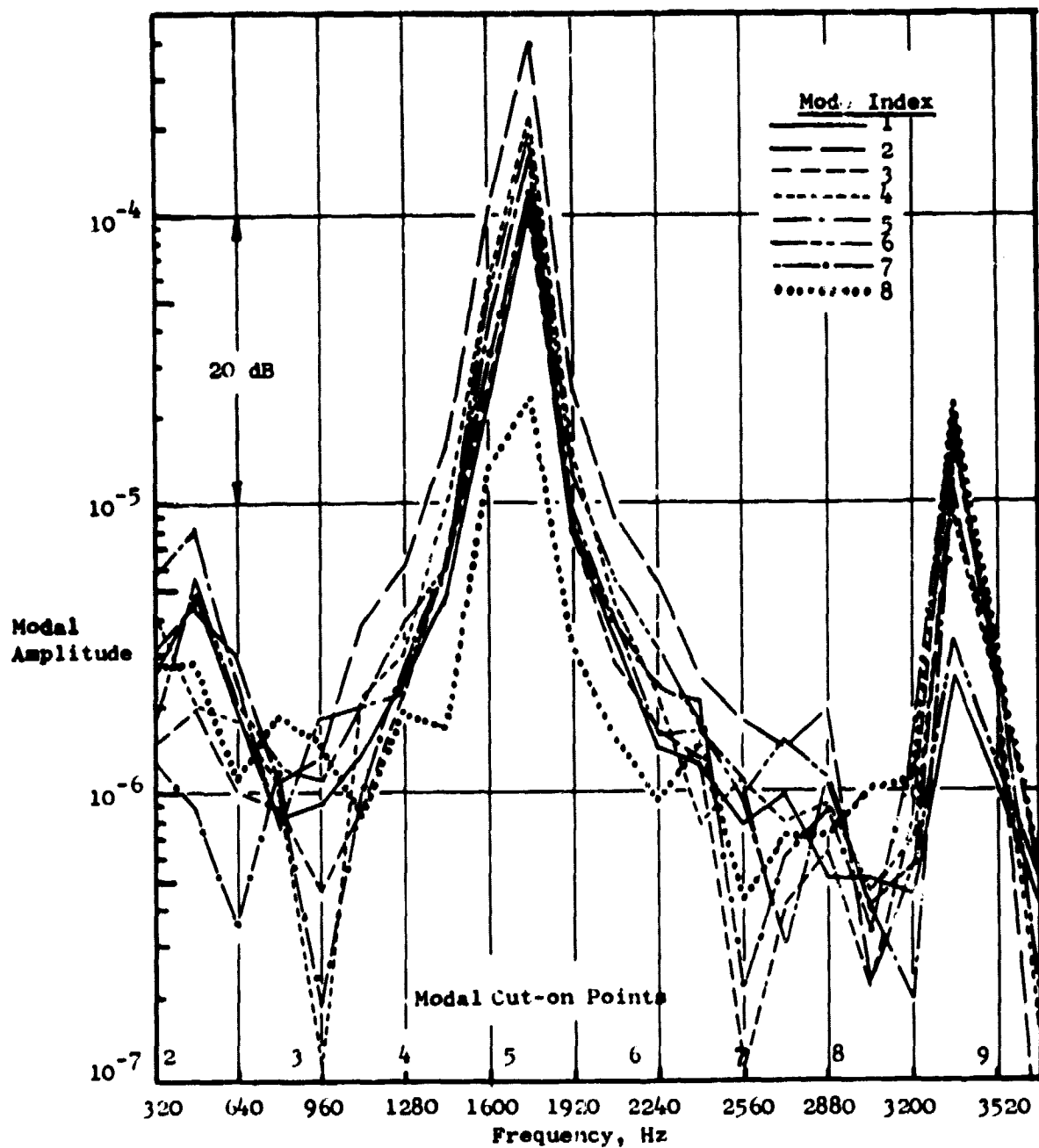
Figure 63. Baseline Radial Mode Spectra.

- 95% Corrected Fan Speed
- Fully Suppressed (12-46)
- 160 Hz Bandwidth
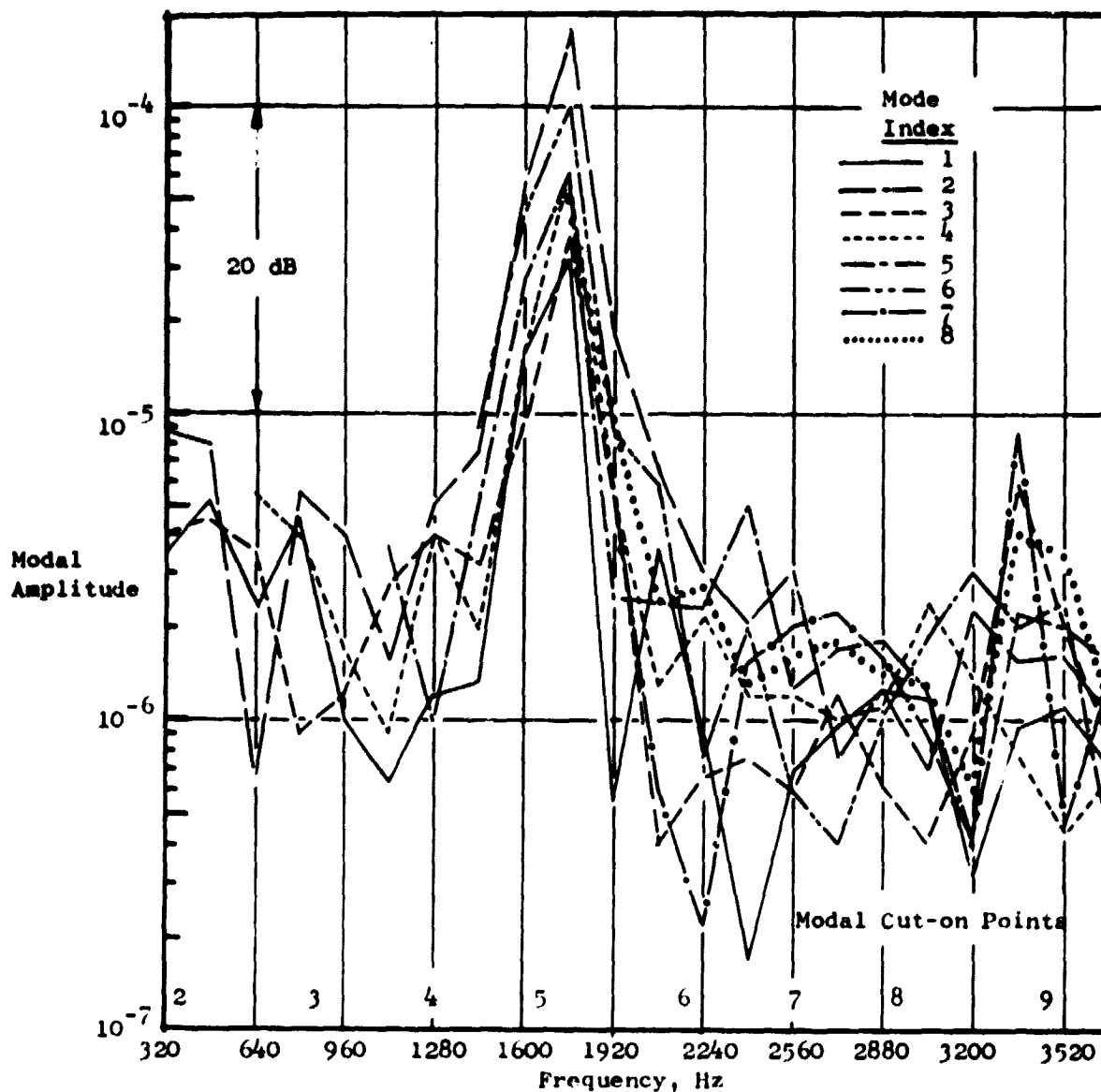
Figure 64.   Fully Suppressed Radial Mode Spectra.
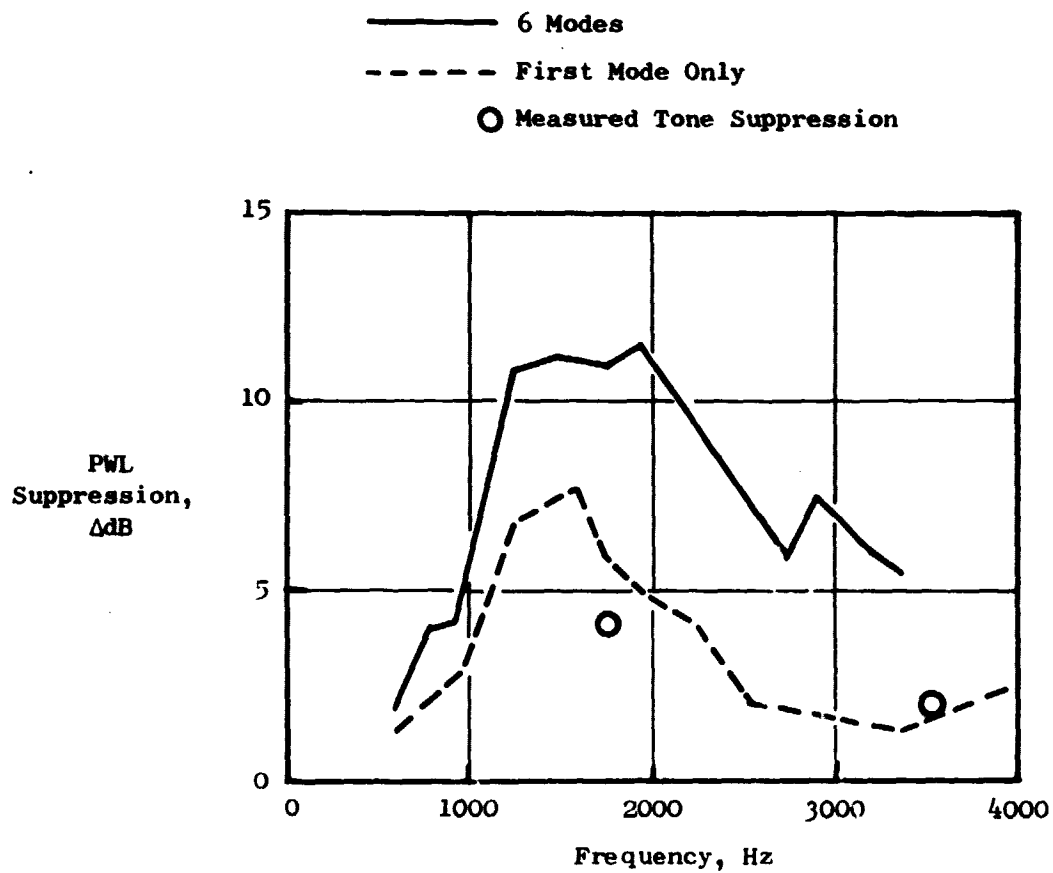
Figure 65.   Predicted and Measured Fan Exhaust Suppression.

c - 2

PWL suppression agrees fairly well with the measured tone PWL suppressions from 20 Hz bandwidth narrowbands. Figure 66 shows the BPF and second harmonic narrowband SPL directivities used to calculate the PWL's.

## 5.3  SPECIAL STUDIES

### 5.3.1  Compressor Stator Variation

The OTW engine has a nominal compressor stator schedule which varies as a function of compressor speed. One of the investigations on the fully suppressed engine included determination of the effect of compressor stator angle on noise at approach power. The need for this comes about when an aircraft has to execute a missed approach. If the compressor could be at high speed (stators closed from the nominal schedule) and generating approach power, then the response time to go to takeoff power would be decreased.

Tests were conducted at approach power with the stators at nominal, +5, and +10 degrees closed from nominal. Corresponding compressor speeds were 12,685, 12,967, and 12,400 rpm, respectively.

Acoustically, there was no significant change in noise at any of the three stator positions. Figures 67 and 68 are typical spectral comparisons at 40° and 120°. This means that the selection of compressor stator angle (nominal to 10° closed) at approach power can be based upon control response criteria with no acoustic penalty.

### 5.3.2  Ground Reflections

When microphones are placed above a reflecting surface as they were for this test, the sound measured at the microphone is the sum of the direct radiated noise and the indirect noise or sound reflected off the surface. These two signals arrive at the microphone with a frequency dependent phase difference and create a series of nulls and reinforcements in the total spectra.

Part of the acoustic instrumentation in the far field sound field included three ground plane microphones at 60°, 90°, and 120°. These microphones were intended to provide information which would allow correction of the 12 m (40 ft) high microphone data to free field. The reader is referred to References 15 and 16 for more extensive discussion of ground reflection theory.

The ground plane microphones, which were placed on a 1.9 cm (0.75 in.) thick sheet of plywood on a pea-gravel base, were used to obtain 6dB or pressure doubling over the lower frequencies. Figure 69 presents ground plane and high microphone baseline levels for takeoff and approach at 60°. 6 dB doubling is evident for only the first four ground plane microphone 1/3-octave bands. Correction of the high microphone data required determination of the phase factor, $\phi$, and the reflection coefficient, Q. The phase factor

○ Baseline (6-68)

△ Partially Suppressed (14-8)

● BPF
● 20 Hz Bandwidth

● Second Harmonic
● 20 Hz Bandwidth
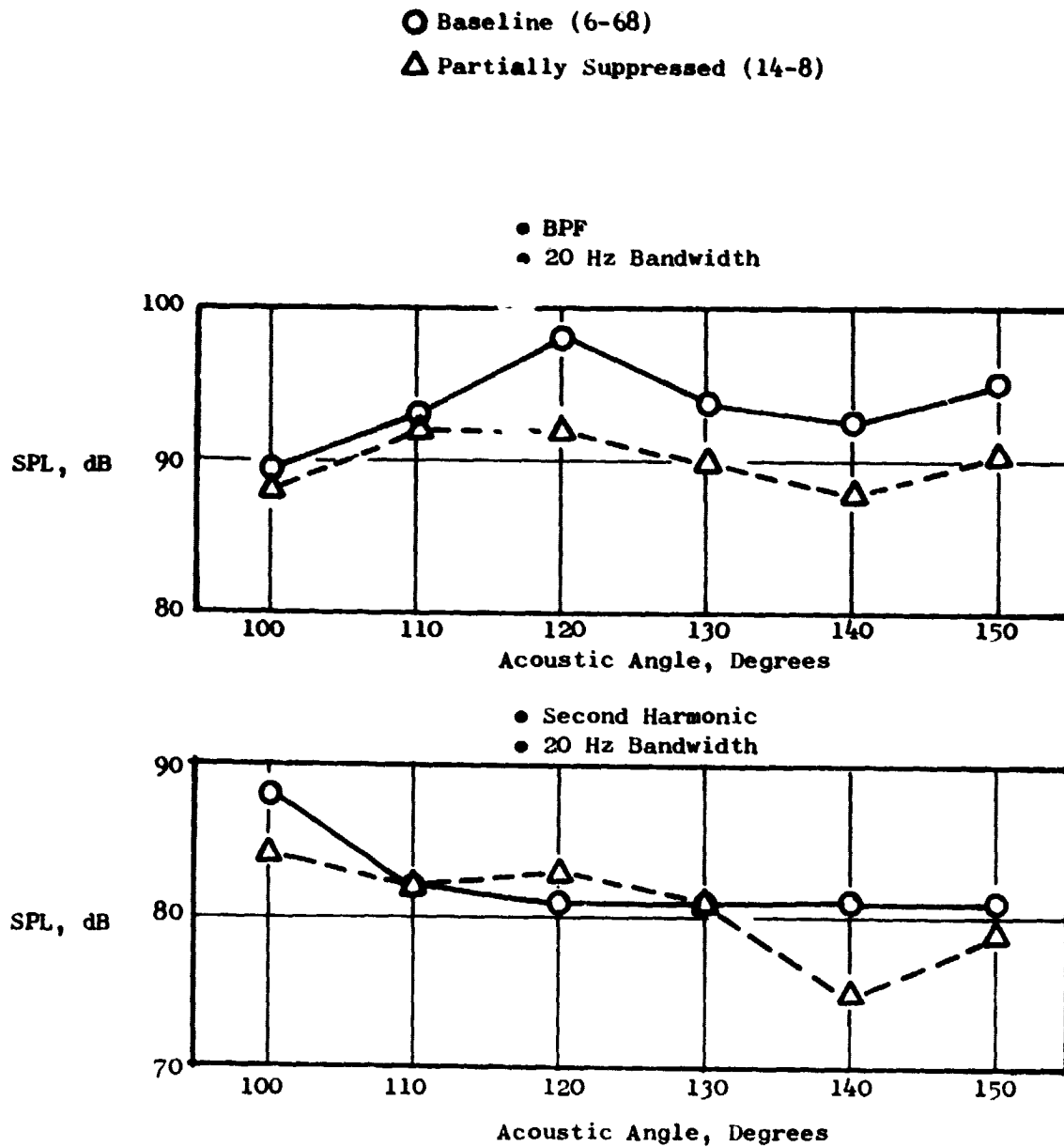
Figure 66. Measured Narrow Band Far Field BPF and Second Harmonic SPL's.

- 81% Corrected Fan Speed
- 152.4 m (500 Ft.) Sideline
- 25° Side Door Angle
- 40° Acoustic Angle

| Stator Angle | Test | Core Speed |
|---|---|---|
| ◯ Nominal | (12-19) | 12685 RPM |
| ▢ +5° Closed | (12-15) | 12967 RPM |
| ◇ +10° Closed | (12-16) | 13400 RPM |
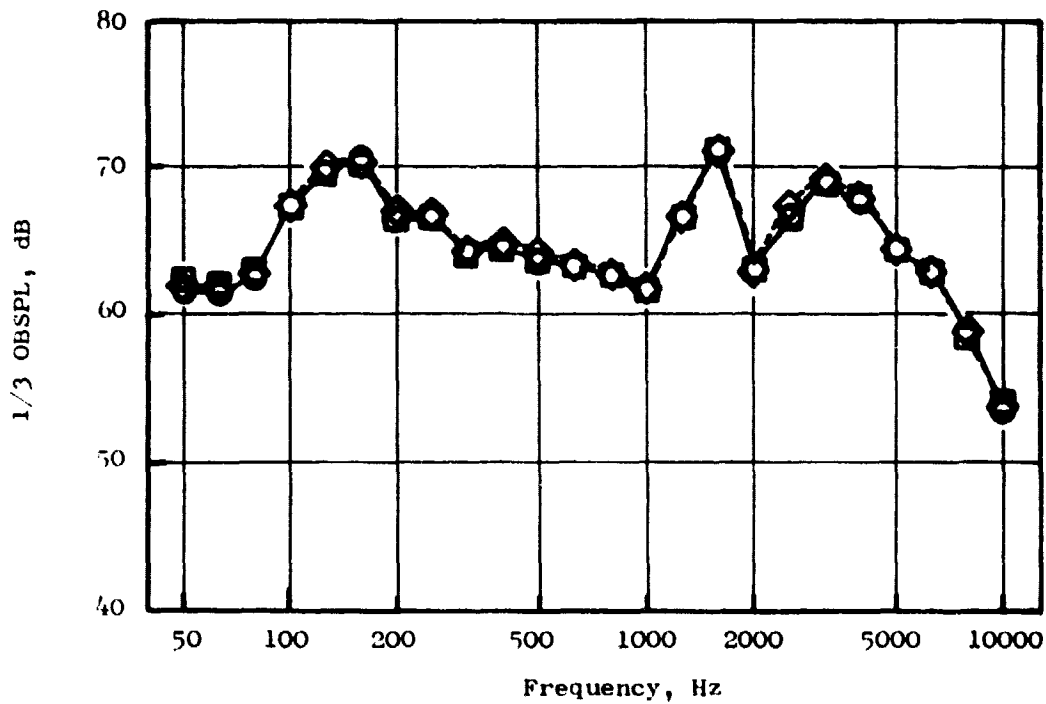


Figure 67. Effect of Core Stator Angle Variation on 40° Spectra.

- 81% Corrected Fan Speed
- 152.4 m (500 Ft.) Sideline
- 25° Side Door Angle
- 120° Acoustic Angle

| | Stator Angle | Test | Core Speed |
|---|---|---|---|
| O | Nominal | (12-19) | 12685 RPM |
| □ | +5° Closed | (12-15) | 12967 RPM |
| ◇ | +10° Closed | (12-16) | 13400 RPM |
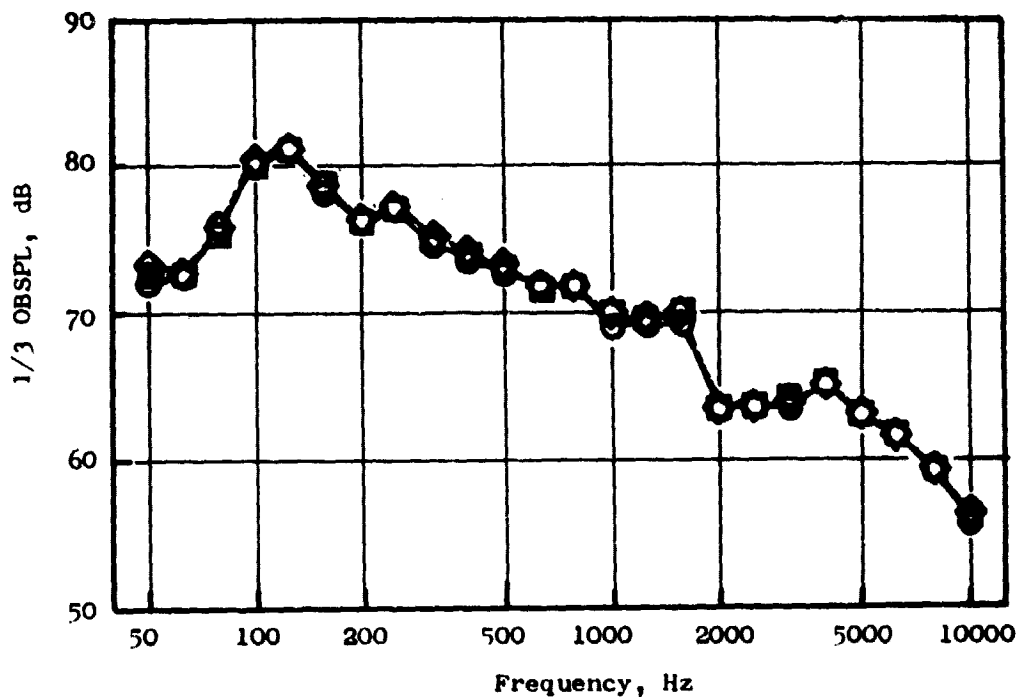


Figure 68.  Effect of Core Stator Angle Variation on 120° Spectra.
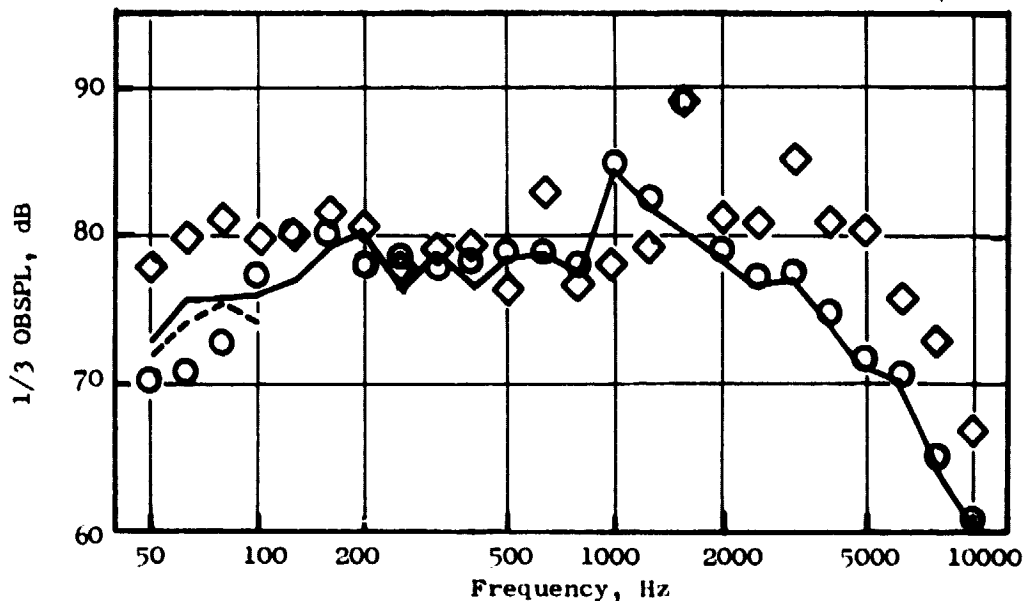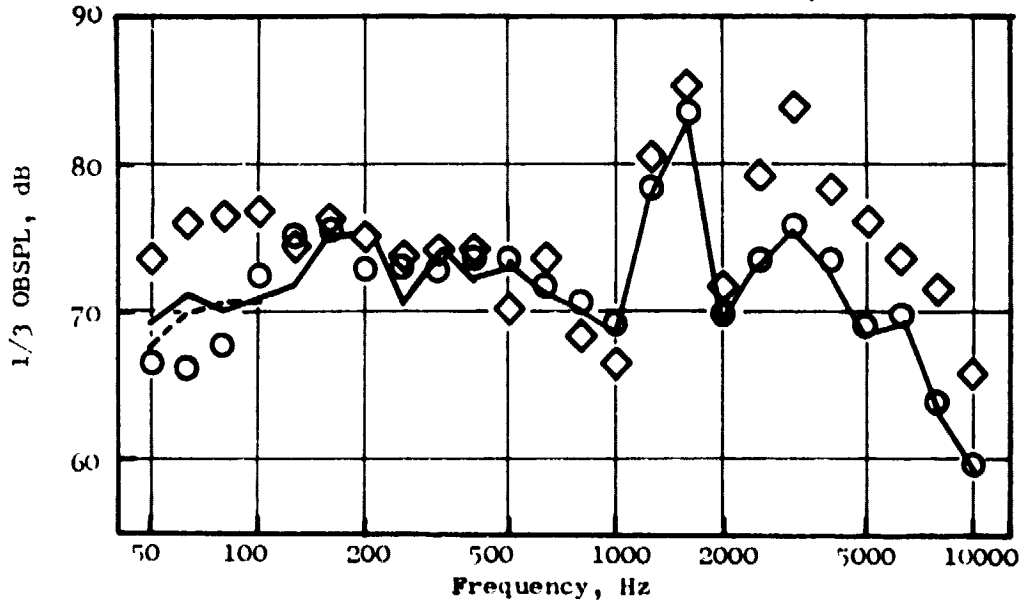
Figure 69. Measured and Free Field Baseline Spectra at 60°.

was determined by ratioing the observed first reflection frequency for the high microphones to the predicted or ideal first reflection frequency for the geometry at the test site. The reflection coefficient was selected initially based upon previous engine tests on this test site and adjustments were made to obtain reasonable agreement with the ground plane microphone data in the first four 1/3-octave bands and to provide a reasonably smooth free field spectrum. The resulting high microphone free field spectra are shown in Figure 69. The corrections for the high microphone are tabulated in Table VIII.

The above high microphone corrections provided reasonable free field spectra for 90° and 120° and were used in subsequent forward thrust system noise calculations.

### 5.3.3  Side Door Variation

The OTW engine had side doors which could be varied to achieve different operating lines on the fan map. Such variability would allow selection of the proper area for flow and high throat Mach number at takeoff and for increased fan pressure ratio at cruise. A convenient standard for side door position was the side door angle. Acoustically, side door angles of 0°, 11.5°, and 25° were tested at select speeds to evaluate various takeoff thrust operating lines. These angles corresponded to exhaust areas of $1.58m^2$ (2444 in.$^2$), $1.72m^2$ (2666 in.$^2$), and $1.90m^2$ (2947 in.$^2$), respectively.

Side door variation was tested at 95 percent fan speed on the baseline configuration. A spectral comparison of the three door angles is presented in Figure 70. There are significant changes in the low frequencies which are due to differences in jet noise levels. The 25 degree side door configuration had the lowest jet velocity and therefore the lowest low frequency noise. This 4 to 5 dB change from 0° door to 25° door in the low frequencies represents a 16 to 19 percent change in velocity assuming an SPL variation of 60 times the logarithm of the velocity ratio. Such a velocity change is consistent with the effective velocity change on the engine using core and fan flow velocities based on measured data and acoustically weighted using the velocity to the 6 power.

There are spectral variations of 2 to 3 dB evident at high frequencies. The fan pressure ratio varies from about 1.37 to 1.32 for 0° and 25° side door angles. This would account for only about 1 dB change in fan noise. (Appendix B of Reference 1). The possibility of more jet noise in these high frequencies than the scale model tests would indicate, as well as fan noise directivity variation with side door angle may account for some of the high frequency differences.

### 5.3.4  "D" Nozzle Asymmetry

The OTW engine has a "D"-shaped nozzle with an aspect ratio of approximately 1.8 (see Figures 3 and 12). Such a nozzle might be expected to exhibit asymmetric noise radiation characteristics (Reference 17).

Table VIII. 12.2 m (40 ft) High Microphone
Ground Reflection Corrections.

● Corrections are to be added
to measured spectra

| Frequency (Hz) | Correction (dB) |
|---|---|
| 50 | +3.0 |
| 63 | +5.1 |
| 80 | +2.3 |
| 100 | -1.4 |
| 125 | -3.1 |
| 160 | -0.8 |
| 200 | +2.7 |
| 250 | -2.6 |
| 315 | +1.3 |
| 400 | -1.4 |
| 500 | -0.9 |
| 630 | -0.3 |
| 800 | -0.7 |
| 1000 | -0.6 |
| 1250 | -0.7 |
| 1600 | -0.6 |
| 2000 | -0.7 |
| 2500 | -0.4 |
| 3150 | -0.6 |
| 4000 | -0.6 |
| 5000 | -0.5 |
| 6300 | -0.6 |
| 8000 | -0.5 |
| 10000 | -C.6 |

- Takeoff Power
- 152.4 m (500 Ft.) Sideline
- 130° Acoustic Angle
- Baseline Bellmouth Configuration

Exhaust Nozzle
Exit Area

| $m^2$ | $in^2$ | Side Door Angle | Test |
|------|------|-----------------|--------|
| 1.58 | 2444 | ◇ 0 Degrees | (6-25) |
| 1.72 | 2666 | ○ 11.5 Degrees | (6-16) |
| 1.90 | 2947 | ▢ 25 Degrees | (6-22) |
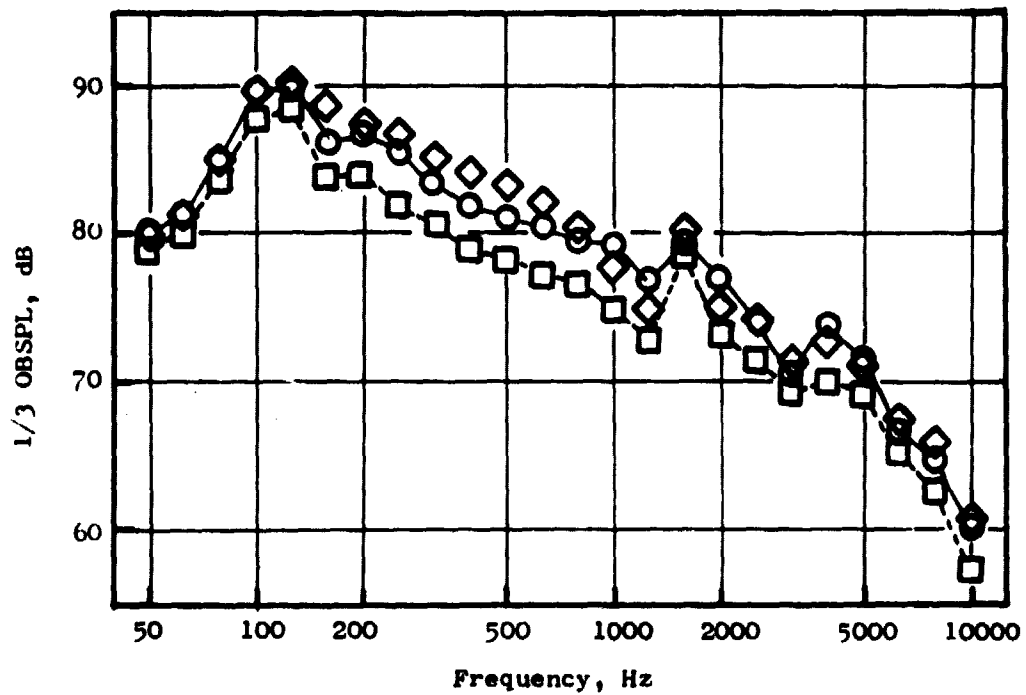
Figure 70. Effect of Side Door Angle on 130° Spectra.

96

Microphones were positioned in the far field to determine if any significant asymmetry over the range of azimuth angles was evident. As was discussed in Section 4.1.1 and shown in Figures 9 and 10, the far field tower at 150° had three microphones on it. The microphones were at 12.2 m (40 ft), 7.8 m (25.6 ft) and 4 m (13 ft) which correspond to aximuthal angles of 20°, 10°, and 0° respectively.

Figure 71 presents free field spectra for the baseline configuration at takeoff and approach. There appears to be no significant low frequency asymmetry over the range of azimuthal angles monitored. At high frequencies, there does appear to be a trend toward lower levels at the engine centerline height (0 degrees azimuth angle).

## 5.4 FORWARD THRUST SYSTEM NOISE LEVELS

The noise requirements for the OTW engine are specified as a total system or aircraft noise level at the operating conditions associated with takeoff and approach operation. These are shown graphically on Figure 72. Specific requirements are given in Table IX.

The takeoff noise goal is 95 EPNdB maximum on a 152.4 m (500 ft) sideline with the aircraft at 61 m (200 ft) altitude and the engines at takeoff thrust. Takeoff flap angle and aircraft speed are given in Table IX. Also shown in Table IX are inlet angle of attack and upwash angles which must be accounted for with regard to fan inlet noise generation and high Mach number inlet, inlet suppression.

At approach, the noise goal is the same as takeoff but the engine is operated at 65% thrust. Flap angles, defined in Table IX; however, are increased for the powered-lift approach.

Since the engine noise levels are to be measured during static testing, a procedure for determining inflight noise levels from static data has been established as part of the contract. This procedure, see Appendix A of Reference 1, establishes the following:

1. Jet/flap noise calculation procedure

2. Extrapolation procedures including air attenuation and extra ground attenuation

3. Doppler shift correction

4. Dynamic effect correction

5. Size correction

6. In-flight cleanup and upwash angle correction

7. Number of engine correction

8. Relative velocity correction for jet/flap noise

9. Fuselage shielding
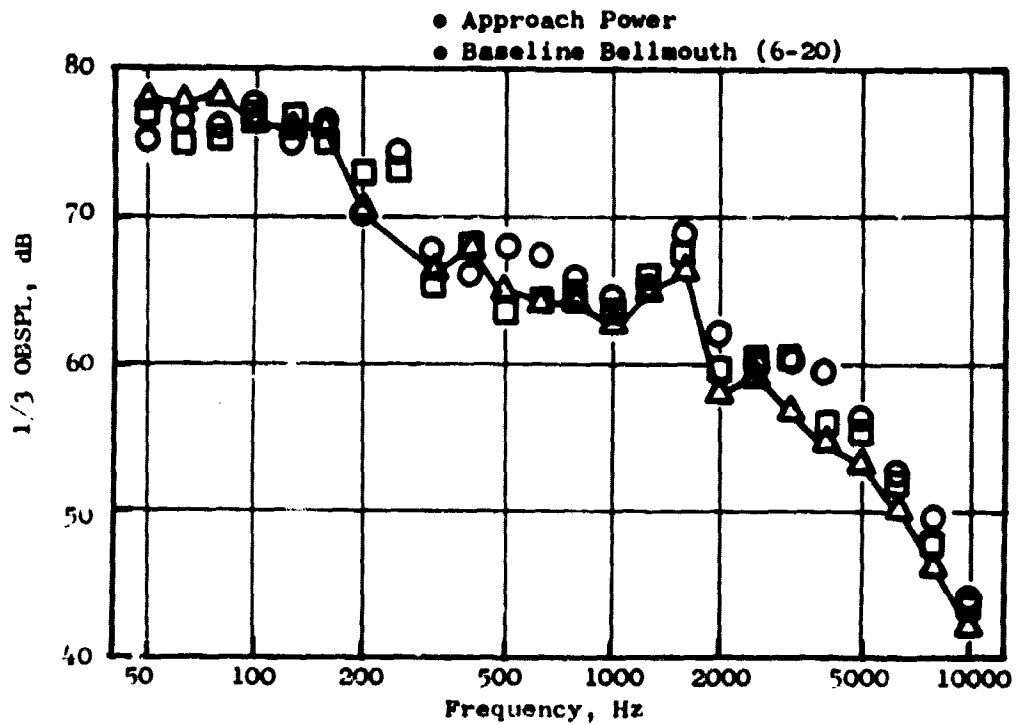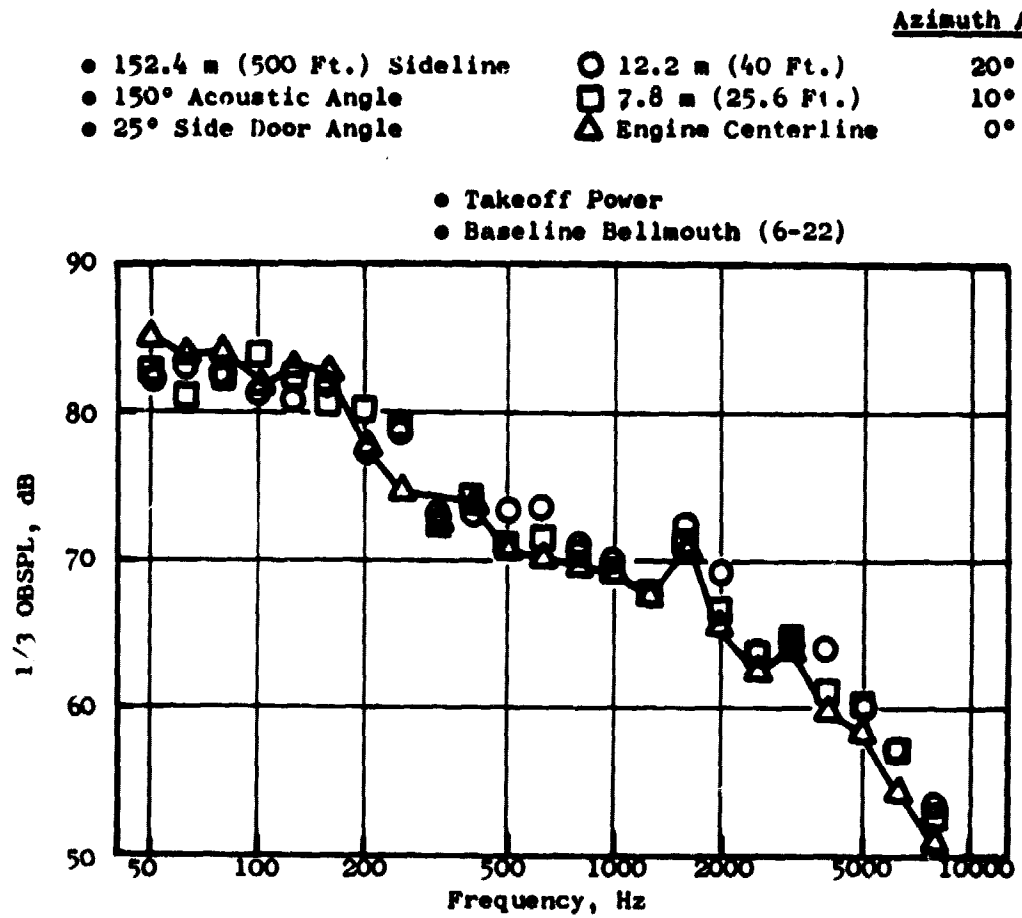
Figure 71. "D" Nozzle Asymmetry Effects.

- 4 Engines
- 400 kN (90,000 Lbs.) Thrust

Takeoff Thrust
61 m (200 Ft.) Altitude

95 EPNdB

Reverse Thrust
(35% T/O Thrust)

100 PNdB

Approach Thrust
(65% T/O Thrust)
61 m (200 Ft.) Altitude

152.4 m (500 Ft.) Sideline

95 EPNdB
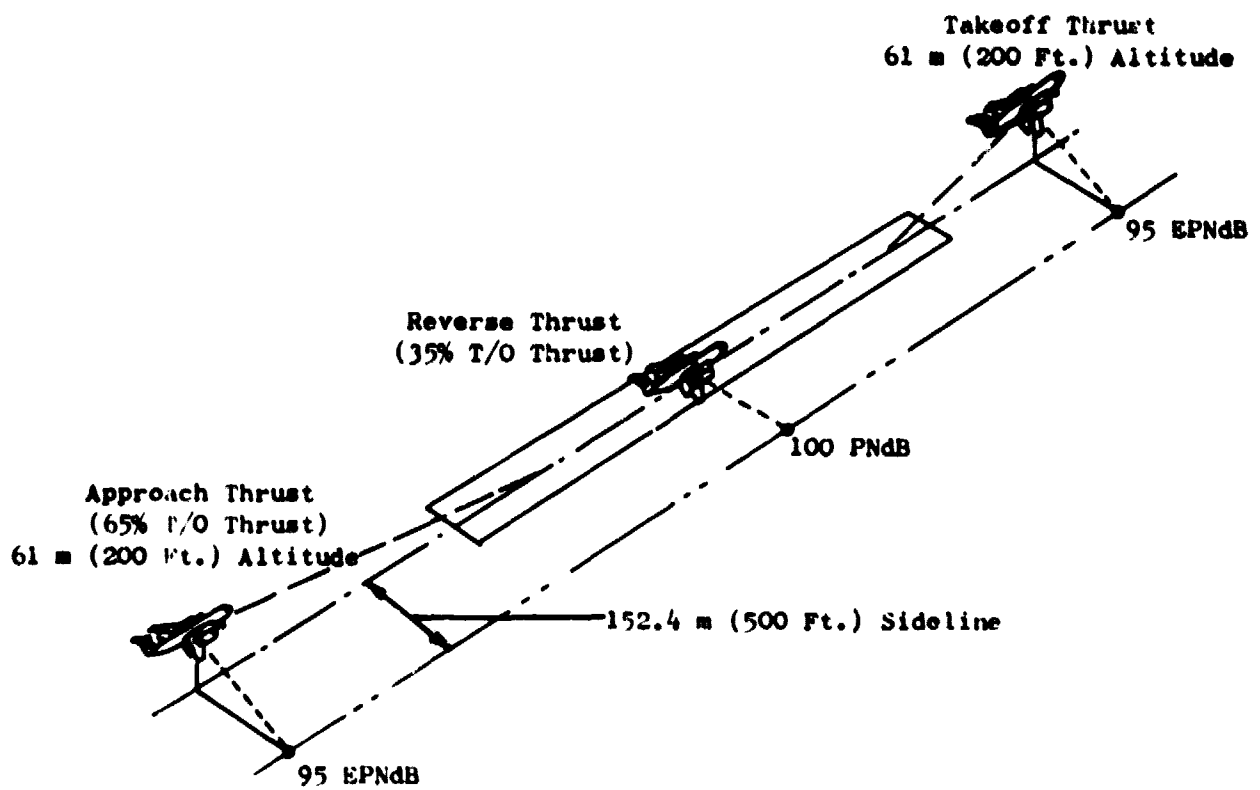
Figure 72. QCSEE Acoustic Requirements.

**Table IX. OTW Engine and Aircraft Flight Characteristics For Acoustic Calculations.**

| Flight Conditions | Takeoff | Landing |
|---|---|---|
| Aircraft Speed, m/sec (knots) | 41 (80) | 41 (80) |
| Flap Angle, degrees | 30 | 60 |
| Climb or Glide Angle, degrees | 12.5 | 6 |
| Angle or Attack, degrees | 6 | 2 |
| Upwash Angle, degrees | 15 | 11 |
| Installed Net Thrust, percent | 100 | 65 |

10.  OTW wing shielding

11.  PNL to EPNL calculation

12.  Dirt/grass ground absorption correction

These calculations are performed on the peak forward and peak aft angles.


### 5.4.1  Takeoff Noise Levels

Using the contract specified procedure from Appendix A of Reference 1, the takeoff noise level for the QCSEE OTW engine at 61 m (200 ft) altitude and 152 m (500 ft) sideline is 97.2 EPNdB.  Table X presents the results for the maximum forward and aft angles.  Jet/flap noise levels contribute significantly to the in-flight-noise level; thus, any reduction to the 95 EPNdB level must include additional jet/flap noise reduction.  Figure 73 illustrates this point by pointing out the effect of increased inlet, fan exhaust, and jet/flap noise reduction required to meet 95 EPNdB.  For example, with jet/flap noise decreased by 2 PNdB, inlet and fan exhaust suppression of 1 and 6, 2 and 2.7, or 3 and 2, respectively, would lower the noise to 95 EPNdB.


### 5.4.2  Approach Noise Levels

Using the procedure spelled out in the contract, with the aircraft configured for approach at the 61 m (200 ft) altitude, the 152 m (500 ft) sideline EPNL is 94.6 EPNdB or 0.4 EPNdB below the goal of 95.0 EPNdB.  The forward and aft constituents are given in Table XI.  In this case, the jet/flap levels are down, primarily due to the lower exhaust velocities.

Table X.  Takeoff System Noise.

- 95.3% $N/\sqrt{\theta}$
- 0.79 Throat Mach Number
- .25° Door Angle (12-18)
- 152 m (500 ft) sideline
- 61 m (200 ft) altitude

| Fully Suppressed | Maximum Forward Engine | Jet/Flap | Maximum Aft Engine | Jet/Flap |
|---|---|---|---|---|
| PNL | 94.8 | 95.8 | 96.8 | 93.2 |
| Total PNL | 99.0 | | 99.1 | |
| EPNL | | 97.2 EPNdB | | |

Figure 73. Takeoff System Noise Trade Study.

Table XI.  Approach System Noise.

- 81% N/$\sqrt{\theta}$
- 25% Door Angle (12-19)
- 152 m (500 ft) Sideline
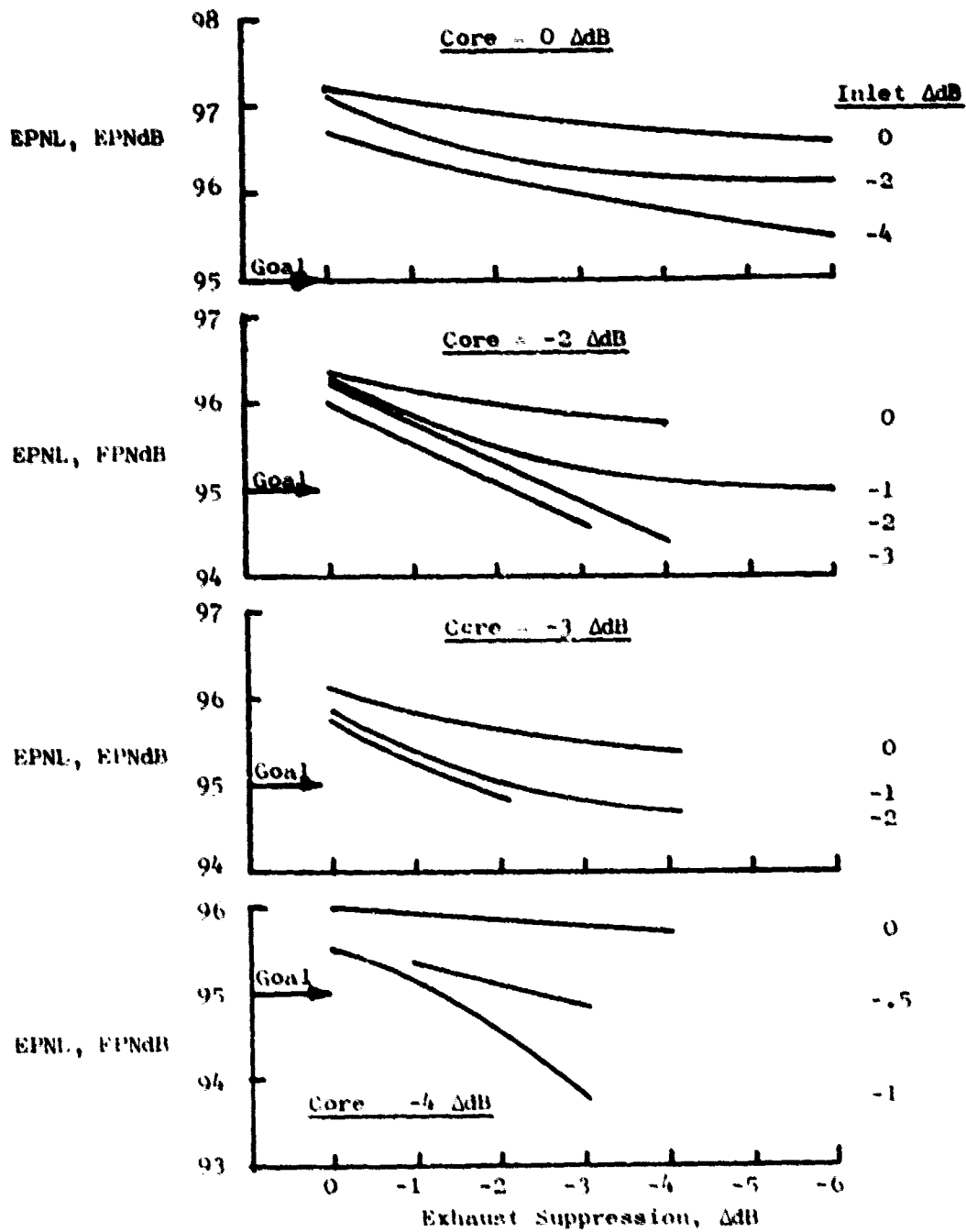- 61 m (200 ft) Altitude

| Fully Suppressed | Maximum Forward | | Maximum Aft | |
|---|---|---|---|---|
| | Engine | Jet/Flap | Engine | Jet/Flap |
| PNL | 95.4 | 89.9 | 90.8 | 87.2 |
| Total PNL | 97.1 | | 93.1 | |
| EPNL | | 94.6 EPNdB | | |

## 6.0  REVERSE THRUST ACOUSTIC RESULTS

### 6.1  FAR FIELD DATA

The fully suppressed OTW engine was tested in reverse thrust mode with target reverser deployed.  To prevent damage to the overhead support structure and instrumentation lines it was deployed so that the flow exhausted downward onto the test pad.  A reingestion shield as shown in Figure 8 was used to prevent hot exhaust gases from entering the inlet.

Data were taken at a series of reverse thrust levels.  All reverse thrust levels were referenced to takeoff static thrust of 90.3 kN (20,300 lb).  Measured engine PNL directivities are presented in Figure 74 for reverse thrust operation.  It is a very flat directivity.  Spectral shapes are given in Figures 75 and 76 at 70° and 110° for the reverse thrust data.  The dip at 200 to 250 Hz is a ground reflection null.  Otherwise, the data appears to be primarily jet noise in shape.  Fan noise at the BPF is barely visible in the spectra.

One of the questions concerning the data is whether the inlet-radiated noise constituent would contribute to far field levels if the reingestion shield were not present.

Spectral comparisons are made in Figures 77 and 78 at 60° and 70° at about 78 percent corrected fan speed which is near 35 percent reverse thrust for both reverse and forward thrust noise levels.  These two figures indicate that up to 2500 Hz, inlet-radiated noise without the shield is lower than the reverse thrust mode.  At frequencies above 3150, inlet-radiated noise from the forward thrust configuration is 2 to 3 dB higher than the reverse thrust levels.  However, if one would add 2 to 3 dB to the reverse thrust levels in these frequencies to account for inlet-radiated noise, there would be little effect (less than 0.5 PNdB) on the PNL since the spectra are controlled by the low frequency jet noise levels of the target reverser.

### 6.2  SYSTEM NOISE LEVEL

The noise goal for the OTW engine in reverse thrust is a peak noise level of 100 PNdB or less on a 152 m (500 ft) sideline with the engine generating a reverse thrust level which is 35 percent of takeoff thrust.

PNL's as a function of fan speed and percent reverse thrust are shown in Figure 79 for 50° to 140° on a 152 m (500 ft) sideline.  These values have been adjusted for atmospheric attenuation and extra ground attenuation as prescribed in Appendix A of Reference 1.  These curves were entered at 35 percent reverse thrust with the resulting PNL directivity shown in Figure 80.  Peak PNL is 101.5 PNdB and occurs at 110 degrees.  Adjustments to this peak PNL as specified in Appendix A of Reference 1 include the following corrections:

| | |
|---|---|
| Engine size | + 0.3 PNdB |
| Number of Engines | + 6.0 PNdB |

- Reverse Thrust
- Fully Suppressed
- 152.4 m (500 Ft.) Sideline

| % Corrected Fan Speed | | % Thrust | Test |
|---|---|---|---|
| ○ | 83.1 | 37 | (11-131) |
| □ | 78.3 | 33 | (11-126) |
| □ | 78.5 | 33 | (11-130) |
| △ | 69.7 | 27 | (11-132) |
| ✕ | 59.4 | 19 | (11-133) |
| ◇ | 41.2 | 5 | (11-134) |
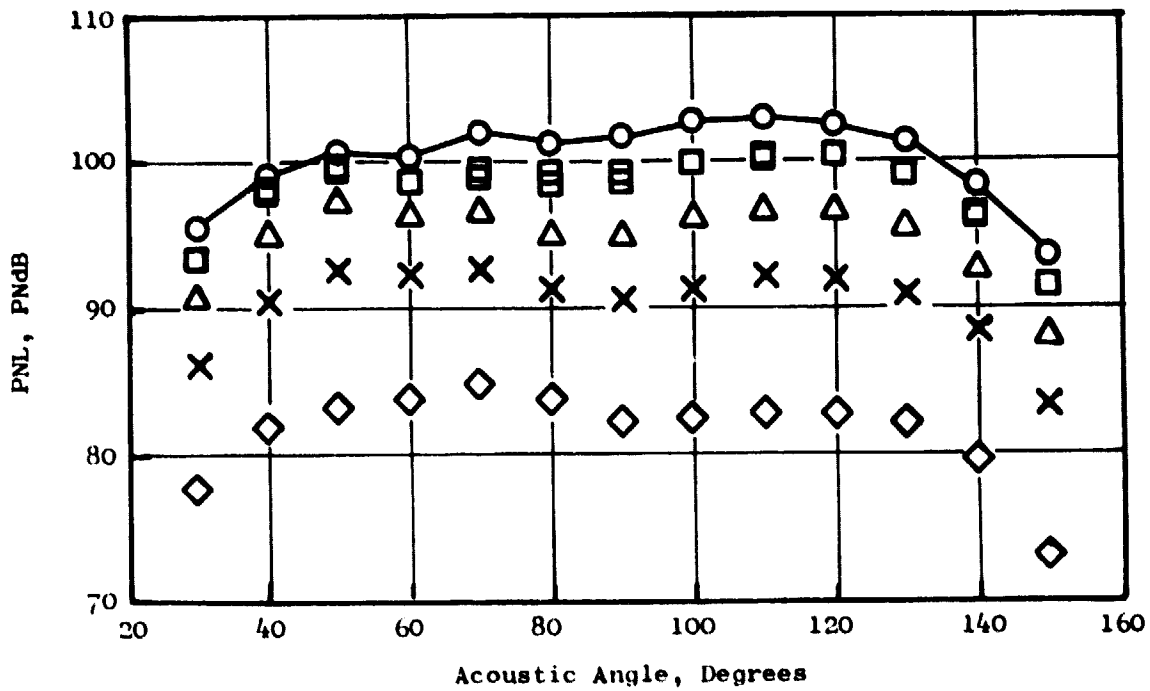


Figure 74.  Reverse Thrust PNL Directivities.

106

- Reverse Thrust
- Fully Suppressed
- 152.4 m (500 Ft.) Sideline
- 70° Acoustic Angle

| % Corrected Fan Speed | % Thrust | Test |
|---|---|---|
| ○ 83.1 | 37 | (11-131) |
| ▢ 78.3 | 33 | (11-126) |
| ▢ 78.5 | 33 | (11-130) |
| △ 69.7 | 27 | (11-132) |
| ✕ 59.4 | 19 | (11-133) |
| ◇ 41.2 | 5 | (11-134) |

Flagged Symbols Denote Band Containing BPF



Figure 75.   Reverse Thrust Spectra at 70°.

- Reverse Thrust
- Fully Suppressed
- 152.4 m (500 Ft.) Sideline
- 110° Acoustic Angle

| % Corrected Fan Speed | % Thrust | Test |
|---|---|---|
| ◯ 83.1 | 37 | (11-131) |
| ☐ 78.3 | 33 | (11-126) |
| ☐ 78.5 | 33 | (11-130) |
| △ 69.7 | 27 | (11-132) |
| ✕ 59.4 | 19 | (11-133) |
| ◇ 41.2 | 5 | (11-134) |

**Flagged Symbols Denote Band Containing BPF**
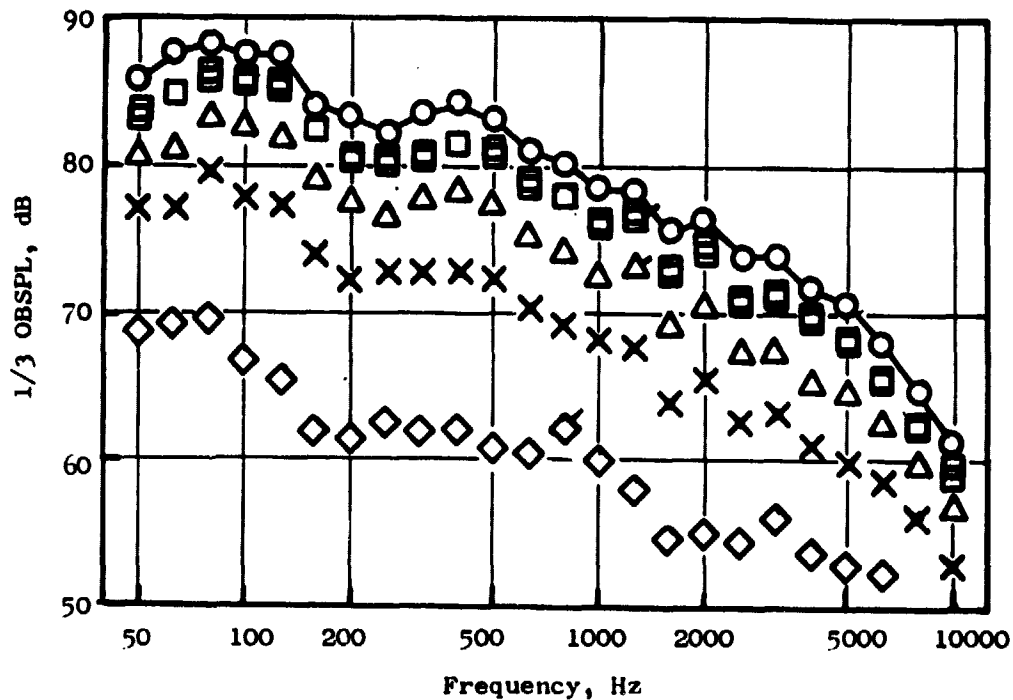


Figure 76.   Reverse Thrust Spectra at 110°.

108

- Fully Suppressed
- 152.4 m (500 Ft.) Sideline
- 60° Acoustic Angle

| % Corrected Fan Speed | Thrust | |
|---|---|---|
| ☐ 78.3 | 33% Reverse | (11-126) |
| ☐ 78.5 | 33% Reverse | (11-130) |
| ○ 78.2 | Forward | (12-22) 25° Side Door Angle |
| △ 80.0 | Forward | (12-07) 11.5° Side Door Angle |
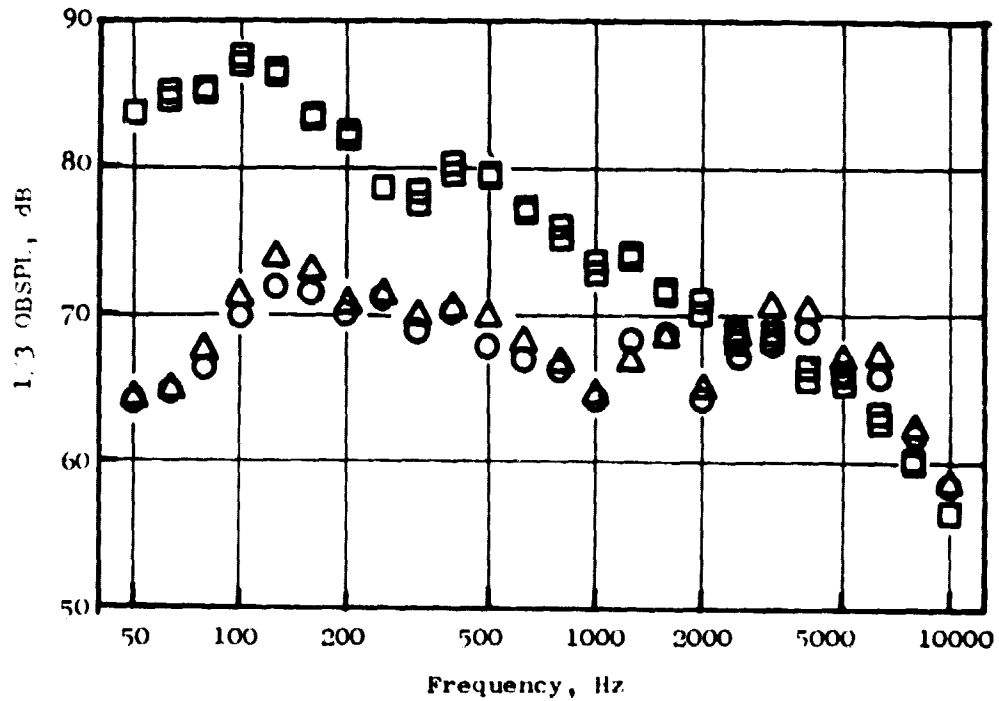


Figure 77.  Forward and Reverse Thrust Spectra at 60°.

109

- Fully Suppressed
- 152.4 m (500 Ft.) Sideline
- 70° Acoustic Angle

| % Corrected Fan Speed | Thrust | Test | |
|---|---|---|---|
| □ 78.3 | 33% Reverse | (11-126) | |
| □ 78.5 | 33% Reverse | (11-130) | |
| ○ 78.2 | Forward | (12-22) | 25° Side Door Angle |
| △ 80.0 | Forward | (12-07) | 11.5° Side Door Angle |
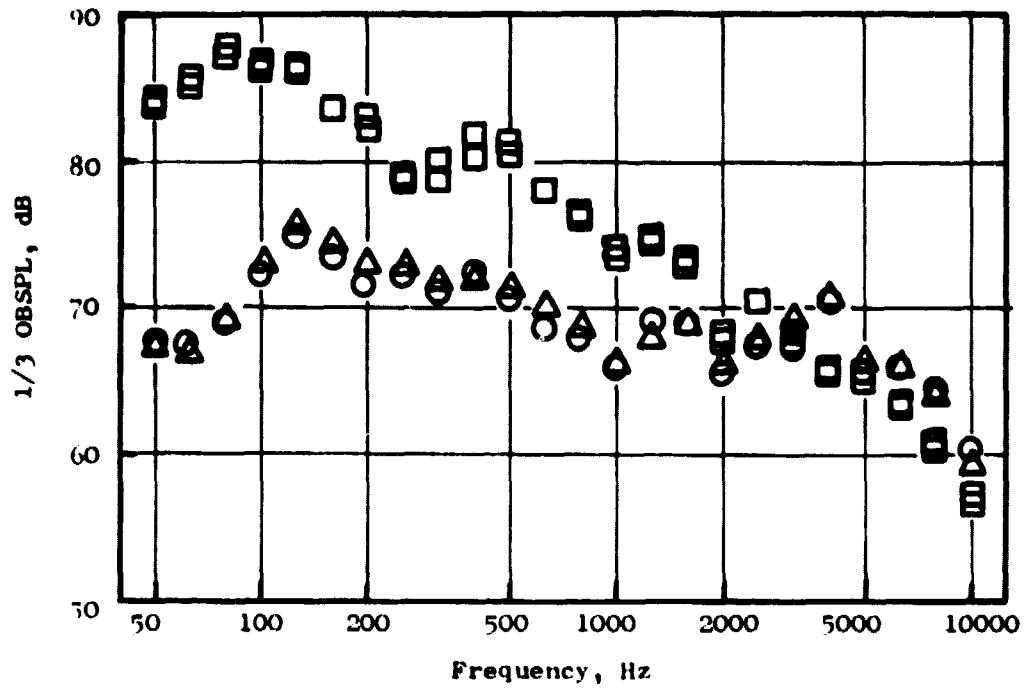
Figure 78. Forward and Reverse Thrust Spectra at 70°.
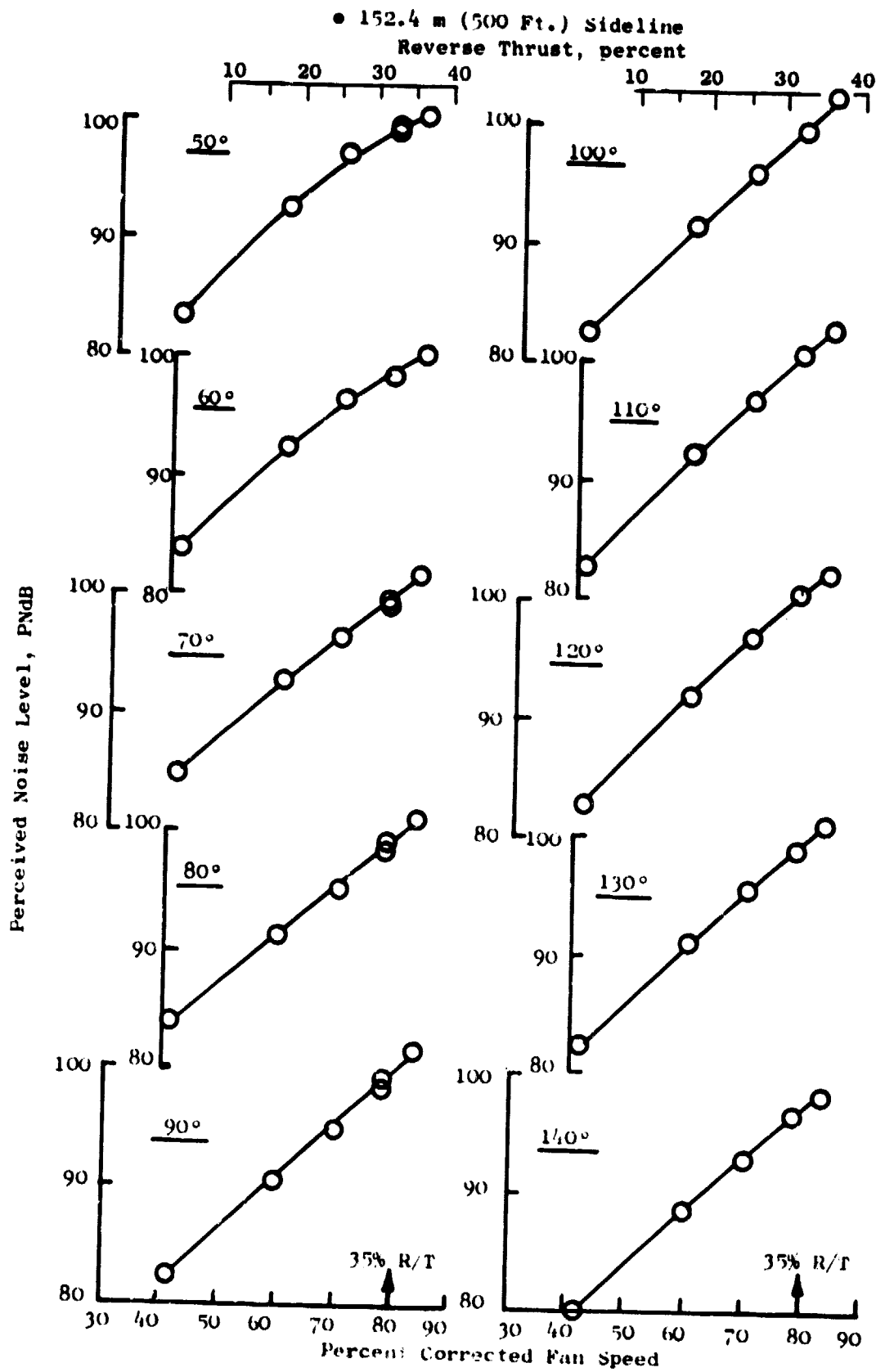
Figure 79.   Reverse Thrust PNL,s as a Function of Percent
Reverse Thrust and Fan Speed.

111

- Reverse Thrust
- 152.4 m (500 Ft.) Sideline
- 35% of Takeoff Thrust
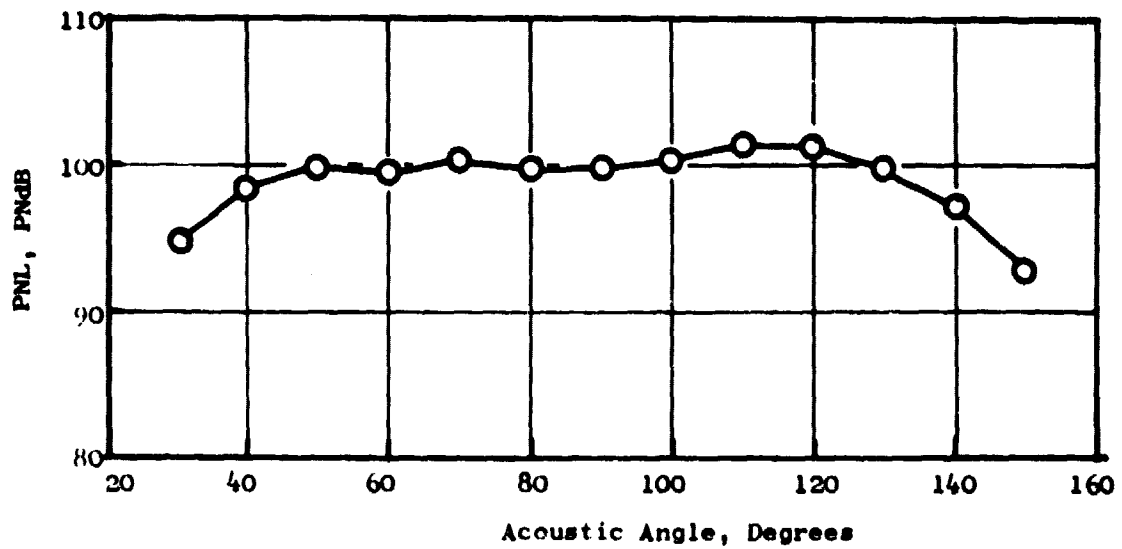


Figure 80. Reverse Thrust PNL Directivity at 35 Percent Reverse Thrust.

| | |
|---|---|
| Fuselage/Shielding | – 1.2 PNdB |
| Dirt/Grass Ground | – 0.5 PNdB |
| Total Correction | + 4.6 PNdB |

Applying this correction means that a short-haul aircraft with QCSEE OTW engines would achieve a peak 152 m (500 ft) sideline noise level of 106.1 PNdB when operating at a reverse thrust which is 35% of takeoff thrust.

The above reverse thrust level is based on the OTW engine mounted on the static test stand with the flow exhausting down onto the pad. During model tests of the OTW thrust reverser as reported in Reference 12, configurations were run with the target reverser exhausting upward as it would be on an aircraft and exhausting downward onto a simulated ground plane as mounted for the engine test. Comparison of the two orientations indicated that noise levels for the downward exhaust configuration increased 1 to 2 PNdB at forward acoustic angles as one would expect assuming that there is a second source of noise, namely, ground impingement noise. However, aft noise levels indicated a decrease of 1 to 3 PNdB depending on pressure ratio and angle. If such directivity differences from the model test are applied to the QCSEE OTW engine data, the reverse thrust level would increase from 106.1 to 107.8  PNdB or 7.8 PNdB above the goal of 100 PNdB.

The contract goal in reverse thrust as mentioned above was 100 PNdB at a reverse thrust level of 35 percent of takeoff thrust. The criterion of 100 PNdB on a 152 m (500 ft) sideline could be met (Figure 78) if the reverse thrust requirement were only 24 percent of takeoff thrust. Since aircraft are not as yet required to use thrust reversers to certify for a given runway length, a lowered level of thrust would still be "icing on the cake" and the noise would meet 100 PNdB. Analytical aircraft stopping distance/noise trade studies (Reference 18) conducted concurrently with flowpath design have shown that high efficiency reverser concepts can be employed at substantially reduced power settings to meet the same sideline noise goals and landing runway length requirements as currently in the QCSEE program.

# 7.0 CONCLUSIONS AND RECOMMENDATIONS

## 7.1 CONCLUSIONS

This report has documented and analyzed acoustic data taken on five configurations of the QCSEE engine. The observations and conclusions from these tests are documented below.

### 7.1.1 Program Goals

At approach the OTW engine achieved a system noise level of 94.6 EPNdB on a 152 m (500 foot) sideline which is 0.4 EPNdB below the goal of 95.0 EPNdB. At takeoff, the system noise level was 97.2 EPNdB or 2.2 EPNdB over the goal of 95 EPNdB, also on a 152 m (500 foot) sideline. In reverse thrust, the maximum 152 m (500 foot) sideline level was 106.1 PNdB or 6.1 PNdB over the objective of 100 PNdB. Achieving 100 PNdB can be accomplished at a reverse thrust which is equal to 24 percent of takeoff thrust.

### 7.1.2 Basic Source Noise

- Good agreement was seen between measured and predicted total engine baseline noise - both forward and aft radiated. The OTW engine noise levels show good agreement with fans of about the same asize when compared on the basis of tip speed (for inlet-radiated noise) and pressure ratio (for exhaust-radiated noise).

- Probability density analysis or the blade-passing frequency (BPF) tone indicates that a random source mechanism such as rotor-turbulence noise is controlling at both forward and aft angles.

- A bank of fans near the inlet was able to dissipate the ground vortex; however, no significant change in noise was observed indicating inflow turbulence not the ground vortex to be a more dominant source noise generator.

- Fan exhaust radial mode measurements indicated strong second order mode dominance at the BPF and higher order modes for the second harmonic.

- Variation of core stator angle at approach power from nominal to 10° closed had no significant effect on noise; therefore, the selection of core stator angle at approach can be based upon control response time.

- Noise changes in the low frequency region were observed with different side door angles. These differences seemed to correlate with 60 times the logarithm of the velocity ratio.

- No significant low frequency asymmetry was observed in the "D" nozzle over the range of azimuth angles monitored.

### 7.1.3 Suppression

- 14 PNdB inlet suppression was achieved with the hybrid inlet at 0.79 throat Mach number.

- PWL changes between the fan face and throat probes show a BPF SPL decrease of 15 dB at 0.79 throat Mach number.

- Exhaust suppression for the fully suppressed configuration was about 6 PNdB compared with a predicted level of 11 PNdB. An apparent lack of attenuation above the peak tuning frequency caused the loss in suppression. This lack of high frequency suppression may be due to treatment regenerated flow noise which is of sufficient magnitude to prevent determination of the fan exhaust suppression.

- A complete evaluation of core suppression in the low frequencies was masked by jet noise: however, some suppression was evident in the data.

## 7.2 RECOMMENDATIONS

Based upon the above discussion, there are areas which could be explored in more depth in future test programs. A series of potential tests is listed below:

1. A test of the fully suppressed engine without the acoustic splitter would determine the effect of the splitter on suppression. Use of a probe just downstream of the treatment in the fan exhaust would provide for measurement of transmission loss in the fan duct.

2. A test of the fully suppressed engine with splitter and with a probe installed downstream of the splitter and treatment would provide transmission loss data.

3. A fully suppressed fan duct but with hard wall core would isolate the effect of the stacked core treatment. This test should include a more complete survey of the "D" nozzle, both acoustically and aerodynamically. The acoustic results should be correlated with far field microphones.

4. An alternate test for recommendation 3 would be to replace the "D" nozzle with a separate flow conical nozzle. This would allow separate surveys of the fan and core flows to separate the two noise sources.

# 8.0 NOMENCLATURE

| Symbol or Abbreviation | Definition | Units |
|---|---|---|
| A | Asymmetry microphone data | - |
| A | Treated surface area | $m^2$ ($ft^2$) |
| BPF | Blade passing frequency | Hz |
| d | Characteristic dimension | m(ft) |
| D | Fan diameter | m(ft) |
| DA | Directional array data | - |
| EPNL | Effective perceived noise level | EPNdB |
| f | Frequency | Hz |
| $f_c$ | 1/3 octave band center frequency | Hz |
| $f_o$ | Peak flow noise frequency | Hz |
| H | Duct height | m(ft) |
| K | Wall Kulite data | - |
| L | Effective treatment length | m(ft) |
| M | Far field, near field, ground plane microphone data | |
| M | Mach number | - |
| N | Fan speed | rpm |
| N | Faceplate holes per unit area | $m^{-2}$ ($ft^{-2}$) |
| $N_f$ | Physical fan speed | rpm |
| $N_c$ | Physical compressor speed | rpm |
| OASPL | Overall sound pressure level re 0.0002 microbar | dB |
| OBSPL | 1/3-Octave Band Sound Pressure Level | dB |
| $P(f, \delta(x))$ | Flow noise power per unit length | watt/Hz/m |
| P-ff | Fan face probe data | - |
| P-flow noise | Sound power of flow noise | watts/Hz |
| PNL | Perceived noise level | PNdB |
| P-N | "D" nozzle probe data | - |
| P-O | OGV probe data | - |
| P-T | Throat probe data | - |
| PWL | Sound power level, re $10^{-13}$ watts | dB |
| Q | Reflection coefficient | - |

116

## 8.0 <u>NOMENCLATURE</u>  (Concluded)

| Symbol or Abbreviation | Definition | Units |
|---|---|---|
| $R_x$ | Reynold's number per foot | $ft^{-1}$ |
| SPL | Sound pressure level, re 0.0002 microbar | dB |
| TL | Broadband transmission loss | dB |
| U | Flow velocity | m/sec (ft/sec) |
| V | Velocity | m/sec (ft/sec) |
| x | Immersion depth | M(in) |
| x | Treatment length | m(ft) |
| β | Attenuation constant | nepers/m |
| δ | Boundary layer thickness | m(ft) |
| θ | Ratio of ambient to reference temperature | — |
| ρ | Density | $Kg/m^3$ ($lbm/ft^3$) |
| φ | Phase factor | — |

# 9.0 REFERENCES

1. "UTW/OTW Preliminary Design Report, Vol I & II," NASA Contractor Reports 134838 and 134839, December 23, 1974.

2. Sowers, H.D. and Coward, W.D., "Quiet, Clean, Short-Haul, Experimental Engine (QCSEE) Over-the-Wing (OTW) Engine Acoustic Design," NASA Contractor Report 135268, March 1978.

3. "Quiet, Clean, Short-Haul, Experimental Engine (QCSEE) Acoustic Treatment Development and Design," NASA Contractor Report 135266, March 1978.

4. "Quiet Clean Short-Haul Experimental Engine (QCSEE) Over-the-Wing (OTW) Final Design Report," NASA Contractor Report 134484, June 1977.

5. Clemons, A., Hehmann, H.W., and Radecki, K.P., "Quiet Engine Program Turbine Noise Suppression, Volume I, General Treatment Evaluation and Measurement Techniques," NASA Contractor Report 134499, December 1973.

6. Stimpert, D.L. and Clemons A., "Acoustic Analysis of Aft Noise Reduction Techniques Measured on a Subsonic Tip Speed 50.8 cm (Twenty Inch) Diameter Fan," NASA Contractor Report 134891, January 1977.

7. "Standard Values of Atmospheric Absorption as a Function of Temperature and Humidity for use in Evaluating Aircraft Flyover Noise," SAE ARP 866, 1964.

8. K.L. Bekofske, R.E., R.E. Sheer, and J.C.F. Wang, "Basic Noise Research Program – Fan Noise – Effect of Inlet Disturbances on Fan Inlet Noise During a Static Test," NASA CR-135177.

9. Kazin, S.B. and Paas, J.E., "NASA/GE Quiet Engine "A" Acoustic Test Results," NASA Contractor Report 121175, October 1973.

10. Kazin, S.B. and Paas, J.E., "NASA/GE Quiet Engine "C" Acoustic Test Results," NASA Contractor Report 121176, April 1974.

11. Bilwakesh, K.R., Clemons, A., and Stimpert, D.L., "Acoustic Performance of a 50.9 cm (20-inch) Diameter Variable Pitch Fan and Inlet," NASA Contractor Report 135117, April 1978.

12. Stimpert, D.L., "Quiet Clean Short-Haul Experimental Engine (QCSEE). Acoustic and Aerodynamic Tests on a Scale Model Over-the-Wing Thrust Reverser and Forward thrust Nozzle," NASA Contractor Report 135254, January 1978.

13. Motsinger, R.E., et al., "Analytical and Experimental Studies of Acoustic Performance of Segmented Liners in a Compressor Inlet," NASA Contractor Report 2882, September 1977.

118

## 9.0 References (Concluded)

14. Motsinger, R.E., et al, "Optimization of Suppression for Two-Element Treatment Liners for Turbomachinery Exhaust Ducts," NASA Contractor Report 134997, April 1976.

15. Anon, "Acoustic Effects Produced by a Reflecting Plane," SAE Aerospace Information Report AIR 1327, January 1976.

16. Savell, C.T., and Stringas, E.J., "High Velocity Jet Noise Source Location and Reduction Task 1 - Activation of Facilities and Validation of Source Location Techniques," FAA-RD-76-79, I, February 1977.

17. "High Velocity Jet Noise Source Location and Reduction, Task 2 - Theoretical Developments and Basic Experiments," Report Number FAA-RD-76-79, II, October 1977.

18. Ammer, R.C. and Sowers, H.D., "Thrust Reverser Design Studies for an Over-the-Wing STOL Transport," NASA Contractor Report 151958, March 1977.

19. Ammer, R.C. and Kutney, J.T., "Analysis and Documentation of QCSEE (Quiet Clean Short-Haul Experimental Engine) Over-the-Wing Exhaust System Development," NASA Contractor Report 2792, June 1977.

20. Olsen, W., Burns, R., and Grosebeck, D., "Flap Noise and Aerodynamic Results for Model QCSEE Over-the-Wing Configurations," AIAA Paper 77-23, presented at the 15th Aerospace Sciences Meeting, Los Angeles, California, January 24-26, 1977.

21. Goodykoontz, J. and Guiterrez, O., AIAA Paper 77-1318 presented at 4th Aero-Acoustic Conference, Atlanta, Georgia, October 3-5, 1977.

22. Phelps, A.E. III, "Static and Wind-on Tests of an Upper-Surface-Blown Jet-Flap Nozzle Arrangement for use on the Quiet Clean Short-Haul Experimental Engine (QCSSE)," NASA TND-8476, June 1977.

23. "Gas Turbine Jet Exhaust Noise Prediction," SAE, ARP876 (Proposed), July 1975.

24. Stimpert, D.L. and Uhl, W.R., "Aero-Acoustic Design and Test of a Multiple Splitter Exhaust Noise Suppressor for a 0.914 m Diameter Lift Fan," NASA Contractor Report 121108, January 1973.

25. Hoerner, S.F., "Fluid Dynamic Drag", Midland Park, New Jersey, published by the author 1958.

# APPENDIX A

## OTW JET NOISE

## 1.0 INTRODUCTION

Noise levels as measured on the engine during this static test include turbomachinery noise sources and jet noise. In practice, an OTW engine would be used with a sophisticated wing and flap system to achieve powered lift. Therefore, for system noise levels simulating the engine in flight the static jet noise must be replaced by the jet/flap noise level. Appendix A of Reference 1 specifies the procedures to be used to extrapolate measured engine data to in-flight conditions.

Prior to OTW engine testing, a scale model test (Reference 12) of the OTW "D" nozzle exhaust system was conducted to provide static jet noise levels which could be scaled to full size and used to remove jet noise from measured engine spectra.

This appendix is intended to document the measured engine velocity profile, compare scaled model jet noise levels with engine data, provide normalized curves of the model spectra shapes, and to briefly describe how jet noise was removed from measured engine spectra.

## 2.0 MEASURED ENGINE VELOCITY PROFILES

A total pressure/total temperature survey was made in the "D" nozzle discharge plane with engine operating conditions of 91 percent corrected fan speed and 11.5° side door angle of 1.72 m$^2$ (2666 in.$^2$) exhaust nozzle area. Subsequent analysis of the data resulted in the engine velocity profiles shown in Figure 81. The core and fan velocities agree very well with the velocities predicted by the cycle for the engine operating conditions.

An effective exhaust velocity using acoustic weighting of V$^8$ on the core and fan ideal velocities results in 265 m/sec (870 ft/sec).

## 3.0 MODEL AND ENGINE JET NOISE COMPARISONS

Acoustic data for the engine were taken at the same conditions as the exhaust survey discussed in the preceeding section. Model data (Reference 12) were available at a velocity of 261 m/sec (855 ft/sec). The model was a single flow system with a relatively flat velocity profile. Spectra from the model and engine are compared in Figures 82, 83, 84, and 85 at acoustic angles of 40°, 90°, 110° and 150°. The model data have been corrected to free field using the corrections established in Reference 16. Engine data are as measured - not free field; however, the model data generally fairs through the reinforcement and ground null patterns and shows very good agreement.
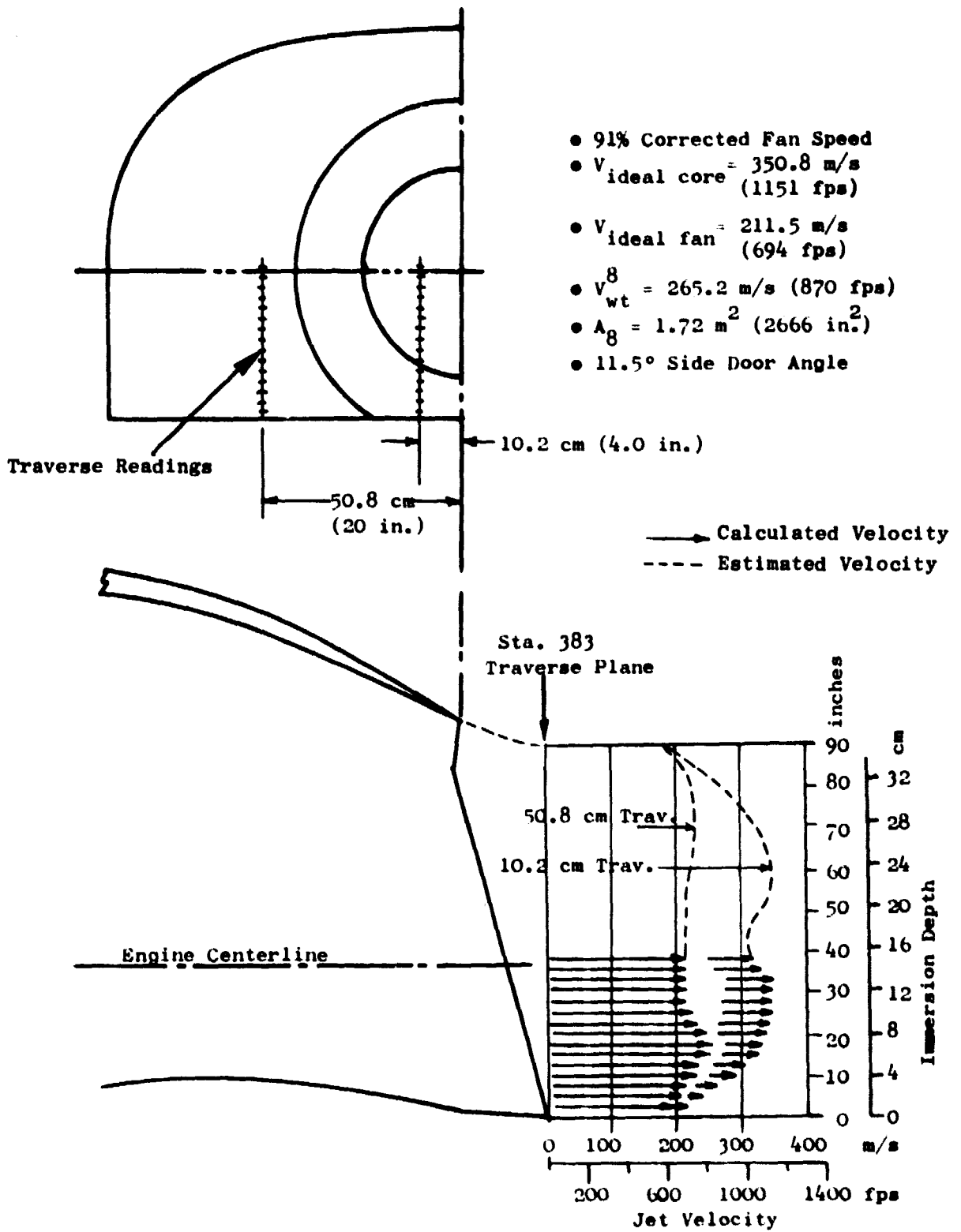
120

- 91% Corrected Fan Speed
- $V_{ideal\ core} = 350.8$ m/s (1151 fps)
- $V_{ideal\ fan} = 211.5$ m/s (694 fps)
- $V_{wt}^8 = 265.2$ m/s (870 fps)
- $A_8 = 1.72$ m$^2$ (2666 in.$^2$)
- 11.5° Side Door Angle
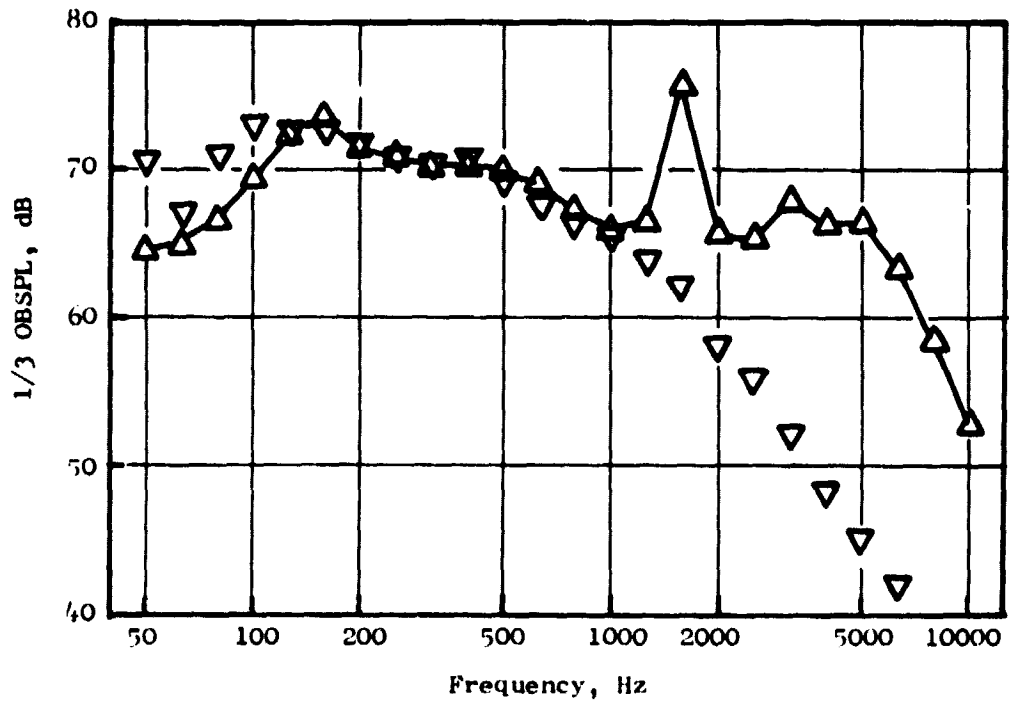
Figure 81. QCSEE OTW Engine Exit Velocity Profiles.

121

Figure 82. Measured Engine Noise and Scaled Jet Noise at 40°.

- 152.4 m (500 Ft.) Sideline
- 11.5° Side Door Angle
- 90° Acoustic Angle

△ Partially Suppressed Engine Noise (14-7)

▽ Scaled "D" Nozzle Jet Noise
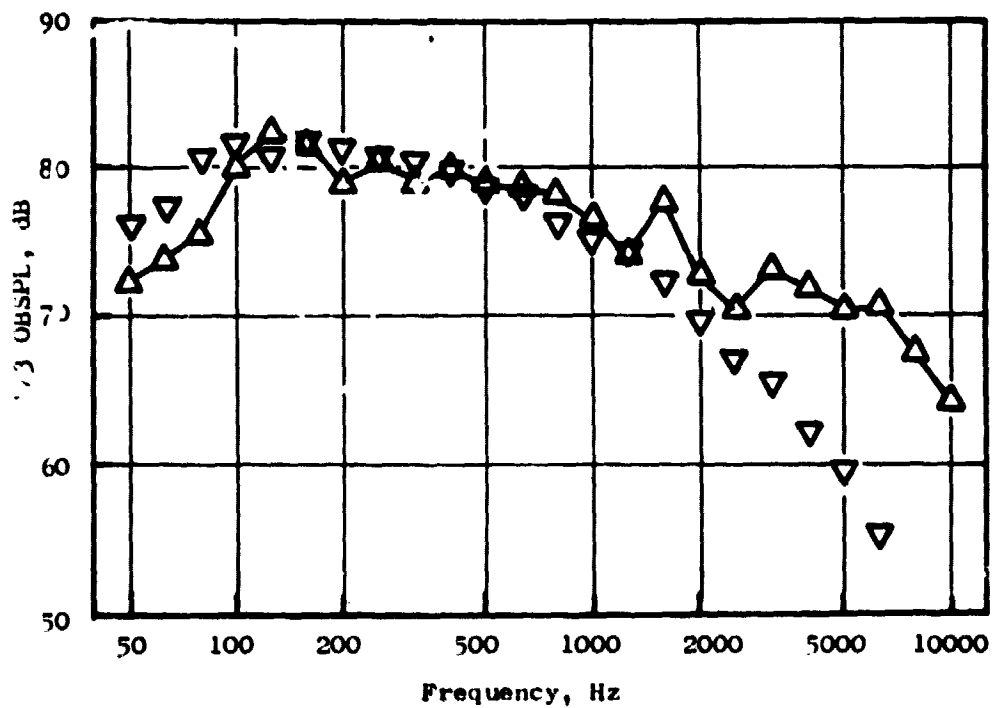


Figure 83. Measured Engine Noise and Scaled Jet Noise at 90°.

● 152.4 m (500 Ft.) Sideline
● 11.5° Side Door Angle
● 110° Acoustic Angle

△ Partially Suppressed Engine Noise (14-7)

▽ Scaled "D" Nozzle Jet Noise
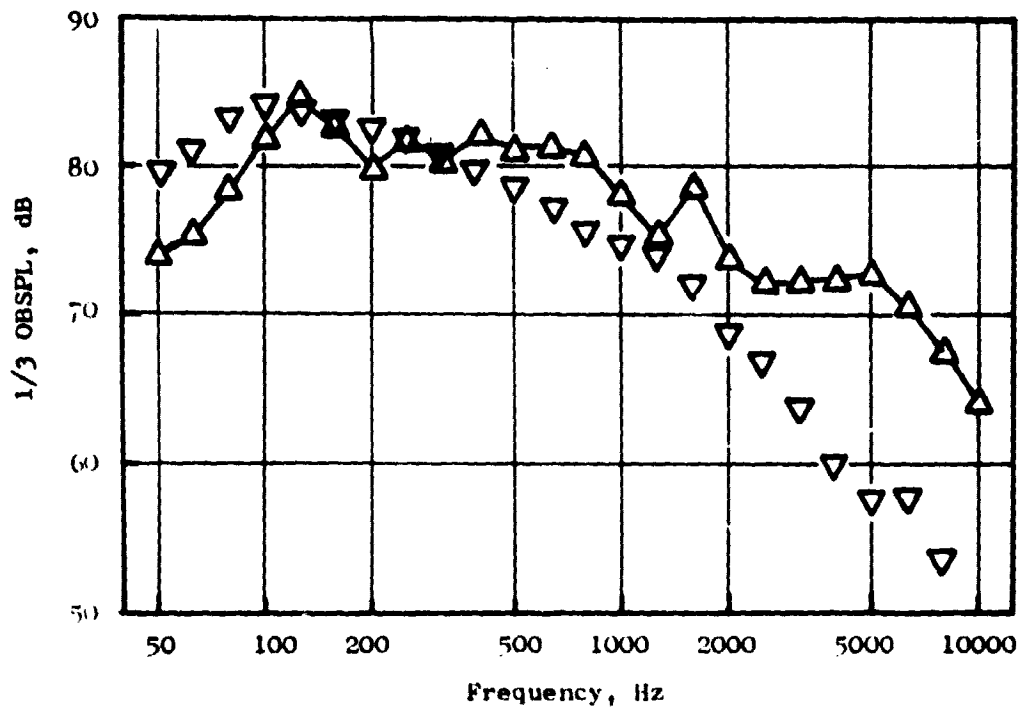


Figure 84.   Measured Engine Noise and Scaled Jet Noise at 110°.

- 152.4 m (500 Ft.) Sideline
- 11.5° Side Door Angle
- 140° Acoustic Angle

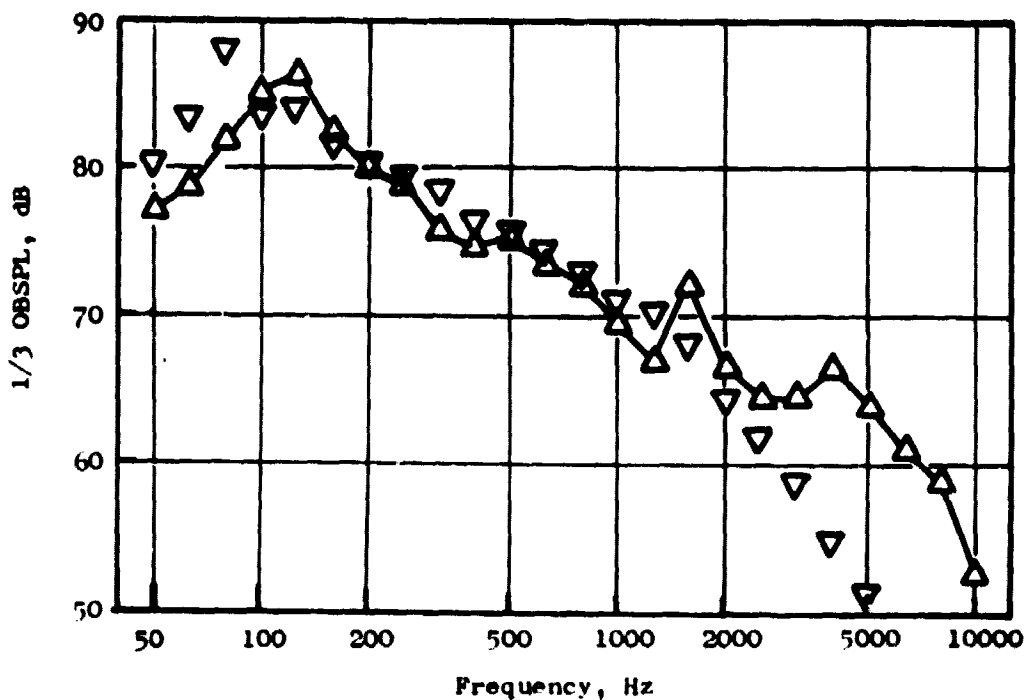△ Partially Suppressed Engine Noise (14-7)

▽ Scaled "D" Nozzle Jet Noise



Figure 85.  Measured Engine Noise and Scaled Jet Noise at 140°.

## 4.0  NORMALIZED SPECTRUM SHAPE

Exhaust velocity surveys were available on the engine only at the one operating condition discussed above.  It was decided to use the model spectrum shape and simply slide it up or down to match the low frequency portion of the engine spectra.  However, before this method could be used, a check was made on the model data to determine if it did have the same spectrum shape at all velocities.

The model data were normalized by plotting OASPL minus SPL as a function of Strouhal parameter (frequency times effective nozzle diameter divided by velocity).  Figures 86 and 87 present the normalized spectra at 80° and 110°, respectively.  Figure 86 also includes 90° data from a second model test of the QCSEE OTW exhaust geometry (References 19, 20, 21, and 22.) This second set of model data also normalizes very well.

For reference, both sets of model OASPL's are compared to predicted conical jet noise in accordance with the procedure outlined in Reference 23.  In Figure 88, this comparison indicates that the "D" nozzle exhaust OASPL's are 4 to 5 dB above the conical nozzle.

## 5.0  STATIC JET NOISE REMOVAL FROM ENGINE SPECTRA

In order to determine the noise of an OTW engine under flight conditions with jet-flap noise, the static jet noise must first be removed from the static engine spectra.  The procedure for doing this for the fully suppressed engine spectra at 110° is used as an example.  Figure 89 shows engine spectra for both baseline and fully suppressed configurations plus the assumed jet noise spectrum shape.

At frequencies of 1600, 2000 Hz, and above 3150 Hz, antilogarithmetic subtraction of jet noise is straight forward and yields jet-less engine levels.  At low frequencies where jet noise and measured engine noise are equal or within a couple dB of each other, engineering judgment must be used.  The procedure for the OTW was to assume that the core suppression was as predicted.  For example, at 500 Hz the predicted core suppression is 11 dB.  Applying this to the baseline level results in engine spectra of 72 dB.  Similarily at 800 Hz, 7 dB core suppression puts the level at 73 dB.  Below 500 Hz, since the engine spectra is all jet noise (no difference between baseline and fully suppressed) a ramp off of 6 dB per octave of low frequency noise from the 500 Hz level was assumed.  For situations such as that at 2500 Hz where the fully suppressed engine and assumed jet are equal, engine noise was assumed to be down 3 dB.

This procedure was repeated for all angles at takeoff and approach power to determine jet-less fully suppressed static OTW engine spectra for system noise calculations.

126

| P/P | Jet Velocity | |
|-----|-------------|---|
| ○ 1.20 | 640 | } JENOTS Data |
| □ 1.25 | 705 | 1/6 Scale Model |
| △ 1.30 | 770 | |
| ▽ 1.35 | 840 | |
| ◊ | 730 | } NASA Data at 90° |
| ◇ | 480 | 1/12 Scale Model |
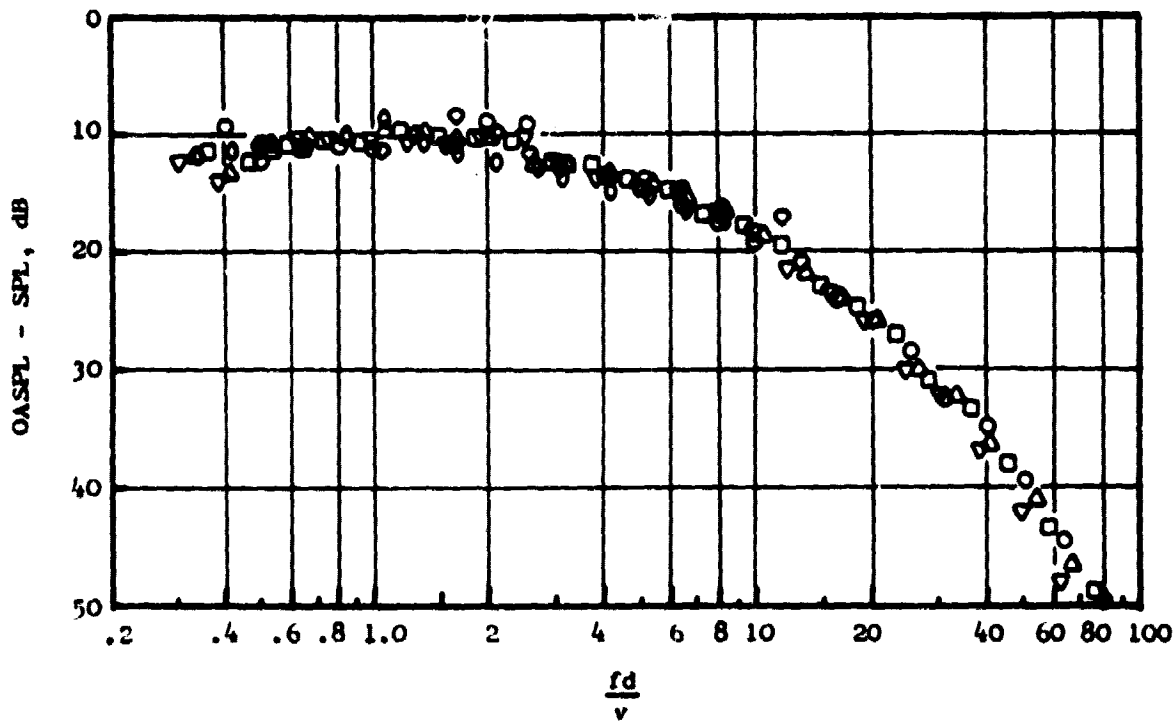


Figure 86.   Normalized Model Jet Spectra at 80°.

127

- 152.4 m (500 Ft.) Sideline
- 110° Acoustic Angle

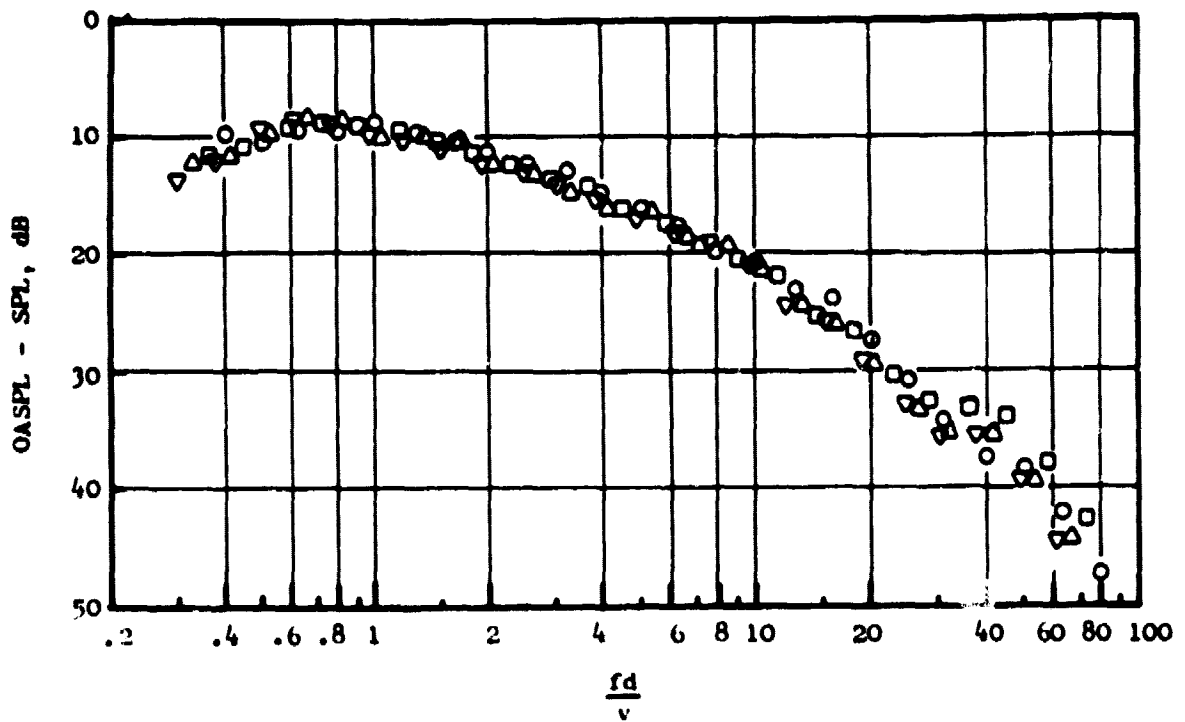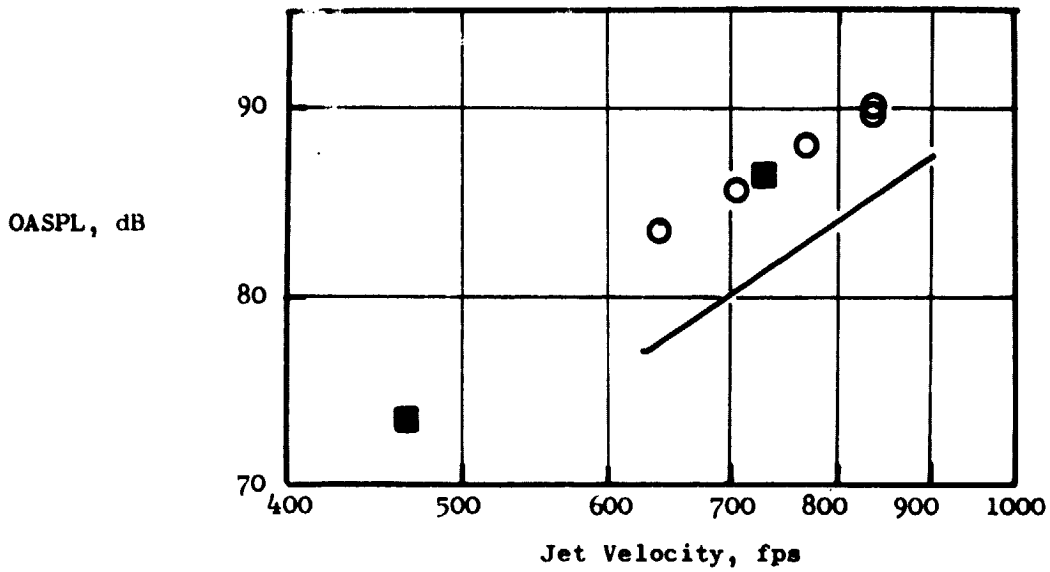| | P/P | Jet Velocity | |
|---|---|---|---|
| ○ | 1.20 | 640 | |
| □ | 1.25 | 705 | JENOTS Data |
| △ | 1.30 | 770 | 1/6 Scale Model |
| ▽ | 1.35 | 840 | |



Figure 87.  Normalized Model Jet Spectra at 110°.

• 152.4 m (500 Ft.) Sideline

O OTW Model Data Scaled to Full Size
—————— Conical Jet Prediction (Ref. 22)
■ NASA Model Data at 90°

• 80° Acoustic Angle



• 110° Acoustic Angle
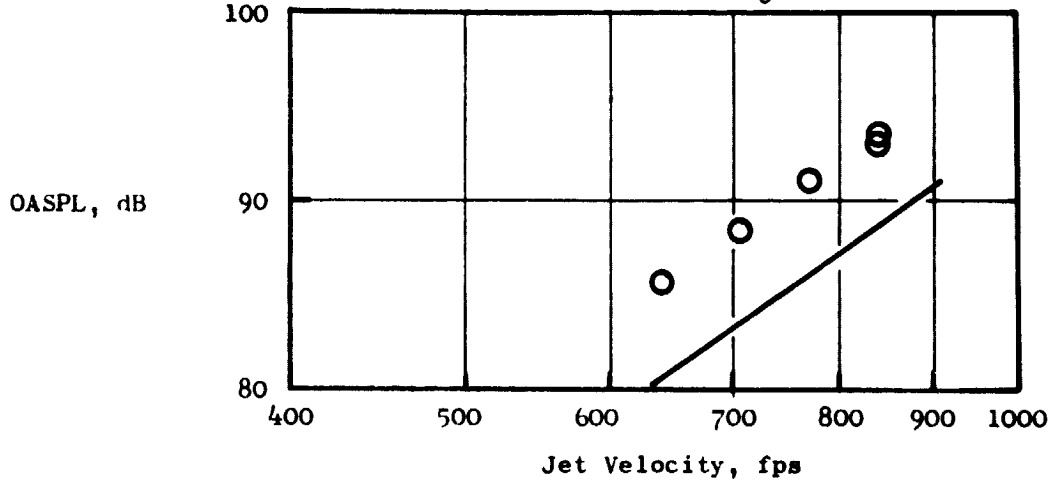


Figure 88.   Comparison of Model OASPL and Predicted Conical Jet Noise.

- 152.4 m (500 Ft.) Sideline
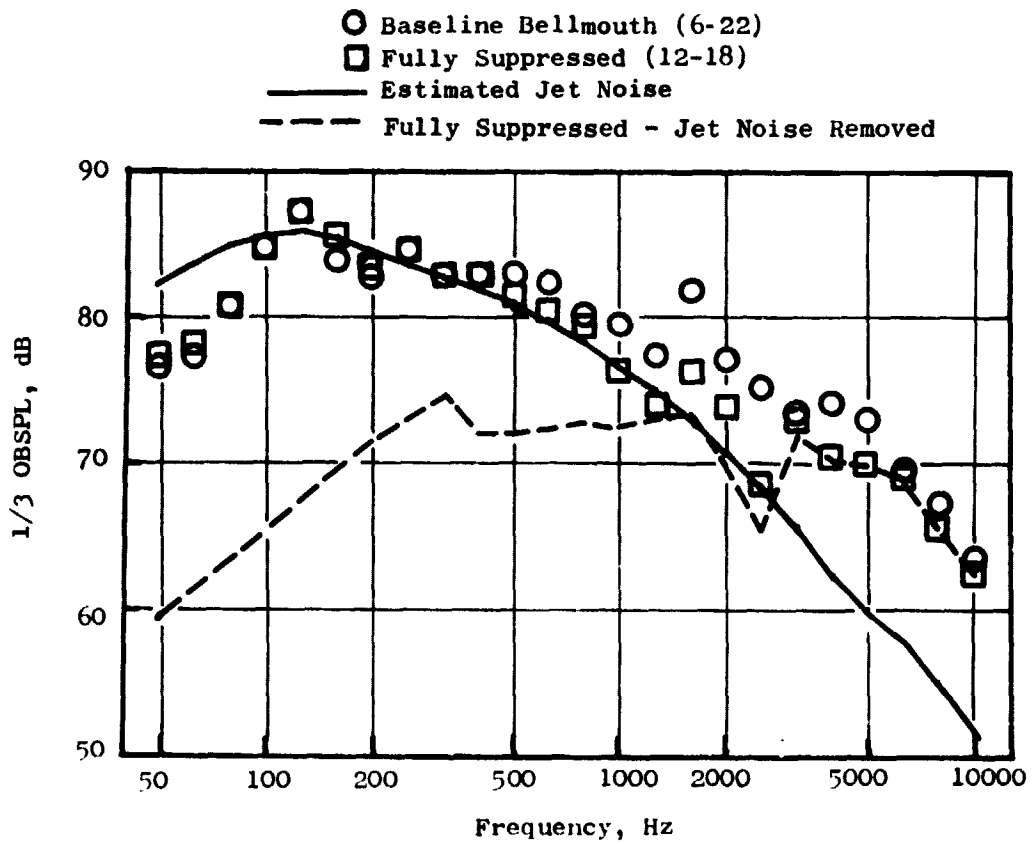- 110° Acoustic Angle

O Baseline Bellmouth (6-22)
□ Fully Suppressed (12-18)
——— Estimated Jet Noise
— — — Fully Suppressed - Jet Noise Removed

Figure 89.  Example of Jet Noise Removal from Engine Spectra.

## TREATMENT REGENERATED FLOW NOISE ESTIMATES

### 1. INTRODUCTION

The OTW engine acoustic test results exhibited an apparent lack of high frequency suppression as was shown in Figure 52. Early estimates as part of the QCSEE preliminary design in References 1 and 3 indicated that flow noise would not be a major contributor to the engine noise levels. However, a review of those early estimates revealed errors which resulted in under-predicting the flow noise by at least 13 dB.

This appendix reviews those earlier errors and presents the equations used to re-predict flow noise on the OTW engine using actual engine performance data.

### 2.0 CALCULATION PROCEDURE

A detailed derivation of the flow noise equations is available in Reference 24. Treatment regenerated flow sound power is given by

$$P_{flow\ noise} = \frac{P(f, \delta(x))}{2\ \beta} \left( 1 - e^{-\beta L} \right) \qquad \frac{watts}{hz} \qquad -1-$$

where

$$P(f, \delta(x)) = \frac{1.6\ M^3\ \bar{U}^3\ \rho\ A \star 10^{-7}}{N\ \delta^2\ L} \qquad \frac{watts}{Hz\ m} \qquad -2-$$

$$\beta = \frac{0.23 \star TL}{L} \qquad\qquad -3-$$

L = treatment length

TL = predicted broadband transmission loss

M = Mach number

$\bar{U}$ = flow velocity

$\rho$ = density

A = treated surface area

N = number of holes per unit area

$\delta$ = boundary layer thickness

The PWL re $10^{-13}$ watts is given by

$$PWL_{flow\ noise} = 10\ \log\left(P_{flow\ noise}\right) + 10\ \log\left(f_c\ 0.23\right) + 130 \qquad -4-$$

where  $f_c$ = 1/3 octave band center frequency

The above equation applies for flow noise below the peak frequency ($f_o$) which is found by

$$f_o = \frac{\bar{U}}{\delta} \qquad -5-$$

For frequencies greater than $f_o$, the flow noise power is reduced by the ratio $\left(\dfrac{f_o}{f}\right)^3$ or the PWL is less by 30 log ($f_o/f$).

Boundary layer thickness was calculated using the following empirical expression

$$\delta = 0.37\ L^{0.8}\ R_x^{-0.2} \qquad -6-$$

where $R_x$ is the Reynold's number per foot. This equation is similar to the expression for boundary layer thickness given in Reference 25 which is

$$\delta = 0.37\ L\ R_x^{-0.2} \qquad -7-$$

For the outer and inner walls the boundary layer thickness grows to about 2.3 cm (0.9 inch) by the end of the treatment. On the splitter, it grows to about 1.27 cm (0.5 inch). For the calculations, a value of 1.78 cm (0.7 inch) was assumed.

At takeoff on the OTW, aerodynamic conditions (based on measured engine data) at the OGV exit are:

M = 0.501

Total Temperature = 322° K (580° R)

Total Pressure = $1.289 \times 10^2\ \frac{kN}{m^2}$ (18.7 psi)

As is apparent from Figure 45, the fan bypass duct area was increased through the splitter region to lower the duct Mach number to 0.38 at takeoff (Reference 4). Flow noise estimates were made at Mach numbers of 0.35, 0.40, and 0.45 to bracket the estimated duct Mach number in the splitter region.

The OTW treated surfaces had variable porosity sections in the duct. The number of holes per unit area were calculated for each section and area weighted to give an average value for the holes per unit area needed in the equation 2. This value for the OTW is 62,900 $\frac{\text{holes}}{\text{m}^2}$ $\left(5840 \frac{\text{holes}}{\text{ft}^2}\right)$.

Results of the flow noise PWL calculations were presented and discussed earlier in the text. Figure 54 shows that calculated flow noise over the range of duct Mach numbers expected for the QCSEE OTW is indeed a major contributor to the engine noise and becomes a floor which precludes determination of aft fan suppression levels.

## 3.0 PREVIOUS QCSEE ESTIMATES

Examination of the previous QCSEE flow noise estimates in Reference 1 and 3 revealed that incorrect values were used for both the number of holes per unit area and the treated surface area. The holes per unit area were too high by a factor of ten and since this parameter is in the denominator of equation 2 the flow noise would be underestimated by 10 db.

The total treated area of the OTW fan bypass duct including the splitter is about $23\text{m}^2$ ($247 \text{ ft}^2$). Early calculations used a value of $10.8\text{m}^2$ ($116 \text{ ft}^2$) which results in underpredicting by 3 dB.

Accordingly, the early estimates were at least 13 dB too low and failed to recognize a potential problem area.